8-2016

Mechanism of Rapid Electron Transfer Reactions involving Cytochrome bc1, Cytochrome c and Cytochrome Oxidase

Jeremy Erik Durchman
University of Arkansas, Fayetteville

Mechanism of Rapid Electron Transfer Reactions involving Cytochrome bc_1, Cytochrome c and Cytochrome Oxidase

A dissertation submitted in partial fulfillment
of the requirements for the degree of
Doctor of Philosophy in Chemistry

by

Jeremy Durchman
Queens University of Charlotte
Bachelor of Science in Chemistry, 2005

August 2016
University of Arkansas

This dissertation is approved for recommendation to the Graduate Council.

_____
Dr. Francis Millett
Dissertation Director

_____
Dr. Bill Durham
Committee Member

_____
Dr. Dan Davis
Committee Member

_____
Dr. Suresh Kumar
Committee Member

Abstract

Electron transfer between mitochondrial proteins complexes represents the primary means by which living things acquire the requisite energy for survival. The coupling of electron transfer to proton translocation creates an electrochemical gradient that drives the synthesis of highly energetic compounds such as ATP. The purpose of these studies is to measure rates of electron transfer and elucidate the important governing factors in the redox events involving cytochrome bc_1, cytochrome c and cytochrome oxidase. Using rapid initiation of redox events triggered by laser flash excitation of ruthenium compounds, and strategically monitoring unique spectral properties of these proteins in the visible region of the electromagnetic spectrum, rates of electron transfer can be determined for native and mutant forms of the proteins. Per Rudolph Marcus' Nobel-winning theory, reorganization energy (λ) and redox potential difference between two centers (ΔG) dictate, to a great degree, the rate of electron transfer -- provided that conformational gating is not rate-limiting. Specifically, the internal kinetics of rapid electron transfer in cytochrome bc_1 from species *Rhodobacter capsulatus* is reported in novel fashion. The effects of substrate and inhibitors on the enzyme are discussed. Rate information for mutant constructs of *R. cap* bc_1 is provided to contribute important structure/function information about the protein and its subunits. Additionally, the effect of altering the redox potential of cytochrome c on kinetic rates of rapid electron transfer to the Cu_A center of cytochrome oxidase is examined, showing for the first time that the electron transfer from cytochrome c to Cu_A obeys Marcus' predictions.

Acknowledgements

In contemplation of all the individuals who have assisted me in this journey, Einstein's quotation "standing on the shoulders of giants" resonates constantly. The vastness of a small group's influence on my life and stark juxtaposition of this immense gratitude to my own tiny role in the universe bring me to regularly give silent thanks to these few. It is indeed rare when we get the chance to immortalize our gratitude beyond the infrequent verbalization, which seems trite, transitory, and in danger of coming across as lip service. Daily, I really try to thank people for the smallest of things -- a favor, or perhaps holding a door. How strange it is to me that we use the same language for something so small as we use when someone does something wonderful to project us in a life-changing manner. In truth, there is no language or verbal mechanism to remind someone each and every moment of what they mean to us. We hope to say it once as well as we can, so that it will stick forever with them -- even when they are themselves feeling down, or ill, or distracted by the all the other individuals in their lives. One can gather hope in the silent sacred promise one makes to himself in the dark when no one else is looking -- the vow that he will carry himself forward in such a way as to honor these giants that aided a flea. Perhaps this, then, is the true place where gratitude lives, breathes, and persists. I will try my best to memorialize you, one and all.

Dr. Frank Millett is a wonderful man, instructor, academic, and mentor. I have never been able to really say how much I owe to him in this experience. I was an orphan mewling in the dark when I joined his group. I found a home with residents Dr. Jeff Havens and Marti Scharlau, my dearest friends and colleagues on the ground. These three formed a core of guidance in terms of how scientific inquiry should be conducted. Dr. Bill Durham

provided hands-on training, guidance, and technical expertise. Dr. Suresh Kumar and Dr. Dan Davis formed the rest of the committee -- supportive, encouraging, and intelligent gentleman that I will never forget. I do not know how to say thank you other than to try to make you proud. I just want you to know that it changed my life, and that I will do my utmost to pay it forward.

My family struggled with me in these endeavors. To Sita, my partner, my rock, my love, who carries the household and parenting when I cannot, to you I want to immortalize my eternal gratitude. It could not have been easy for you, though you never complained, and I hope you know I would pick you first for any battle I might ever face. I am sorry if you've ever doubted that. To my children Lennon, Michael, and Alexander -- I love you all. Please do not aspire to be like me, but rather be greater as I know you can. My mother, Lynn, my brothers Matt and Tom -- though distant in space, you have always had my back. My father Erik -- your untimely passing brought great sorrow to me but I still have your hands. I look at them everyday and I see your fingers. I wish we'd had more time as I think of some activity every day we will never get to do together again.

I want to thank all faculty and staff in Fayetteville and Fort Smith -- Dr. Lois Geren, Marilyn Davis, Dr. Wes Stites, Heather Jorgenson, Leslie Johnson, Mona Dyer, Dr. Jim Belcher, Dr. Dave McGinnis, Todd Phipps, and Liz Williams, to name a few.

Lastly, for all the wonderful life lessons, I would like to thank Dr. Paul Adams and Mrs. Amy Yearry (nee' Webb). I learned from you both that the greatest achievements come when the stakes are high and the mountain is unforgiving. In the event of inclement weather at the summit, I will not ever forget, thanks to you, that other routes may exist, and that discretion is the better part of valor.

Table of Contents

List of Figures

Chapter 1: Introduction to Metabolism, Biological Electron Transfer, the Mitochondrial Enzymes Involved Therein, and a Novel Methodology Employed Toward the Study of These Seminal Relationships

1.1 The mitochondrial electron transport chain and its production of ATP

Throughout the course of time, man's position in the universe has held an understandable aura of mystique and wonder for scientists, philosophers, poets, and anyone that has experienced the miracle of birth or the heartache of tragedy. The metaphysical questions of how and why life exists are among the most important and debated questions that define our species. And while science alone may never answer the questions as to why life exists, the study of metabolism on a molecular level has revealed some important information into our understanding regarding how life exists and persists. While one may identify many things and conditions necessary for life, there is one indisputable requirement that must be included and acknowledged, and which is the point of interest in studying metabolism: energy. All living organisms exist as fundamentally challenged entities, sharing the common obstacle of overcoming an entropic, energetically unfavorable dynamic in their environmental surroundings. From the cumulative sum of the interactions each living thing has with its environment, there is a necessity to build, sustain, and reproduce against this running current of entropy. By harvesting the energy harnessed in chemical bonds, living organisms manifest a compelling case of local "negentropy," a term first coined by Erwin Schrödinger to rationalize the phenomenon of the existence of life and order in a universe that generally favors disorder. Given that energy is neither created nor destroyed, per the First Law of Thermodynamics, the processes of metabolism must be extremely efficient in order to result in a net gain of

energy for an organism. On a molecular level, organisms require an efficient means of coupling and storing the energy yields of their metabolic intake, which is accomplished by metabolizing food sources to produce a chemical species that serves as the primary electrochemical energy source used by the cell, known as adenosine triphosphate (ATP). In order to produce ATP, electrons are transferred between intermembrane protein complexes while simultaneously establishing and maintaining an electrochemical potential across the biological membrane via the "pumping" of protons. Selective pressures on these redox proteins have led to the evolution of a highly efficient and conserved means of coupling, as exemplified by the homology found within the diversity of known species in the evolutionary timeline. The electron transfer systems of metabolism found in the mitochondria of animals, in the chloroplasts of plants, and in the plasma membrane of bacteria all share essential structural motifs, functional roles, and enzymatic features. Thus, though primarily this discourse will, when possible, address this biological system in its relevance to human beings, on a larger scale these same considerations would be applicable to all living species. The ubiquitous frequency and presence of these systems in species great and small strongly reinforces the seminal importance of electron transfer to supporting life in its providence of the energetic solution to the thermodynamic hurdle of entropy (1).

The mitochondrial electron transport chain, as depicted in Figure 1.1-1, consists of a series of protein complexes, which convey electrons along the inner mitochondrial membrane. The free energy yielded by the redox reactions is spent to actively transport $[H^+]$ across the membrane against the concentration gradient from low $[H^+]$ to high $[H^+]$, i.e. from the mitochondrial matrix to the intermembrane space. Since the inner membrane is

impermeable to direct proton transfer, the gradient that is established by this translocation generates an electrochemical potential across the inner membrane, driving the phosphorylation of adenosine diphosphate (ADP) to create ATP [ADP + P_i --> ATP + H_2O]. This reaction is catalyzed by ATP synthase, which allows protons that have been actively pumped against the concentration gradient to then flow from the low pH intermembrane space {positive side (P)/cytosolic} to the high pH {negative side (N)/ interior} mitochondrial matrix. To broadly summarize, the energy obtained from caloric intake is invested in this proton gradient, which creates the impetus for creation of ATP, the energetic currency of biological systems. Thus, an overview of electron transfer and the proteins involved in the electron transfer protein complex follows (2).

The electrons from glycolysis and the citric acid cycle, as carried in the form NADH, are introduced to the electron transfer chains at Complex I (NADH dehydrogenase, NADH-coenzyme Q reductase). Mitochondrial Complex I has a molecular mass of 980 kDa, as many as 8 redox centers, and consists of over 44 different subunits; it is by far the most complex enzyme of the mitochondrial electron transfer chain. A core portion of 14 subunits is highly conserved across prokaryotes and eukaryotes alike, suggesting a highly conserved role. As a result of this complexity, its structural characterization and the precise mechanism of its action have yet to be fully elucidated. What is known is that upon binding NADH by the single flavin cofactor of Complex 1, the two electrons from NADH are passed through a series of Fe-S cofactors to reduce coenzyme Q and form ubiquinol (UQH_2). In doing so, for every two electrons passed through the enzyme from a single NADH carrier, 4 protons are pumped toward the low pH (high [H^+]) side of the membrane. In terms of structure in regards to proton pumping, Complex I contains a series of transmembrane

helices that form four novel, discontinuous, and somewhat flexible proton channels, each composed of two distinct halves. Each channel has a central lysine contained and important glutamate residues modulating pKa to serve as potential H^+ donor/acceptor pairs. No less than 9 iron-sulfur (FeS) clusters serve to couple electron flow to the pumping of protons. Outside of requisite expenditure associated with conformational shifts, most of the energy generated in the redox process is dedicated to the reduction of quinone, which is contained in the membrane and serves to carry electrons for reducing cytochrome bc_1. These are discussed in greater detail in the following sections (2, 3).

Complex II follows Complex I and is the only integral membrane protein of the inner mitochondrial membrane that is also part of the TCA cycle. This enzyme, also referred to as succinate-Coenzyme Q reductase or succinate dehydrogenase in the literature, is the smallest complex of the electron transfer chain at 140kDa mass and is comprised of only 4 subunits. It functions to oxidize succinate to fumarate, an activity that is concomitant with the reduction of a bound FAD to yield $FADH_2$. $FADH_2$ then passes its electrons sequentially through an Fe-S cofactor to form ubiquinol (UQH_2) via reduction of coenzyme Q substrate. With a combined pool of reduced electron carrier UQH_2 achieved from the activities of Complexes I and II, there is a readily available source of substrate for processing by cytochrome bc_1 (2).

As indicated, the ubiquinol (UQH_2) molecules produced by Complexes I and II are in turn used by cytochrome bc_1 (also known as Complex III, or ubiquinol-cytochrome c reductase). This novel pathway, termed the Q-cycle, ultimately provides electrons to reduce cytochrome c coupled with proton pumping across the inner membrane. One of the unique features of this cycle is the bifurcation of electrons traveling two distinct pathways

through cytochrome bc_1. As each ubiquinol molecule is oxidized, one electron follows the most energetically favorable chain, termed the high potential chain. This high potential chain consists of an Fe-S cluster and cytochrome c_1 heme redox center, while the other electron proceeds through a less favorable pathway in terms of sheer redox potential driving force. This electron re-reduces an equivalent of the oxidized ubiquinone, producing a semiquinone radical (UQ-). A second turnover of the enzyme provides the electron to then reduce this radical, regenerating the substrate ubiquinol for further cycling. Each turnover results in two protons pumped from the matrix. Thus, in terms of accounting, in consideration of the two turnovers and net products of both the high and low potential chains of cytochrome bc_1 through a completed Q-cycle, the enzyme pumps four protons to the P-side and reduces two equivalents of cytochrome c. Cytochrome bc_1 and its mechanism will be discussed further in Chapter 2 (2,4).

Cytochrome c (Cc) is the recipient of electrons from heme c_1 of cytochrome bc_1. With a molecular weight of ~12 kDa, Cc is a small and highly soluble protein that plays an important, non-enzymatic role in this system. Despite not catalyzing a biological reaction, it serves primarily as an integral shuttle between the otherwise relatively situated, stationary pair of cytochrome bc_1 and cytochrome oxidase, (Complex IV, CcO). In addition, it is also the electronic recipient in numerous other redox pathways, and will be discussed in greater detail in Chapters 2 and 3. Like a wire connecting two electrical components, it is not possible to overstate its significance in ensuring that this biological circuit is complete (2).

Cytochrome oxidase represents the sequential end of the mitochondrial electron transport chain. Electrons are transferred to cytochrome oxidase from cytochrome bc_1 via cytochrome c, where they are received by molecular oxygen, producing H_2O. Cytochrome

oxidase has a molecular weight over 160kDa and consists of more than 10 subunits. It contains two pairs of different heme and copper cofactors (hemes a and a_3, and copper centers Cu_A and Cu_B). Electrons from cytochrome c are passed sequentially from Cu_A to heme a, then transferred to the binuclear center of hemes a_3/ Cu_B. From a stoichiometric standpoint, Complex IV pumps four protons across the membrane for every four electrons passed through the complex. The overall reaction can be written as:

$8H^+_{(in)} + 4e^- + O_2 \dashrightarrow 2H_2O + 4H^+_{(out)}$ (2).

The proton gradient established by the mitochondrial electron transfer chain yields an electrochemical potential, with both electrical and concentration impetuses acting as a driving force for protons to flow back across the inner membrane. Per Peter Mitchell's Nobel winning theory, the free energy difference across the inner membrane may be expressed as a term accounting for both factors of the electrochemical potential as:

$$\Delta G = RT \ln\left(\frac{[c_2]}{[c_1]}\right) + ZF\Delta\Psi$$

where c1 and c2 are the respective concentration of the species across the membrane; Z is the charge on the species; and F is Faraday's constant of 96,485 C/mole electrons (3). Since the concentration gradient in this case is that of $[H^+]$ and is thus singly positive, equation 1.1 can be simplified to:

$$\Delta G = RT \ln\left(\frac{[H^+_{out}]}{[H^+_{in}]}\right) + F\Delta\Psi$$

In this manner, the proton gradient established by the electron transfer chain is readily utilized by ATP synthase to produce ATP. By allowing protons to then travel back across the membrane to the inner mitochondrial matrix, the energetically favorable direction of

proton mobilization, i.e. high [H^+] to low [H^+], acts as the mechanical force to turn the F_1 subunit by rotating a portion of the F_0 subunit, termed the c-ring. The rotation of the c-ring causes the nucleotide binding sites of the F_1 subunit to synthesize ATP from ADP and P_i. This final culminating process concludes the process of metabolism, as ATP is the energetic currency that is used by the cell, and thus the organism, to carry out the various functions necessary for survival (2,4).

Figure 1.1-1 Depiction of the various constituents of the mitochondrial electron transport chain. The enzymatic components function in order to produce an electrochemical membrane potential with H^+ pumped from the matrix to the intermembrane space, with electrons serving as electrogenic balance

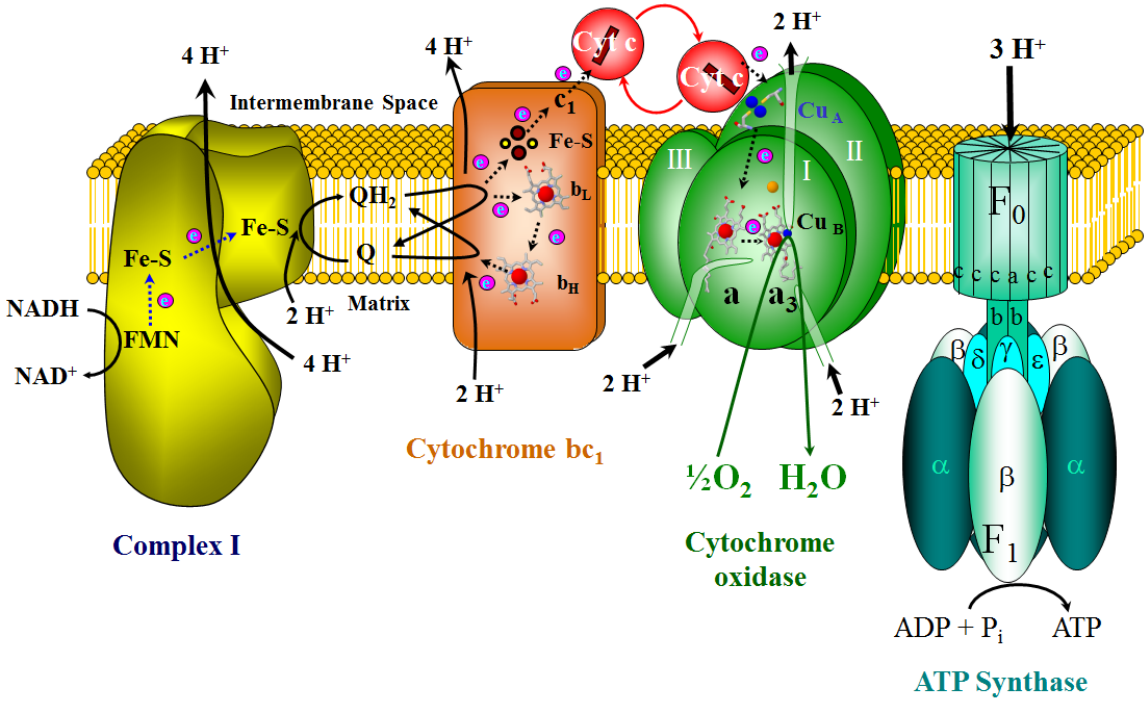

1.2 Introduction to electron transfer

In the previous section, the significance of electron transfer events to living organisms, as occur between the protein complexes of the electron transfer chain to generate an H^+ gradient, is made apparent. Obtaining a usable energy course in the form of a chemical species such as ATP provides the organism with a means by which to store energy and control energy consumption efficiently. Electron transfer between protein cofactors, and the coupling of this electron relocation to H^+ flow, is a salient feature of several other metabolic conversions (1). The poignance and relative ubiquity of electron transfer reactions have driven collective scientific efforts to accurately model these types of systems. Fundamentally, the rate of a chemical reaction is related to the Arrhenius equation, which incorporates the concept that some initial thermodynamic hurdle must be overcome to achieve an activated state to achieve the creation or breaking of a chemical bond, represented by the following equation:

$$k = A\exp\left(\frac{-E_A}{RT}\right)$$

where E_A is the activation energy, R is the constant 8.3145 J/(mol/K), T is temperature in K, and A is the pre-exponential proportionality term. However, for reactions limited to true transfer of electrons between two species such as those found in the mitochondria, the making and breaking of chemical bonds is not a factor. As the transfer of the electron is itself not a rate-limiting reaction coordinate in these types of systems, Arrhenius theory does not adequately model experimentally determined data (5). Rather, a theoretical description of an electron transfer event must incorporate the Franck-Cordon principle, which asserts that, in order for electron transfer to occur between two species in solution,

it must be assumed that the actual charge transfer is much more rapid than any requisite nuclear rearrangements. These nuclear rearrangements are in fact understood to be the rate-limiting reaction coordinates when no chemical bond is being made or broken, and when no slower conformational gating is required. While this facet of the principle presents a relevant distinction to Arrhenius, Franck-Cordon in its purest form also falls short in accurately summarizing biological electron transfer. Specifically, one problem with the Franck-Condon principle is that it asserts that vertical excitation from a ground to an excited state upon harmonic/vibrational overlap is a necessity, which mandates an energy input. However, since biological electron transfer still occurs even in the dark, the Franck-Condon principle alone leaves an important question unanswered -- in the absence of light, from where might this excitation energy originate? Upon the alignment of the ground and excited states, this energy must come from somewhere (1, 6-8).

Rudolph Marcus, to whom credit for revolutionizing the topic of electron transfer reactions must be given, reconciled the incongruencies presented by both the Arrhenius and Franck-Condon theories. Marcus essentially combined the Arrhenius and Franck-Condon approaches, as follows: Given an electron transfer reaction but prior to the charge transfer, the nuclei of atoms immediately surrounding each redox center (termed inner sphere, or λ_{in}) and the long range nuclear orientations influenced by the charge at each redox center (termed outer sphere, or λ_{out}) must be in configurations necessary to accommodate the charge transfer. The sum of λ_{out} and λ_{in} is broadly described simply as λ, and is termed the reorganization energy. The applied rationale of reorganization energy in the complex arena of biological electron transport mandates a certain geometric and harmonic symmetry that must be in place both before and immediately after the actual,

instantaneous electron transfer occurs. In order to fuse these independent theories into mathematical application, Marcus modulated Arrhenius' equation. He accomplished this by redefining the Arrhenius activation energy ($\Delta G^{\ddagger}$ or E_A) as the composite of two independent yet linked, and possibly even counteracting variables (depending on specific circumstance). Referred to as the redox potential driving force (ΔG) and reorganization energy (λ), this represents Marcus's seminal achievement (9,10). In order to simplify the thought process with respect to these complex systems, Marcus viewed both the product and reactant states, and all the nuclear reconfigurations pertaining to both, as energetic parabola. This greatly simplifies hundreds of possible reaction coordinates defining the system into two simple parabolic functions described by the same basic constraints, yet displaced along both axes as shown in Figure 1.2-1. In accordance with Hooke's Law, and as seen in the figure, the activation energy may be expressed in this modified version of the Arrhenius equation as:

$$\Delta E_A = \left(\frac{-(\Delta G + \lambda)^2}{4\lambda RT} \right)$$

Thus, the rate of electron transfer may be described as:

$$k = A \exp\left(\frac{-(\Delta G + \lambda)^2}{4\lambda RT} \right)$$

The pre-exponential term, A, may also be described as the rate of electron transfer that would proceed in the absence of a required activation energy, as such:

$$k = k_0 \exp\left(\frac{-(\Delta G + \lambda)^2}{4\lambda RT} \right)$$

where k_0 is the rate of electron transfer when $\Delta G = -\lambda$ (5,10,11).

From a mathematical perspective, Marcus' theorem makes an unusual prediction for rates as a function of varying values of $-\Delta G$. Using Figure 1.2-2 as a reference, one might logically conclude from the outset that a greater driving force, as marked by increasing values of $-\Delta G$, would only speed up an electron transfer. This is consistent with the physical concept of force and its influence on rates -- for example, a moving object, like a car or a baseball, could theoretically be accelerated to the speed of light given enough force. However, at the molecular level, this holds true only up to a point. Specifically, Marcus theory predicts that the rate of electron transfer will actually decrease if ΔG is significantly greater than $-\lambda$, a situation that Marcus denoted as the "inverted region." At this point and beyond, the redox potential, which is the driving force and represented by the free energy term, ΔG, becomes so great that it actually decreases the rate of reaction. While somewhat counterintuitive, this is possible because increasing the driving force beyond a certain critical point results in an increase in the activation energy ($\Delta G^{\ddagger}$ or E_A), meaning a greater overall energy input is required to achieve the transition state. This decreases the probability of any single donor molecule transferring its electron to an acceptor, and a net lower k_{et} is expected from the Marcus equation under these circumstances for pure electron transfer reaction involving no chemical bond breaking/formation.

It should be noted that Marcus' developmental work was done on electron transfer between inorganic iron atoms (Fe^{+2} and Fe^{+3}), while the connection to biological systems was not made until later. When applied to biological systems, Marcus' theory presents significant evolutionary implications for exactly what selective forces might have acted in the evolutionary sequence. Specifically, biological redox proteins have likely undergone a

gradual tuning process that must have reconciled the two contributing, and yet sometimes competing, factors of redox potential driving force and the reorganization energy in order to maximize the efficiency and rate of electron transfer. This phenomenon partially explains why extremely large (> .85-.90V) potential differences are not observed between biological redox couples, as the implicitly high $\Delta G^{\ddagger}$ ultimately makes the electron transfer event slower and less efficient. This might also be used to rationalize how added complexity, involving systems with more steps and/or redox centers, might have evolved from primordial simplicity to achieve present day levels of elegance and intricacy. The selective forces of evolution acting on such a multi-component system to achieve maximal efficiency must at a minimum include $-\Delta G$ and λ, as they pertain to $-\Delta G^{\ddagger}$ for any given step. Provided that conformational gating is not the rate-limiting step in an electron transfer, ΔG and λ will dictate the true rate of electron transfer (k_{et}) for a step (1,6,12,13).

The incorporation of Marcus' perspectives into the biological arena required some modification, which is discussed in this section. For example, since biological redox reactions for the most part occur between redox centers separated by some distance, the pre-exponential term (A) can be further clarified as a function of Boltzmann's constant and temperature, as such:

$$A = \left(\frac{4\pi^3}{\hbar^2 \lambda k_B T} \right)^{\frac{1}{2}} H^2{}_{AD}$$

where H_{AD} is an electronic coupling term that represents the probability of an electron being transferred between the redox donor and the acceptor (1). Thus, the full expression of the classical Marcus theorem becomes:

$$k_{et} = \left(\frac{4\pi^3}{\hbar^2 \lambda k_B T} \right)^{\frac{1}{2}} H^2{}_{AD} \exp\left(\frac{-\left(\Delta G^\circ + \lambda\right)^2}{4\lambda RT} \right)$$

Furthermore, because electronic coupling term is itself a function of the distance between the redox centers, Hopfield proposed that the H_{AD} term may be represented as:

$$H_{AD} = H^0{}_{AD} \exp\left(-\beta(rDA - r_0)\right)$$

where β is a measure of the capacity of the separating medium to allow for electron transfer between the two centers (14).

Several different approaches have been used to determine the value of β for biological redox reactions, as it is of particular mathematical importance to Hopfield's expansion of Marcus' pre-exponential term. For example, Gray *et al.* measured intracomplex rates using photoexcitable ruthenium compounds for several proteins and derived a general value for β of -1.1 $Å^{-1}$ (1,7). Some redox proteins with comparable redox center distances were found to have vastly different intramolecular electron transfer rates,, which indicated that a unique β value for each redox system might be likely. In light of these findings, Beratan *et al.* introduced a model of pathway analysis to include all the potential pathways for electronic coupling through the protein medium involving the coupling of the redox centers. Using this system of analysis, bonding pathways may be assigned an average β value of -1.1 $Å^{-1}$, while non-bonding pathways can be assigned an average β value of -2.0 $Å^{-1}$ (1,15).

Alternatively, Moser and Dutton have proposed a different approach to estimating β values in order to simplify the rather complex nature of prior models. This approach essentially treats the protein matrix between redox centers as a single homogenous

barrier. An average β value of -1.4 $Å^{-1}$ was empirically determined to be appropriate for several different redox protein systems (11,12,16,17). By simplifying the complex quantum mechanical concerns of prior models, the Moser-Dutton equation holds a considerable advantage to these other models in terms of utility (18,19). One of the important conclusions of this establishment of a singular value for β is that it suggests a certain independence of electron transfer from at-large protein structure. This may have provided some evolutionary advantages, possibly decreasing selective pressure and thereby yielding more possibilities for optimization**.** Since redox potential and reorganization energy have such a drastic impact on the kinetics of redox proteins, as addressed by Marcus, these together may compose a more limited and focused subset of evolutionary options for the fine-tuning of redox reactions. The considerable homology found within these systems across the evolutionary spectrum stands as a testament to the success of these archetypes. Orientations of redox centers with respect to one another appear to have been established early in the evolutionary timeline. Later evolutionary design may have taken a more subtle yet quite effective approach to modulating redox reactions and relationships by simply altering the distances between cofactors (12,16,17,19-22).

Figure 1.2-1 Graphical depiction of Marcus Theory, indicating donor (D) and acceptor (A), with parabolic expression the pre- (R) and post-electron transfer (P) states. Per Hooke's law, these are considered identical parabola simply displaced on the x-axis. The redox driving force (ΔG), and reorganization energy (λ) are indicated as important electron transfer parameters. Under these circumstances, where redox driving force (ΔG) = 0, and given reorganization energy (λ), the activation energy ($\Delta G^{\ddagger}$ or E_A) = $\lambda/4$.

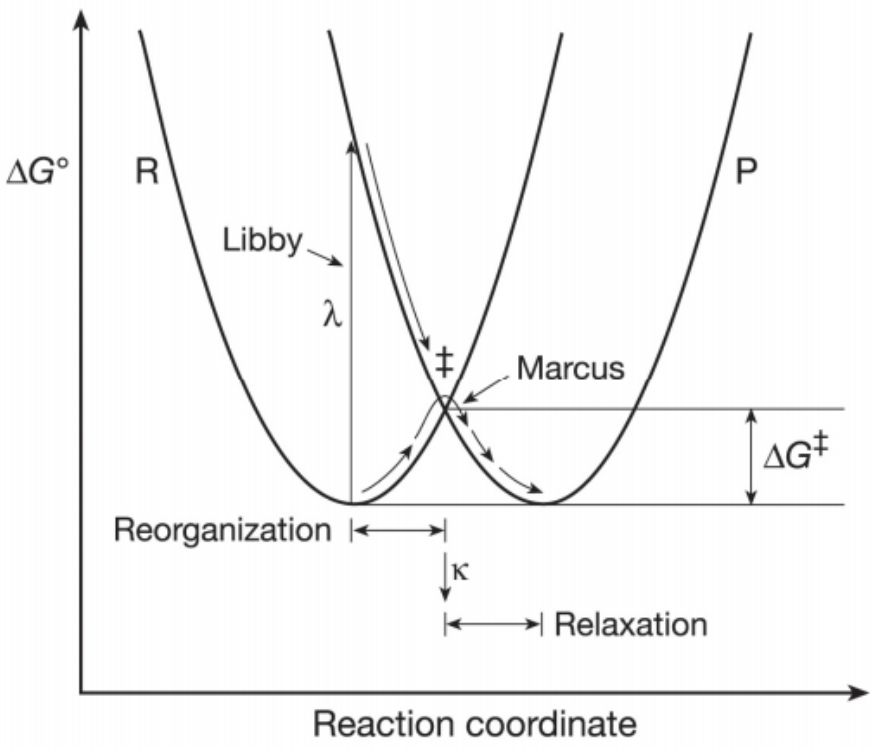

The ***reorganization energy (λ)*** is defined as the change in Gibbs energy if the reactant state ($D|A$) were to distort to the equilibrium conformation of the product state ($D^+|A^-$) without transfer of an electron.

Figure 1.2-2 Depiction of Marcus theory of electron transfer to conceptualize the effect of increasing redox potential (ΔG^0) on reaction rates as governed by activation energy ($\Delta G^{\ddagger}$ or E_A). As the redox driving force becomes greater, rate is shown to predictably increase until $-\Delta G^0 = \lambda$. Once redox driving force ($-\Delta G^0$) exceeds reorganization energy (λ), the activation energy actually begins to increase and rates begin to decrease, described as the inverted region.

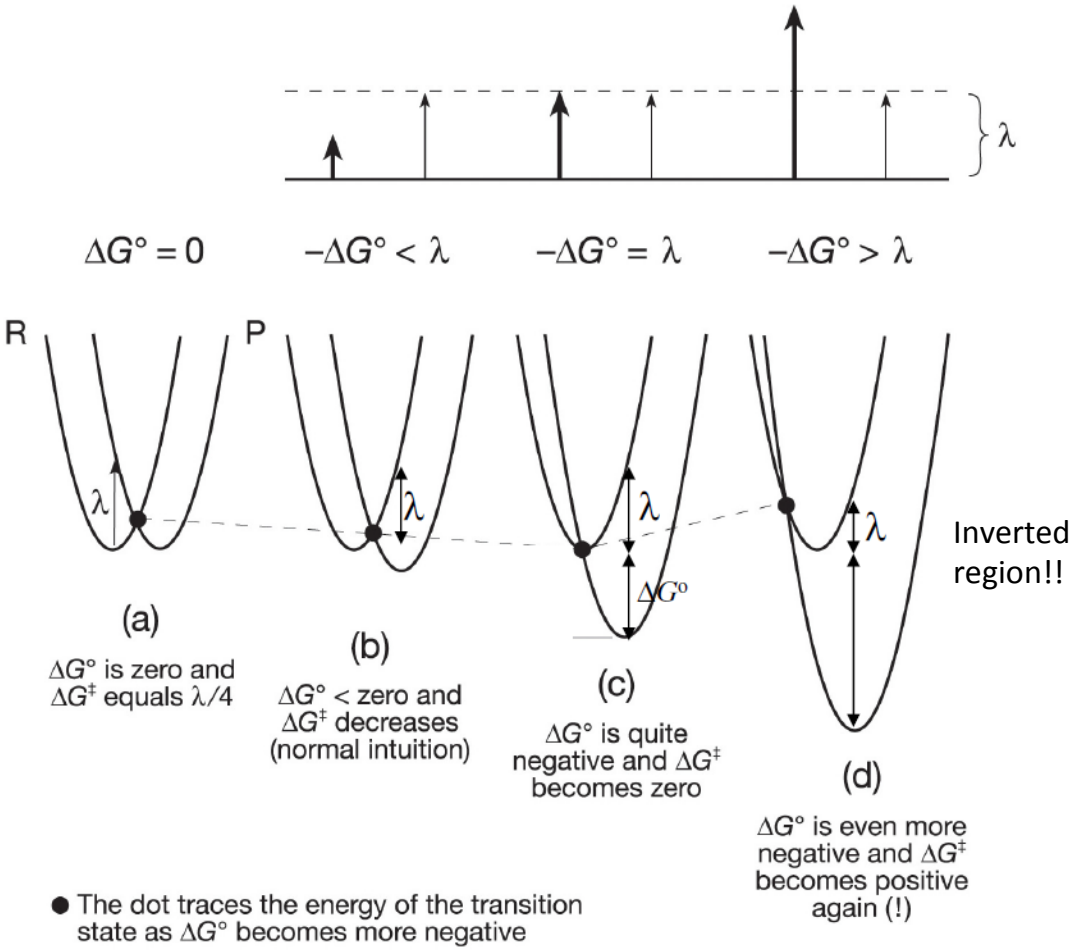

1.3 The methodology of laser flash photolysis

As discussed above, the rate of electron transfer between redox centers is very rapid as compared to the necessary nuclear rearrangements accompanied by that transfer of charge between them. From a fundamental standpoint, it stands to reason that any method designed with the specific intent of studying the rates of electron transfer between redox proteins must also be very rapid. In fact, if the goal is to determine the true rate of electron transfer, the method must be faster than the biological electron transfer event itself regardless of what may be the rate-limiting step. Otherwise, the method is itself rate-limiting, and, while perhaps useful in a semi-quantitative manner in the determination of limits or for relative comparison, methods such as these are unable to quantitatively assess true rates of electron transfer. For example, one such means of studying biological electron transfer has been the use of stopped flow experiments. These are conducted by directly injecting two redox proteins into a buffering solution and monitoring redox-dependent spectral changes as the electron transfer takes place. However, stopped flow experiments are limited by the rate of mixing and subsequent diffusion of the two proteins into the solution to interact with one another, such that resolution is typically limited to timescales on the order of milliseconds. While not useful for the true determination of kinetic rates, these types of experiments have nevertheless been extremely beneficial in the study of biological electron transfer for the purposes of establishing redox relationships and identifying important criteria necessary for electron transfer reactions to take place. Through comparison of relative rates of distinct systems or species, or as a comparison of rates of native wild-type protein to that of a mutant construct, a great deal of information can and has been surmised from such experiments. These experiments are also relatively

low cost, consume little time, and can often provide valuable insight into the viability of a project or study. Yet, one is highly unlikely to even remotely approach a measure of true electron transfer rates at the biologically, catalytically relevant scale using this type of methodology.

The combined efforts of the labs led by Frank Millett and Bill Durham at the University of Arkansas-Fayetteville have introduced, developed, and refined an alternative method of measuring biological electron transfer. This method utilizes the unique photoactive properties of ruthenium compounds to initiate electron transfer reactions. These compounds vary in composition and may be covalently attached to strategic sites on redox proteins, such as specific amino acid residues, or they may be freely diffused into solution. Rapid laser-flash photoinitiation of sufficient excitation energy triggers activation of the ruthenium complex to the metal-to-ligand charge transfer state. Depending on the particular ruthenium complex and the parameters of the biological redox center, the rapid reduction or oxidation of the redox cofactor occurs on the nanosecond timescale, several orders of magnitude more rapid than stopped flow techniques. Heme proteins, such as the ones that are present in the mitochondrial electron transport chain, have large absorption characteristics within the visible region, such that the subsequent, catalytically relevant changes in redox state after the flash-initiation can be monitored as the system responds to the light-activated electron stimulus. A range of ruthenium compounds have been synthesized to be used for these types of studies to offer a unique perspective into true rates of electron transfer previously unobtainable using more conventional methods.

A diagram of the laser instrumentation setup is shown in Figure 1.3-1. The laser flash is directed to the sample to initiate the electron transfer between the ruthenium

compound and biological redox protein. The broad spectrum light from a tungsten lamp is focused into the sample and is modulated by a high-pass filter, which serves to prevent sample degradation. These components act to direct light through the sample for analysis at pertinent wavelengths as directed by the monochromator. Signals, after amplification by the photomultiplier tube, are conferred to the oscilloscope to generate files of transmittance transients, which are further processed to absorbance transients. Computer software can be used to determine kinetic rate constants and amplitudes from these absorbance vs. time transients.

Figure 1.3-1 Laser instrumentation setup, indicating laser flash, tungsten lamp with lens and high pass filter to minimize potentially destructive interfering light transmittance to the sample, monochromator for wavelength selectivity, photomultiplier tube (PMT) for signal amplification, and oscilloscope. Raw signals processed through fitting software to generate transients, pictured in bottom left. Figure courtesy of Dr. Jeff Havens.

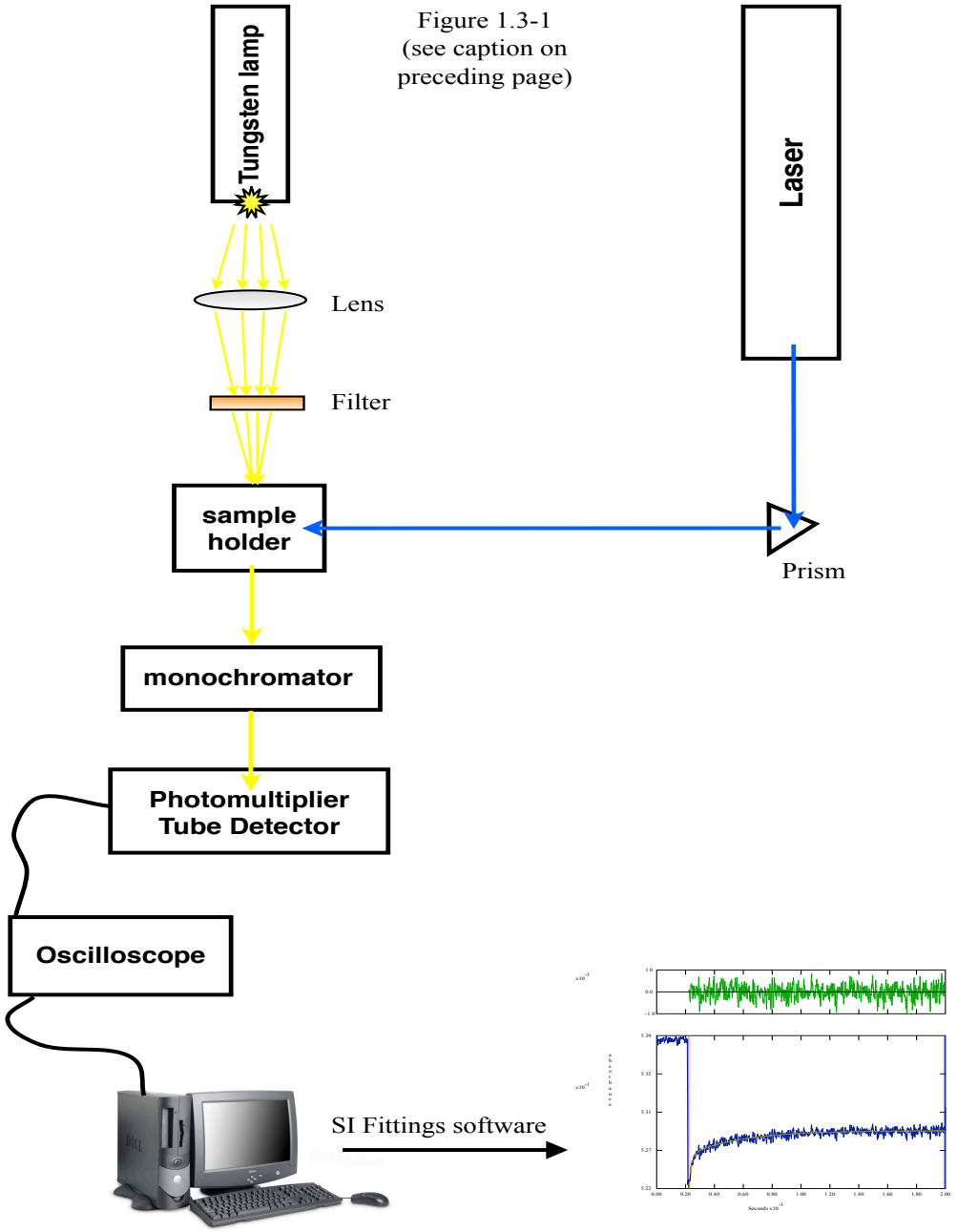

Chapter 2: Kinetic Studies of the cytochrome bc_1 enzyme of *Rhodobacter capsulatus*

2.1 Introduction to cytochrome bc_1 and its importance

Cytochrome bc_1, also known as Complex III of the electron transport chain is an integral component of the aerobic energy harnessing system found in the inner mitochondrial membrane of all eukaryotes and the plasma membrane of prokaryotes. Through a series of highly concerted and controlled electron transfers in sequence, the carbon-carbon bond energy of foodstuffs are metabolized by the enzymes of the electron transport ensemble to actively create an electrochemical gradient of H^+ -- these protons are then allowed to cross the mitochondrial membrane from the intermembrane space in order to drive the production of ATP via the terminal ATP synthase enzyme. Cytochrome bc_1 is located at the approximate midpoint of this process, such that its importance to the existence of life on this planet is quite difficult to overstate. Authors have estimated that this enzyme and homologous photosynthetic cytochrome b_6f account for 30% of total bioenergetic flux and transmission in the biosphere (23,24). From a practical standpoint, this enzyme is thus a valuable point of study for several reasons. First, its centrality to survivability for an organism makes it a viable target for control through the use of antimicrobial and antifungal agents. Of specific interest, then, is the means by which these agents inhibit and/or alter the behavior of cytochrome bc_1 of one species, while in turn not also disrupting the bioenergetic cycle of another species. This has potential applications in several profitable arenas, such as in the development and implementation of pesticides and antibiotic medicines. As a result, the studies of bc_1 by the Millett/Durham collaboration, as well as other labs, have employed these agents to further elucidate the native, uninhibited enzymatic process by which this protein receives electrons from its native substrate quinol

and transfers them to the mobile electron shuttle cytochrome c. Secondly, this enzyme has received increasing amounts of interest and attention in recent years regarding its production of superoxides and reactive oxygenated species (ROS), which have been increasingly implicated in numerous roles detrimental to human health and physiology (25-34). Beyond these practical applications, and the enzyme's core significance in the scheme of metabolic energy transduction, a full understanding of cytochrome bc_1 is likely to shape and contribute to the theoretical paradigms regarding the nature of enzyme-mediated catalysis. For example, many of the proposed mechanisms for bc_1 require a destabilization of the activated intermediate, which is contrary to many other enzymatic models. The models that exist for many other enzymes typically involve the stabilization, and not the destabilization, of such an intermediate. Why would nature digress from a fairly standard mode of catalysis in such a manner? It is with these lines of questioning and pertinent application in mind that it is of enormous scientific value to investigate and advance knowledge of this enzyme.

2.2 Function and features of cytochrome bc_1

Eukaryotic cytochrome bc_1 from various species can be comprised of as many as 11 subunits, while prokaryotic species can be found with as few as three subunits (35). Despite this diversity, it is believed the functional core of these subunits is conserved in terms of sequence and fold. By extension, this remarkable level of conservation strongly suggests functional equivalence for the enzyme across species, despite the differences that persist in subunit variance and complexity (36,37). Additional subunits found in the eukaryotic forms of the protein are thought to simply aid and assist in regulatory processes and/or assist in the prevention of possible deleterious side reactions as compared to their prokaryotic predecessors (36,38,39).

The structure of the bc_1 dimer is shown in the schematic below in Figure 2.2-1, while a comparison of prokaryotic bc_1 and eukaryotic bc_1 are shown in Figure 2.2-2. The enzyme exists as a homodimer, with each monomer containing two functional chains: the high potential c chain and the low potential b chain, hence named for the c- and b-type hemes each contains. These two chains provide the separate yet linked interactive redox pathways of a bifurcated electron transfer pathway that is one of the most seminal and unique characteristics of this protein. Figure 2.2-3 is provided to illustrate this novel functionality as first suggested by Peter Mitchell (top), with a schematic of the current consensus of the Q-cycle as more information from crystal structures has been gathered (bottom) (35). To summarize, the substrate of the enzyme, quinol, arrives at the binding site reduced bearing electrons generated from Complex I, whereupon it is oxidized to quinone. This binding site is located proximal to the low pH side of membrane, i.e. nearer to the intermembrane space; this site, designated Q_o, is positioned between the high and low

potential chains in a manner such that when the quinol is oxidized to remove two electrons, the first electron is transferred to the iron sulfur protein (known as the ISP or the [2Fe2S] cluster in the literature for its atomic composition) of the high potential chain. Tracking that electron, the ISP is thought to then conformationally rotate to bring the FeS redox center into the proximity of the c-type heme c_1. This facilitates a redox equilibration with heme c_1 until the mobile shuttle cytochrome c arrives in its oxidized form to accept the electron and proceed to cytochrome oxidase (40-46). Meanwhile, the electron taking the route of the low potential chain passes through heme b_L to reduce heme b_H. Subsequent interaction with either a quinone or semiquinone at the Q_i site, as shown in Figure 2.2-4 (grey ribbon marked by anticmycin in green), is believed to conserve the electrogenic partition to the proton motive force and regenerate the quinol substrate. This process is commonly termed the Q-cycle as first named and proposed by Peter Mitchell, a long theorized and generally accepted mechanism in the field even before X-ray crystallographic studies were conducted to further support its existence from a structural standpoint. This bifurcated transfer of electrons and the cycling of quinol, semiquinone, and quinone forms of the substrate are coupled to the abstraction of cytosolic protons proximal to the Q_i site. For their respective roles in proton pumping, in fact, Mitchell coined the designation of the two sites Q_o and Q_i in reference to the proton pumping "out" and "in," respectively. Overall, the enzyme functions to convert the free energy of redox reactions into the chemically useful form of a proton motive force back across the membrane that generates ATP via ATP synthase. From a stoichiometric evaluation, this concerted activity involves the successful oxidation of one quinol to pump four protons to the intermembrane space of the mitochondrion against the concentration gradient -- from low $[H^+]$ to high $[H^+]$-- while the

electrons are efficiently passed to cytochrome oxidase via cytochrome c. The subsequent fate of these electrons will be discussed in Chapter 3 (4).

Despite prokaryotes having no mitochondria, the function of cytochrome bc_1 is quite similar to that of eukaryotes, with the exception that the enzyme is situated in the external cell membrane. Figure 2.2-5 serves as a visual of cytochrome bc_1 and its relationship to the photosynthetic reaction center for such organisms. Rather than Complex I, the large photosynthetic center P870 acts as the source of electrons to reduce quinone, thus maintaining a sufficient quinol pool for bc_1. Light of sufficient excitation wavelength absorbed by the photosynthetic center triggers the elevation of electrons to an excited state, denoted as P870*, drastically changing the redox potential of P870 from +.5V to -.9V -- a difference of ~ -1.4V (see Figure 2.2-6). The electron is transferred through a series of redox centers towards the cytosol of the bacterium, where they are transferred to oxidized quinone to produce quinol. Protons are drawn from the cytosol into the interstital space in the bilayer in order to facilitate the production of the quinol substrate. Similar to eukaryotic bc_1, prokarytic bc_1 functions to oxidize the quinol substrate; this process uses heme c_1, the [2Fe-S] ISP cluster and its seminal rotational mechanism, and the b hemes as previously described in full detail in Section 2.2. By extracting electrons from quinol, protons are similarly liberated and pumped back to the extracellular periplasmic space. As discussed, the ATP synthase enzyme utilizes this established electrochemical gradient to allow protons to flow to the interior space of the membrane in archetypical fashion. This results in the phosphorylation of ADP to form ATP for the bacteria's energy needs. Cytochrome c2 acts to replace donated electrons to P870 by recycling the electrons from bc_1, wherein the cycle can begin anew. For the purposes of this study, and given the

ubiquitous role of bc_1 in the simplest to the most complex organisms, we seek to gain insight into the inner workings of bc_1 for *Rhodobacter capsulatus* (*R. cap)* for comparison to previously characterized Rhodobacter sphaeroides (*R. sph*). By extension, we seek to use these assessments at the prokaryotic level to hypothesize of the enzyme for other species.

A basic question that might be formulated from the initial introduction to this theoretical mechanism is: What does the additional complexity of this bifurcation accomplish? After all, it would be much more simple, and thus far less expensive from the metabolic investment standpoint, to have a single redox center-containing protein for the electrons to traverse en route to cytochrome c, rather than taking on the additional costs of constructing a larger protein with multiple redox centers. In fact, cytochrome c in itself has a single redox center and has been proven to be very successful and efficient in electron transfer -- why not, perhaps, employ a similarly small, simple protein to act as the intermediate between Complexes I and III? The answer to this and related questions can be answered by acknowledgement of at least two different factors, wherein the complexity and investment can be argued to yield worthwhile dividends. First, it is feasible that electron transfer could proceed even if a non-bifurcated pathway was in place, given a suitable redox-mediating entity in place of bc_1 and provided that Marcus Theory constraints of driving force and reorganization were met. However, the electron transfer would not yield the concomitant mobilization of protons across the membrane, which is the seminal goal of the entire electron transport chain. In such a hypothetical case, sacrificing the contribution of bc_1 to the electromotive proton gradient would result in fewer protons being actively transported across the membrane against the concentration gradient, resulting in decreased ATP production per glucose molecule. Similar to an overall

comparison of the relative complexities of prokaryotes and eukaryotes, evolution has favored the additional systemic complexity and costs for the sake of greater net gains and efficiency. To do so, the electron in the low potential chain is the electrical impetus for the proton uptake from the cytosol into the cycle, such that even though it is not directed downstream to cytochrome c and on towards cytochrome oxidase, its emergence at the Q_i site to be recycled back to reduce a quinone or semiquinone is just as important as the role of the electron taking the high potential chain. Secondly, employment of a single redox center or pathway in place of bc_1 would extract only one electron at a time. Since each quinol (QH_2) delivers two electrons to Complex II, in the timeframe of turnover for such an enzyme to return to a suitably oxidized state in order to receive the second electron, a highly reactive semiquinone (SQ) radical would persist. Thus, for the purposes of efficiency and such as to minimize the existence of the radical SQ and its potentially deleterious side reactions, the complexity of bc_1 and bifurcation has considerable merit over hypothetical alternatives.

Mitchell recognized that in his proposed Q-cycle some level of redox control must be present in order to suppress side reactions, such as those that occur as a function of oxygen radicals or the delivery of electrons along the same chain. The necessity of the existence of such stringent control mechanisms has led to much debate on theoretical models proposed to account for the enzyme's efficiency and/or the general missive to avoid problematic side reactions from radical formation in the process. The difficulty of elucidating the intricate redox exchanges occurring within this single enzyme with multiple active components has yielded several variants on the Q-cycle model (4). It has been suggested that the various kinetic methodologies used to study cytochrome bc_1 are at least partly responsible for the

lack of consensus in conclusions that are drawn from the various and somewhat conflicting results of studies. One at-large problem is the fact that many interactions occurring in the enzyme are "hidden," as kinetics experiments measure the slowest, rate-limiting step and mask faster events taking place in the mechanism (23).

Though many challenges exist in the study of bc_1, much progress has been made by using inhibitors of bc_1 to modulate the kinetic activity of the enzyme. These inhibitors fall into two separate clases: P_m-type (myxathiazol, azo-oxystrobin, and MOAS/methoxyacrylate compounds) and P_f-type (famoxadone, JG-144, stigmatellin). These denotations refer to whether, upon binding, they tend to mobilize (P_m) or fix (P_f) the ISP. X-ray crystallographic studies from the late 1990's have shown that the presence of such inhibitors in the Q_o pocket changes the orientation of the ISP. For example, when P_m-type myxathiozol is bound, the inhibitor appears to bind closer to heme b_L and, notably, without any bonding contact with the ISP. This serves to separate, or block, the ISP from the low potential b heme proximity to yield a more mobile, disordered state that cannot be detected in the crystal. When P_f-type stigmatellin is bound, in contrast, the ISP is oriented towards the b subunit, where a ligand of the [2Fe2S] cluster, His^{161}, and a carbonyl group of the inhibitor form a hydrogen bond. Thus, the ISP is stabilized at the b position, and is hence considered fixed. These structural studies suggest that the ISP is a mobile shuttle, which first binds nearer the b-heme to accept an electron from quinol. Subsequent rotation of the ISP towards heme c_1 results in ISP oxidation in the high potential chain previously discussed. Mutational, cross-linking, and EPR studies have corroborated the mobility of the ISP and this mechanism. The controlled motion of the ISP domain has been proposed to be a possible gating mechanism to prevent deleterious side reactions and retain proper

electron direction within and through the enzyme. Rapid kinetics studies of *Paracoccus denitrificans* bc_1 by Havens *et al.* show significantly increased rates of electron transfer from the ISP to heme c_1 for P_m inhibitors, as monitored at 552nm using the same method and conditions employed in this study. P_f inhibitors, on the other hand, have been shown to slow the rate of electron transfer between the redox centers to 20-25% of the rate of the uninhibited enzyme. These results, taken together with crystallographic studies and EPR results from multiple groups, strongly suggest that the conformations of the Q_o site, the ISP binding crater, and the orientation of the ISP are closely linked together (47).

It would thus seem that the path and mechanism of the high potential chain is relatively well understood, and the rate-limiting step of electron transfer, the ISP rotation, is a generally accepted feature of cytochrome bc_1. It is safe to say that many of the details and mechanistic features of the low potential chain, however, are still topics in an ongoing, spirited debate. There is mounting evidence for a functional role of cytochrome bc_1 as a dimer, rather than just a structural feature. The bulk of the current debate in recent years has to do with whether or not intermonomer electron transfer occurs across the dimeric interface. Structural evidence suggests that the distance between the dimers is too great for catalytically relevant electron transfer in the micro- to millisecond timeframe to occur, but for one exception. At a bridge formed by the two hemes b_L in the center of the dimer, the distance tapers to 14 Å, which is just at the limit of distances between redox centers that can reasonably facilitate catalytically relevant electron transfer (48).

In February 2013, Anthony Crofts reviewed the mechanism of bc_1 electron transfer, a review in which many of the early efforts that sought to prove or support the existence of intermonomer electron transfer were considered unsubstantiated for essentially a single

reason: genetic crossover. These studies that were maligned by Crofts hinged on the premise of knocking out the Q_o site of one monomer in addition to deactivating the Q_i site of the other monomer, in turn yielding a heterodimeric mutant that must transfer electrons across the dimer in diagonal fashion. The crossover argument originated from the experimental experiences of the Croft group, which indicated that strains designed to force intermonomer electron transfer essentially showed the same kinetics as wild type enzyme. Upon follow-up investigation, it appeared that the active colonies had reconstructed the wild-type monomers via crossover recombination of the unmodified portions of the plasmid construct to recreate either the fully functional homodimer, or heterodimers with at least one completely functional monomer. Thus, their attempt to create a mutant designed to enforce intermonomer electron transfer was unsuccessful, a result that led to the conclusion that intermonomer-limited mutants could simply not compete under photosynthetic conditions with strains that had functional monomers (49). Prior to the Crofts review, Swierczek *et al.* reported that the "electronic bus bar" across the dimer in the double knockout intermonomer interaction mutant yielded activity of ~17% of wild type; however, doubt was cast on this result due to the reasonable possibility for recombination (50). From Crofts' perspective, it was arguable that what activity existed could be from a fraction of the protein population with wild-type reconstructs (49). Other researchers performing similar types of work through 2012 were similarly challenged on this basis. It was apparent that in order for the field to advance on this issue, a way to cross-link or otherwise produce and purify these informative constructs with high fidelity was necessary.

While many of the details about the nature of bc_1 have been elucidated, important questions remain about the interaction of the b-hemes and the possibility of intermonomer electron transfer. Figure 2.2-7 shows a skeletal view of cytochrome bc_1 to address the important redox centers and the distances between them, emphasizing the proximity of heme b_L groups where intermonomeric electron transfer is theorized to take place. As challenges to data indicating intermonomer electron transfer were largely driven by an argument based on recombination, in 2013 the Osyczka group published evidence using a technique designed to circumvent the prospect of recombination. This generated some very compelling data that seems to support the theory of intermonomer electron transfer across the dimeric interface. This methodology used to obtain these results involved covalently fusing two different monomers together at the b heme position: a b subunit from *Rhodobacter capsulatus* and a b subunit from *Rhodobacter sphaeroides*, both containing *R.cap* FeS and c_1 components. The engineered plasmid -- in which two cytochrome b subunits are replaced with a single fused hybrid of the two b subunits, one from each species -- is remarkable. In comparison to the group's previous studies, this system provides the unique advantage of safeguarding against genetic recombination to maintain the desired constructs on the genetic level. The 17.6% difference between the two encoded base pairs on the plasmid is sufficient difference to lower the frequency of recombination, while the 90% similarity, based on primary amino acid sequence, means that the fusion protein functions comparable to wild type. Strep-tag affinity is employed for purification, with Western blotting used to confirm presence of the Strep tag and thus the fusion protein of the correct size: two times larger than cytochrome b in the membranes. This fairly exotic system was further manipulated to include mutations G158W, H198N, and H212N as

knockout points of Q_o and Q_i sites. The authors cite relevant intermonomer electron transfer across the dimer from one b_L to another as indicated on a 50ms timescale. Controls of double Q_o and double Q_i mutants showed no electron transfer, such as might be expected. The results are the most recent from this group to have been published and strongly indicate that intermonomer electron transfer does appear to occur (48). With regards to *R. cap* bc_1, the research group of Fevzi Daldal has contributed a great deal to the understanding of this complex protein. In their 2013 article, Lanciano *et al.* discuss the formulation and kinetic studies of heterodimeric protein that has been designed to force intermonomer transfer. The use of a two-plasmid system is employed, yielding a mixture of proteins that are further separated using affinity tags in sequence. This provides the additional advantage of yielding both hetero- and homodimeric constructs from a single flask. The use of two plasmids does not necessarily prevent the reversion of the proteins to wild type form in a genetic crossover, but the use of the affinity tags is employed to discern between the various dimer populations produced and separate them accordingly. Once the dimers are assembled, they retain their orientation. Mass spectrometry was employed to probe marker peptides to verify presence of the affinity tags and mutant. Similar to the Osyczka group's findings, Lanciano *et al.* report significant cytochromes (c + heme c_1) reduction as measured at 550nm, indicating a functional ISP. More importantly, with regard to the issue of intermonomer electron transfer, the 560nm signal visibly shows the initial reduction of the b hemes followed by their slow oxidation as electrons traverse the low potential chain.

Once the proteins are produced, both the Osyczka and Daldal groups use comparable systems and conditions to measure the rates of electron transfer in their

proteins. The use of chromatophores containing photosynthetic reaction centers has its advantages, but the resolution and quantification of fast phase electron transfer is not one of them. Detection in this type of system is to a large extent rate-limited by diffusion of cytochrome c to heme c_1, while the rate-limiting step in the protein has been shown to actually be rotation of the ISP. Thus, the true rate of electron transfer cannot be determined using this type of system. Per Marcus Theory, the transfer of electrons is instantaneous once reorganizational energy constraints are met and the geometries of the redox centers are sufficiently oriented for the transfer event. Evolutionarily, the electron transport chain has been honed by time and selection to minimize the reorganizational component to create a masterpiece of speed and efficiency, catalyzing reactions on the micro- to millisecond timescale. However, the use of chromatophores yields information in the 100-200ms timescale at best, meaning that the actual electron transfer event is missed and one is simply observing the state of system components afterwards. The use of photoreaction centers has undoubtedly been proven to be capable of yielding important information, yet we have the unique advantage of supplementing their data with our own in order to quantify true rates of transfer associated with the enzyme. In order to achieve this, the methods of fast phase electron transfer employed by the Millett/Durham group significantly diverge from the use of chromatophores, as described in Chapter 1.

Figure 2.2-1 Structure and orientation of the bc_1 dimer in the membrane bilayer, with symmetrical sites indicated along with Q_o and Q_i substrate processing sites (51).

Cytochrome bc_1 exists as a dimer in the native state

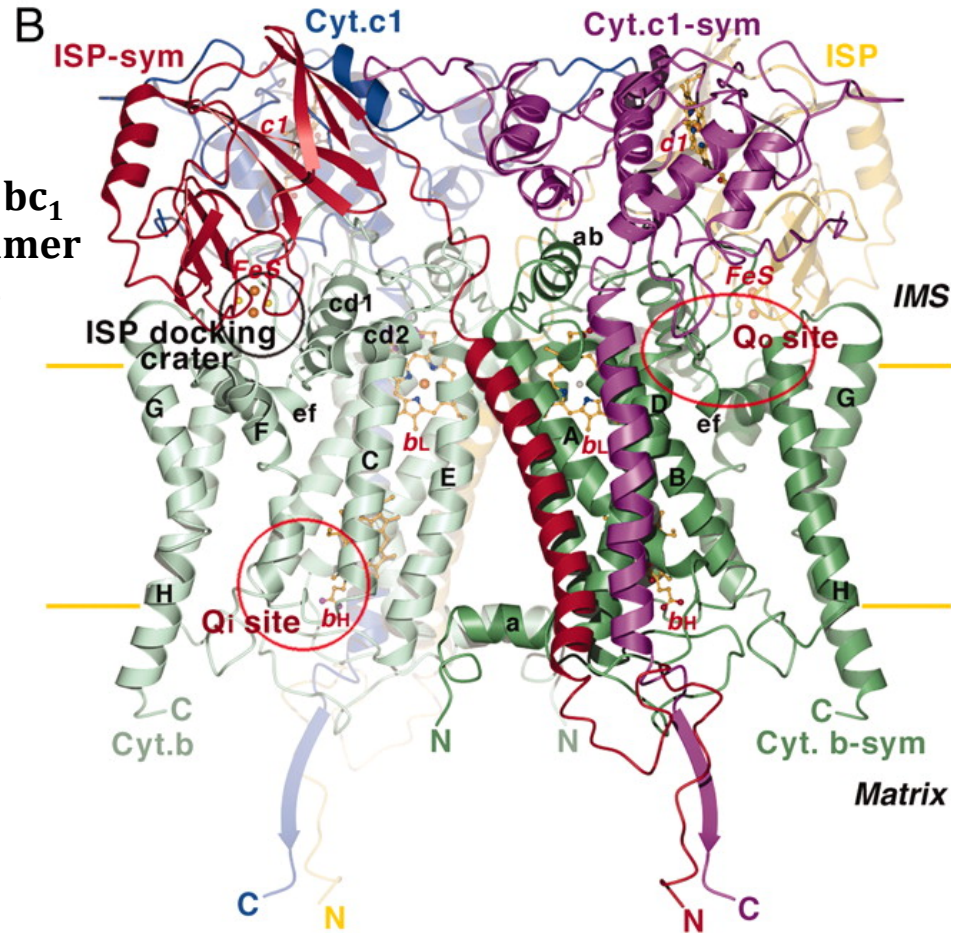

Figure 2.2-2 Comparison of crystal structures of prokaryotic vs. eukaryotic cytochrome bc_1 (35)

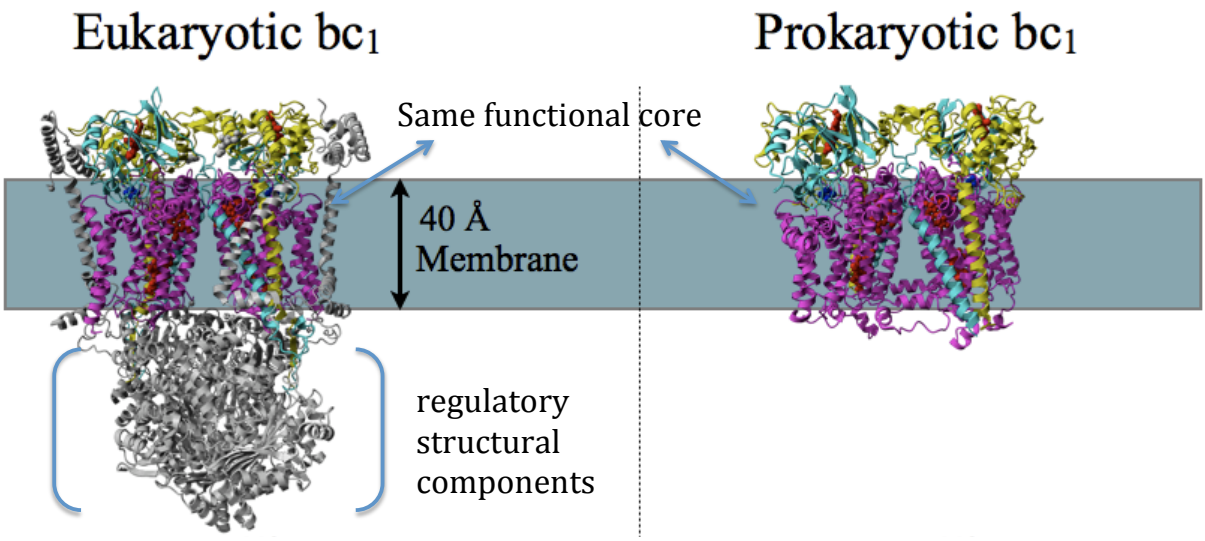

Figure 2.2-3 The Q-cycle as originally proposed by Peter Mitchell (top), and a schematic of the currently accepted consensus of the Q-cycle as supported by crystal structure evidence (bottom) (35).

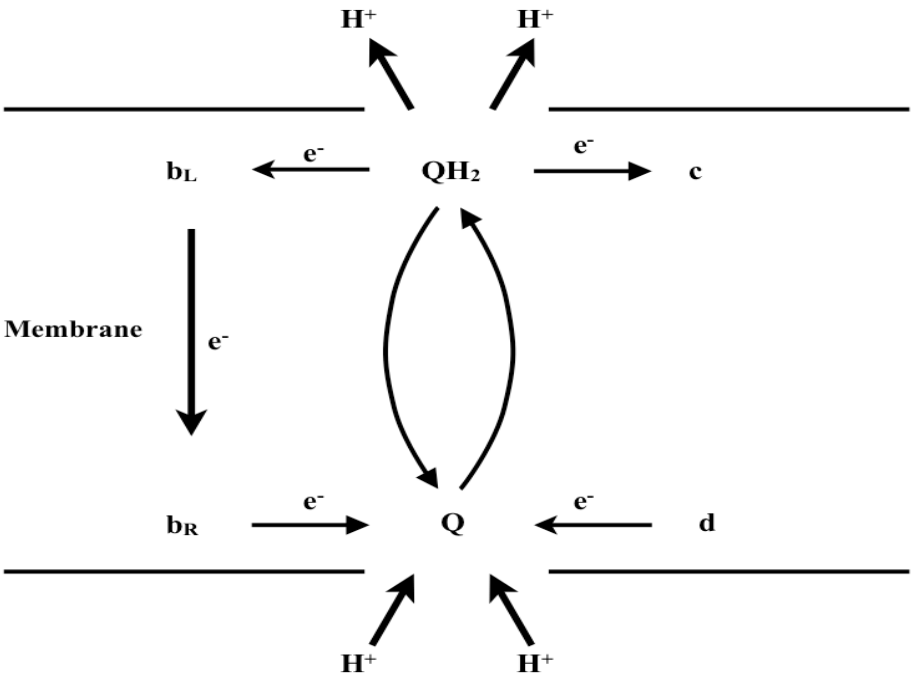

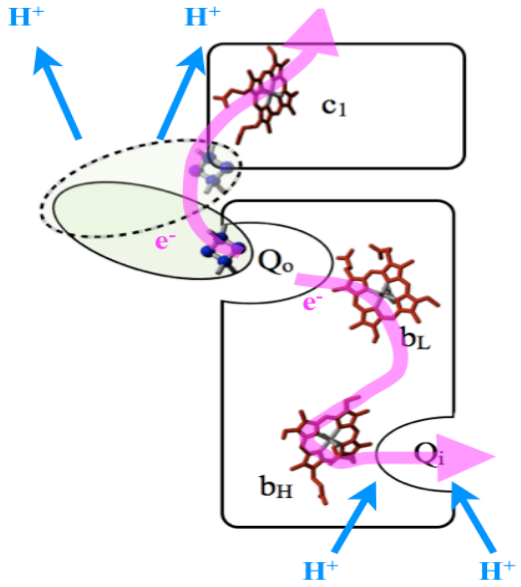

Figure 2.2-4 Ribbon diagram of cytochrome bc_1 in two different conformational states. These are defined by the orientation of the FeS cluster (dark blue) in its rotational state. In its b-state, the FeS is closest to the b hemes (grey ribbon with heme colored red). In the c_1 state, the reduced FeS is oriented towards the heme c_1 group (green ribbon, with heme c_1 in red) to facilitate electron transfer. While in the b-conformation, stigmatellin (cyan) binds at the Q_o site, while antimycin (green) binds at the Q_i site.

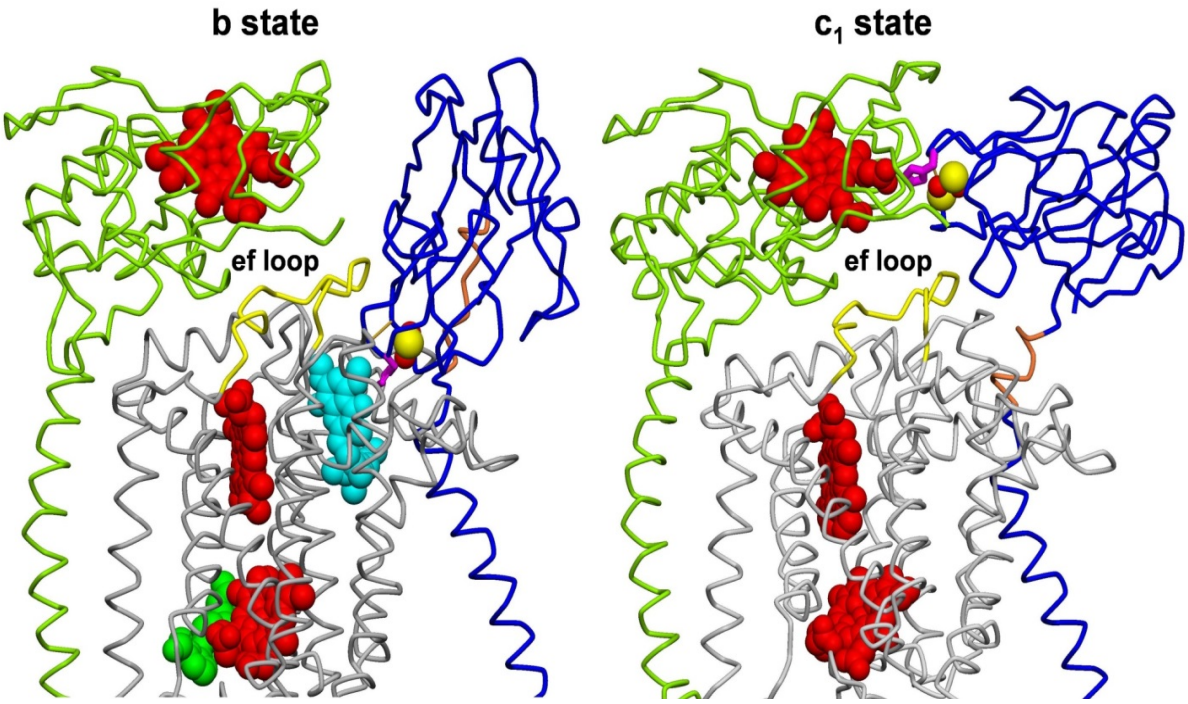

Figure 2.2-5 Schematic depicting the relationship of bc_1 to the photosynthetic center in photosynthetic *Rhodobacter sphaeroides*. Key similarities include the rotation of the ISP and homology of the enzyme as compared to eukaryotes.

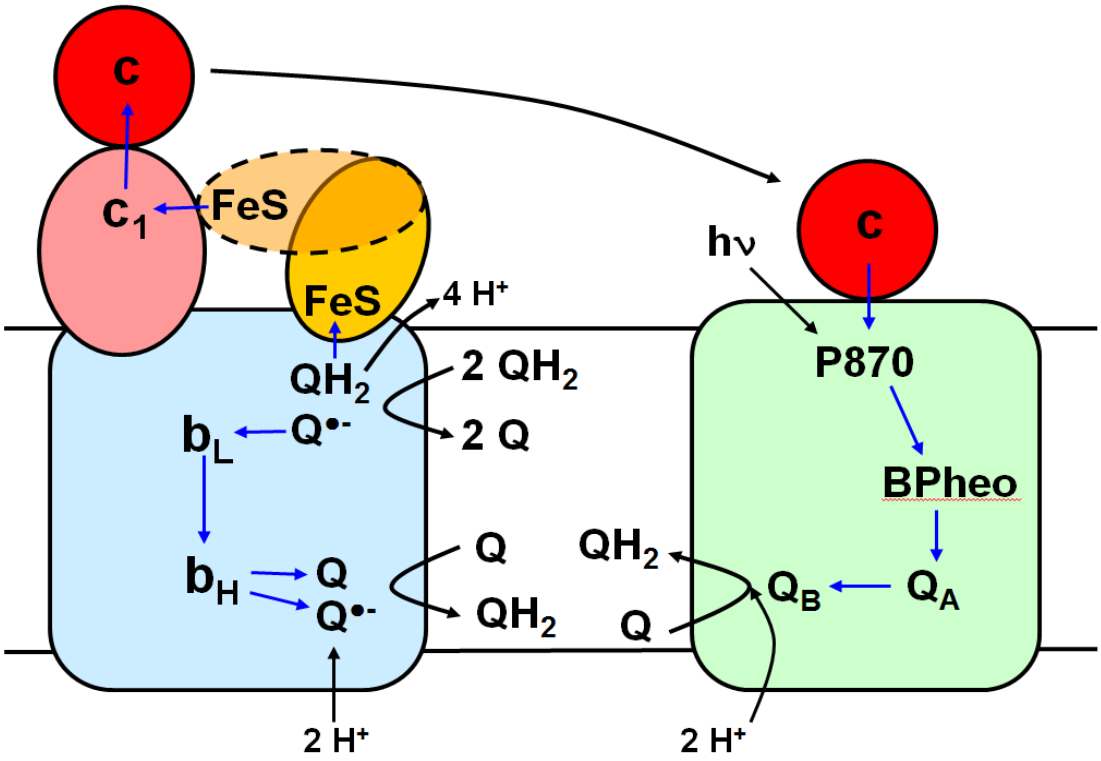

Figure 2.2-6 Redox potentials involved in photoexcitation of P870 and the subsequent electron transfers through the photosynthetic reaction center to drive reduction of quinone to quinol.

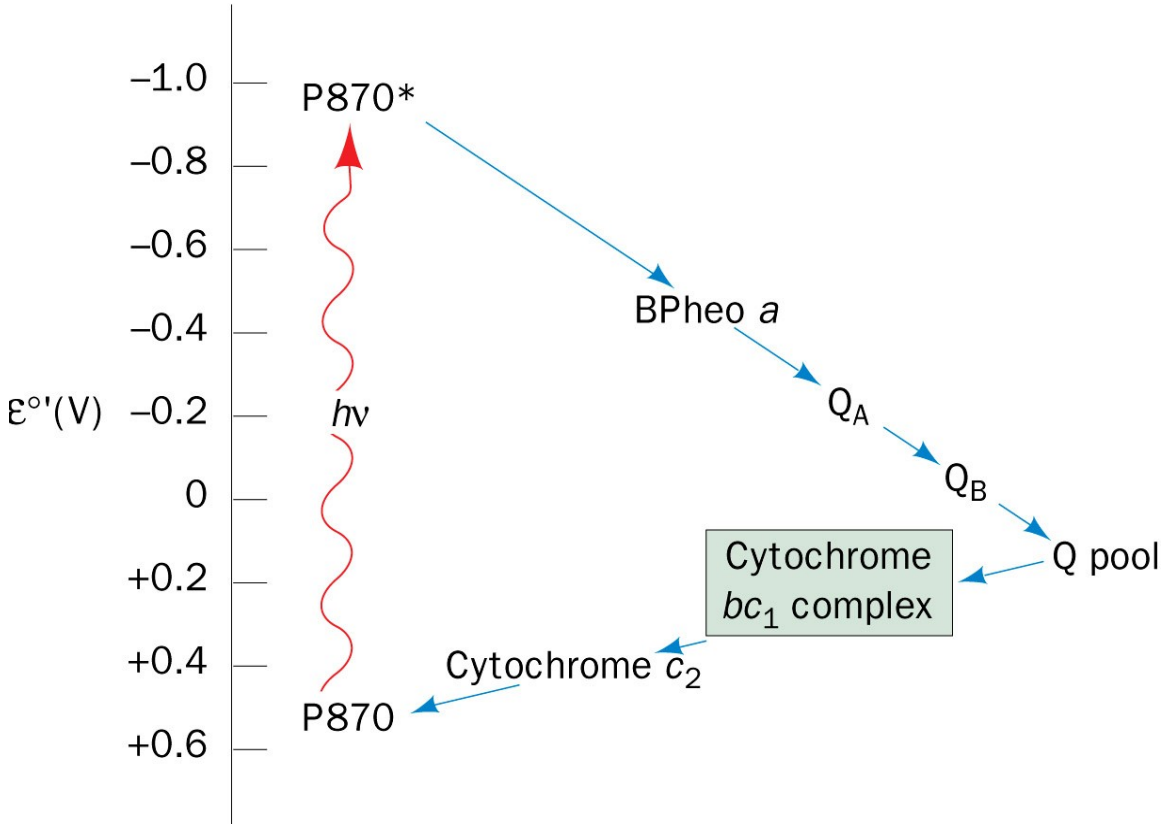

Figure 2.2-7 Figure indicating redox potentials and distances found in cytochrome bc_1. Intermonomeric ET across dimer of bc_1 is theorized to take place across the heme b_L redox centers (51).

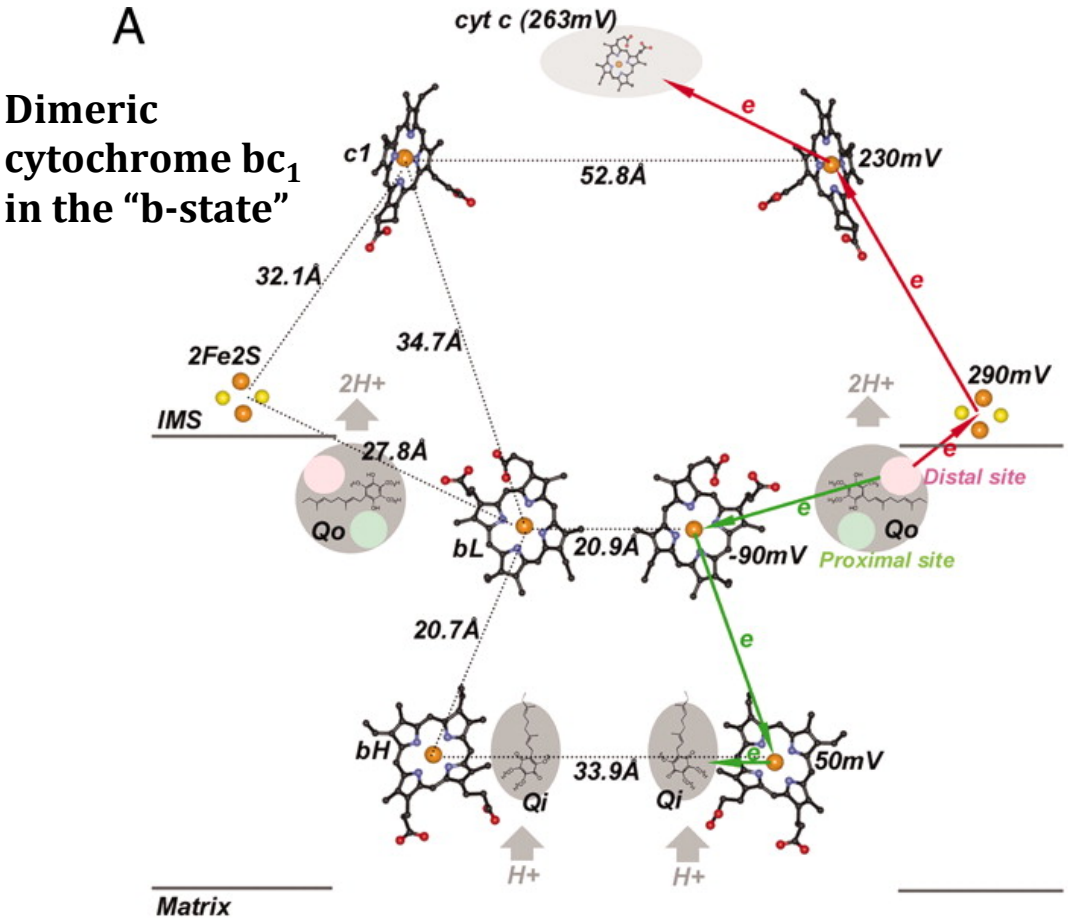

2.3 Flash initiation of redox events within cytochrome bc_1

Throughout the experiments described in this section, flash initiated redox events within cytochrome bc_1 are initiated as shown in Figure 2.3-1 (top). In this method, Ru_2D seres as a cytochrome c surrogate to rapidly oxidize the ferrous c_1 subunit of cytochrome bc_1. From a spectral standpoint, this phase is indicated b a rapid decrease in the absorbance of the sample at 552nm, which indicates oxidation of the heme redox center. After this flash oxidation, the experimental pathway then tracks the increase in absorbance at 552nm as heme c_1 is re-reduced, which corresponds to the electron transfer from the pre-reduced ISP to the heme c_1 subunit. For *Rhodobacter sphaeroides*, this phase has been reported to be 80,000 s^{-1}, a value which serves as a point of comparison in the current studies regarding similar species *Rhodobacter capsulatus.* Upon oxidation, the mobile ISP is capable to move towards the Q_o site to oxidize the quinol substrate. The ISP is itself re-reduced in this process, which can be monitored via the slower phase in the 552nm transients. Further evidence of bifurcated turnover at the Q_o site can be monitored at an isosbestic point for heme c_1 at the 560nm wavelength, where the redox status of the heme c_1 component of the system is eliminated from consideration. Therefore, any observed changes in the spectrum at this wavelength correspond specifically to changes in the redox state of the b hemes associated with the low-potential chain. The reduction of the b-hemes, as monitored at the 560nm wavelength, thus correlate to the rates of the slower phase re-reduction of the ISP as monitored at 552nm. The details of these spectral relationships have been firmly established by several prior studies for the purpose of examining the internal kinetics of cytochrome bc_1.

In the current experiments, initial conditions deviate from those in prior studies due to the redox state of the low potential chain prior to flash. Specifically, these experiments are conducted under conditions favoring reduction of the b hemes across the population of bc_1 macromolecules prior to the flash initialization. It was noted that there is likely an equilibration of redox states across the b-hemes. As described in subsequent sections, this was achieved via maintaining anaerobic conditions and providing ample reduced substrate. It was noted that even under these conditions, the extent of re-oxidation of hemes b does not return to the pre-flash baseline. Accounting for the extinction coefficient of heme b_H at 560nm and heme c_1 at 552nm, two equivalents of heme b_H are observed to be oxidized following a single turnover at the Q_o site.

Using *R. cap* cytochrome bc_1 constructs provided from the group of Fevzi Daldal, the experiments below were designed to determine important, novel rate information for the bc_1 enzyme for the species. In addition, the experiments were performed to provide insight into the possibility of intramonomer electron transfer.

Figure 2.3-1 Schematic of inorganic complex Ru_2D being employed as a cytochrome c analog, serving to oxidize the c_1 subunit upon laser flash initiation and providing information about the internal kinetics of the enzyme (top). Alternatively, ruthenium complexes covalently attached to cytochrome c can, upon laser flash photolysis, oxidize cytochrome c to create an analogous electron transfer cascade (bottom).

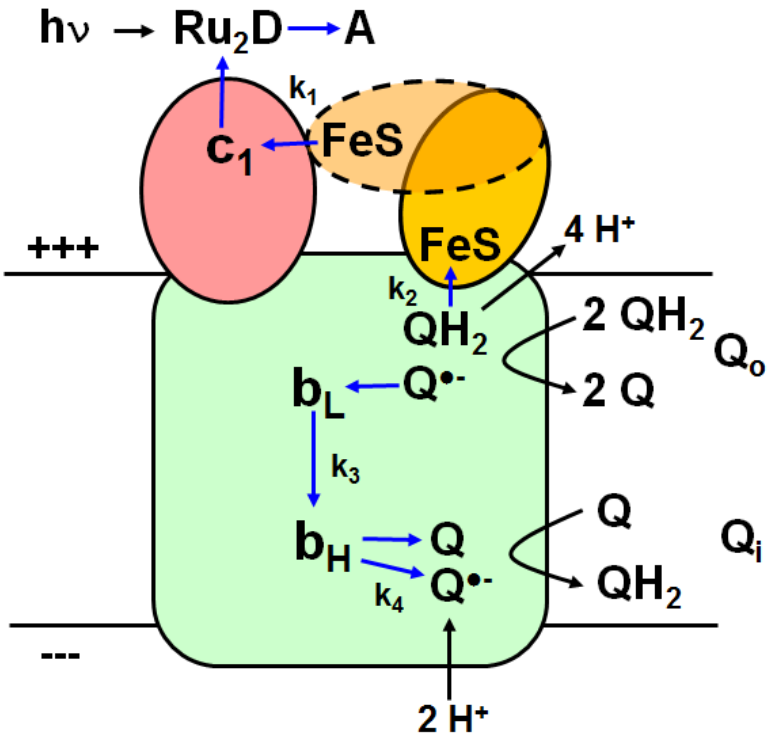

2.4 Materials and methods

As mentioned, we employ an alternative technique to examine cytochrome bc_1 to characterize fast-phase kinetics using laser flash photolysis. Using the binuclear ruthenium complex Ru_2D and laser flash excitation, we photooxidize heme c_1 to initiate a cascade of electron transfers. Prior to this event, quite simply, the system is poised in a mostly reduced state; the b-hemes typically just equilibrate to a partially reduced state, based on the UV-Vis analysis at 560nm where their characteristic absorbance can be monitored. This reduced state is facilitated by the use of one of two reducing systems: ascorbate with TMPD as redox mediator, or the enzyme succinate dehydrogenase/succinate combination. The protein is ~5uM in 300uL volume, anaerobic as degassed by N_2 in a sealed cuvette with septum. The ISP is pre-reduced via decylubiquinol in solution, which is added as an analog of the native substrate quinol. Lauryl maltoside at .01-.02% simulates a membrane-like environment to stabilize the protein in our typical choice of buffer: 20mM Tris-HCl buffer at pH=8.0, along with sacrificial oxidant cobaltpentaamine chloride -- $[Co(NH_3)_5Cl]Cl_2$. Unlike for some ruthenium complexes, which are covalently attached to the protein, the Ru_2D is dispersed freely in the solution. Upon flashing, the Ru_2D is oxidized and draws the electron from heme c_1; the ISP is then able to interact with and reduce heme c_1, which we track by monitoring the 552nm transient as it is re-reduced by the ISP. Similarly, we perform analysis at 560nm to track the low potential chain of the b-hemes, which gradually become more reduced relative to their starting pre-flash equilibrated, primarily oxidized state, as electrons pass through that fork of the bifurcated pathway.

The following section is a summary of the experiments completed on the *Rhodobacter capsulatus* enzyme cytochrome bc1 as analyzed via laser flash photolysis. All

reactions were conducted with 4-6uM enzyme with 20uM Ru_2D in 20mM Tris-HCl buffer at pH=8.0 with .01% lauryl maltoside. 5mM cobalt pentaamine chloride, $[Co(NH_3)_5Cl]\ Cl_2$, was used as a sacrificial oxidant for the system. In order to poise the system in a reduced state prior to flash, succinate dehydrogenase was used along with its native substrate succinate in most of the experiments, as indicated for each experiment below by [SCR/succinate] for concision. However, the combination of ascorbate and the redox mediator TMPD was used in some experiments; these experiments are indicated with [TMPD/ascorbate]. Quinol substrate was added in the form of decylubiquinone (DBQ) at 80-100uM. The addition of inhibitors was typically in the range of 10-25uM, depending on the inhibitor and observed efficacy.

2.5 Results:

The first experiments were designed to study the wild-type *R. cap.* bc1 to assess the native rates of electron transfer from the FeS cluster to heme c_1, and the internal electron transfer of the b-hemes. Figure 2.5-1A shows a rate constant k = 14,000 s^{-1} for the enzyme as measured at the 552nm wavelenght. Occurring in the absence of native or added ubiquinol, using TMPD/ascorbate as the reducing system, this indicates the rate of electron transfer through the high potential chain, the electronic pathway as the electron is transferred from the [FeS] cluster to heme c_1. Figure 2.5-1B shows the 559nm transient for this sample of enzyme on the same timescale, which showed no discernable b-heme reduction over the course of the same experiment. This indicates a vacant Q pocket and resultant lack of low-potential chain electron transfer. Measured rates are understood to be purely monoexponential in nature, and the mathematical fits reflect this by disregarding the possibility of enzymatic turnover and its associated rate constant k_2.

Figure 2.5-2 shows the effect of 50μM P_f-type inhibitor famoxadone, with rate constant k_1 of electron transfer from the ISP to heme c_1 reduced with k = 5000 s^{-1}. The physical effect(s) of inhibitor binding at Q_o reduce rate of electron transfer to 36% that of uninhibited sample at 10:1 ratio (inhibitor:protein). No significant effect was observed on signal amplitude as compared to uninhibited enzyme. Additional famoxadone, raised two-fold to 100μM in sample, did not yield any additional effect on the measured rate constant.

In order to assess the effect of added substrate DBQ to an otherwise quinol deficient sample, additional experiments were performed using (succinate/SCR) as the reducing system. Prior to addition of DBQ, no measurable electron transfer was observed at either the 552nm or 560nm wavelengths. Addition of 100μM DBQ resulted in the evolution of

strong signal, yielding rate constants k_1 = 5000 s^{-1}, and k_2 = 1500 s^{-1} as shown in Figure 2.5-3 at the 552nm wavelength (Figure 2.5-3). With the decylubiquinol present, the rate constant of electron transfer through the low potential chain was measured to be 1500 s^{-1}, a value similar to that of k_2 measured at 552nm (Figure 2.5-4).

To assess the effect of the potent P_f - type inhibitor stigmatellin, a sample was separately prepared to consist of 4μM cyt bc_1 in a 300 μL solution of 20 mM Tris-HCl, pH 8.0, 20 μM Ru_2D, 5 mM $[Co(NH_3)_5Cl]^{2+}$, 100 μM decylubiquinol, 2 mM succinate, 50 nM SCR, 4 μM TMPD, and 1 mM ascorbate. The 552 nm transient is shown as Figure 2.5-5. This sample was in what would be described as a maximally reduced state, using both the SCR/succinate and the TMPD/ascorbate reducing systems. Uninhibited sample performed consistent with Figure 2.5-3; however, stigmatellin virtually slowed the rate of electron transfer to neglible levels.

Additional mutants were provided by the Daldal lab, which incorporated the addition of 1 (Ala+1) or 2 (Ala+2) alanine residues inserted into the neck region near the ISP. The presence of additional amino acid residues in this region changes the orientation of the ISP. For the Ala+1 mutant, this results in a reduced rate of electron transfer with a value of ~700 s^{-1}. This is shown with the 552nm transient in Figure 2.5-6A, while Figure 2.5-6B shows a concomitant rate of electron transfer to the b-hemes as monitored at 560nm, with a value of ~800 s^{-1}. The addition of a second adjacent alanine to create the Ala+2 neck mutant showed virtually no significant electron transfer on the timescales of the experiment (results not shown).

Figure 2.5-1 Flash initiated electron transfer within cyt bc_1 in absence of ubiquinol. Reaction conditions consist of 5 µM cyt bc_1 in a 300 µL solution of 20 mM TRIS-HCl, pH 8.0, 20 µM Ru_2D, 5 mM $[Co(NH_3)_5Cl]^{2+}$, 5 µM TMPD, 1 mM ascorbate. (A) The 552 nm transient shows the rapid oxidation of heme c_1 by Ru_2D, followed by re-reduction of heme c_1 by the ISP with a rate constant of 14,000 ± 2000 s^{-1}. (B) The 559 nm shows no discernable b-heme reduction, indicating a vacant Q_o site.

A

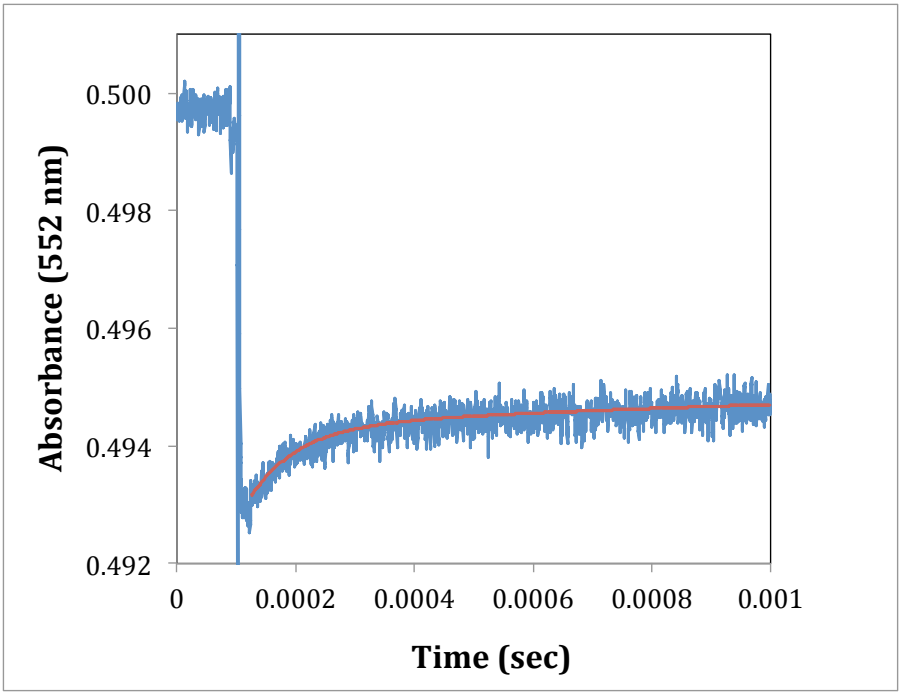

B

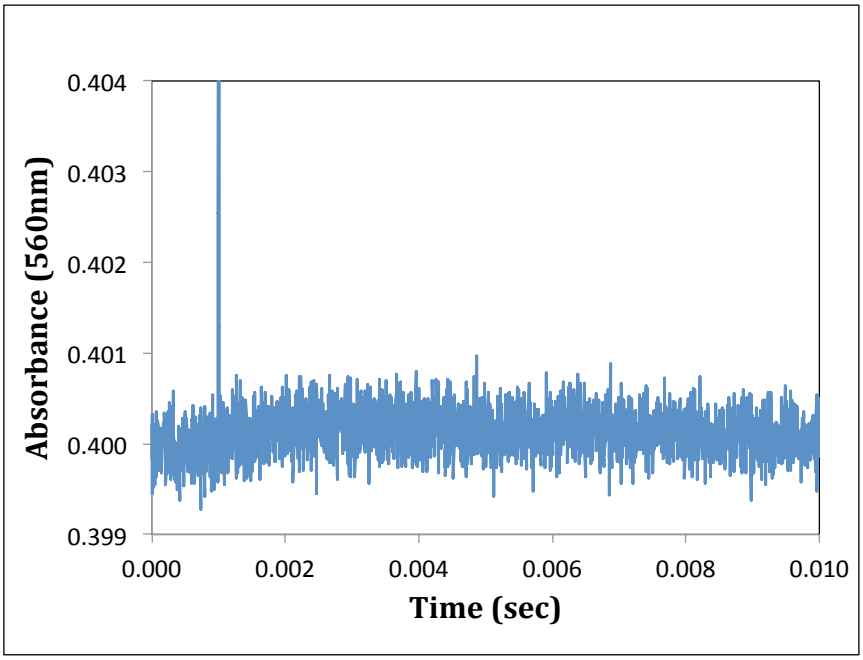

Figure 2.5-2 Effect of famoxadone on electron transfer in cyt bc_1. Reaction conditions consist of 5 μM cyt bc_1 in a 300 μL solution of 20 mM TRIS-HCl, pH 8.0, 20 μM Ru_2D, 5 mM $[Co(NH_3)_5Cl]^{2+}$, 5 μM TMPD, 1 mM ascorbate, as in Figure 2.5-1, except with addition of 50 μM famoxadone. The rate constant for electron transfer from ISP to heme c_1 is 5,000 ± 1000 s^{-1}.

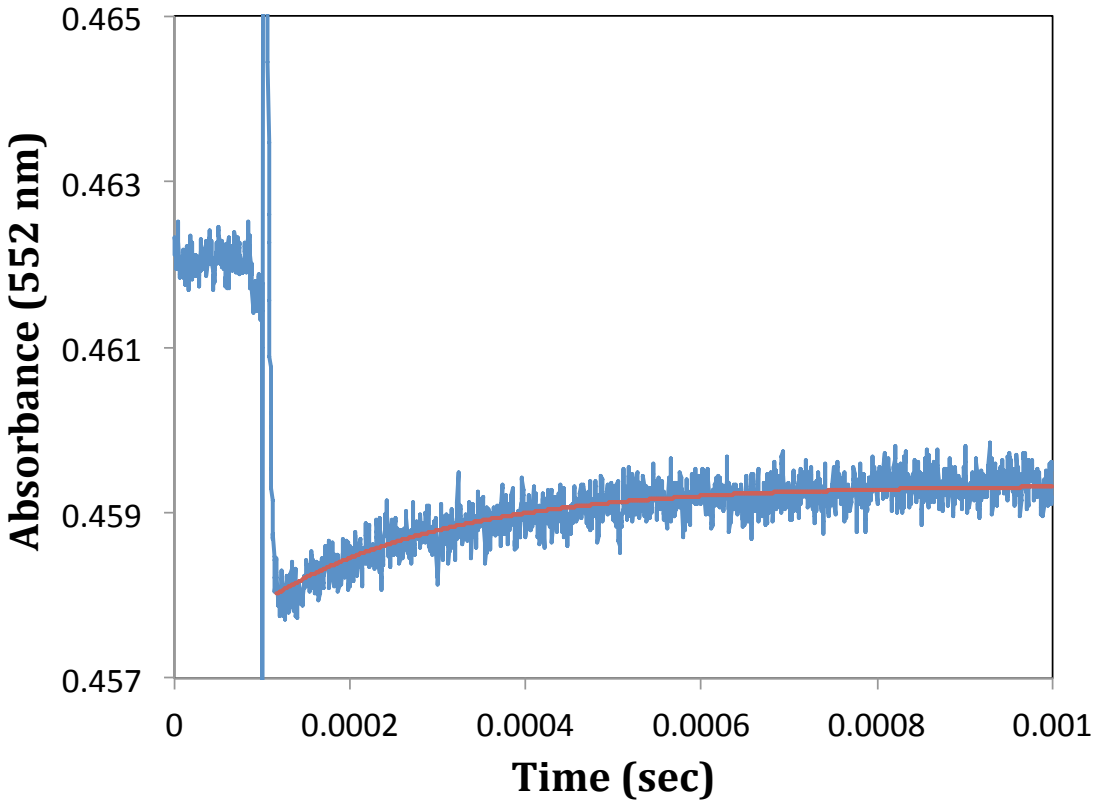

Figure 2.5-3 Effect of ubiquinol on electron transfer within cytochrome bc_1. Reaction conditions consist of 5 µM cyt bc_1 in a 300 µL solution of 20 mM TRIS-HCl, pH 8.0, 20 µM Ru_2D, 5 mM $[Co(NH_3)_5Cl]^{2+}$, 100 µM decylubiquinol , 2 mM succinate and 50 nM SCR. The 552 nm transient shows the rapid oxidation of heme c_1 by Ru_2D, followed by biphasic re-reduction of heme c_1 by the ISP with rate constants of 5,000 ± 1000 s^{-1}, and 1,500 ± 150 s^{-1}.

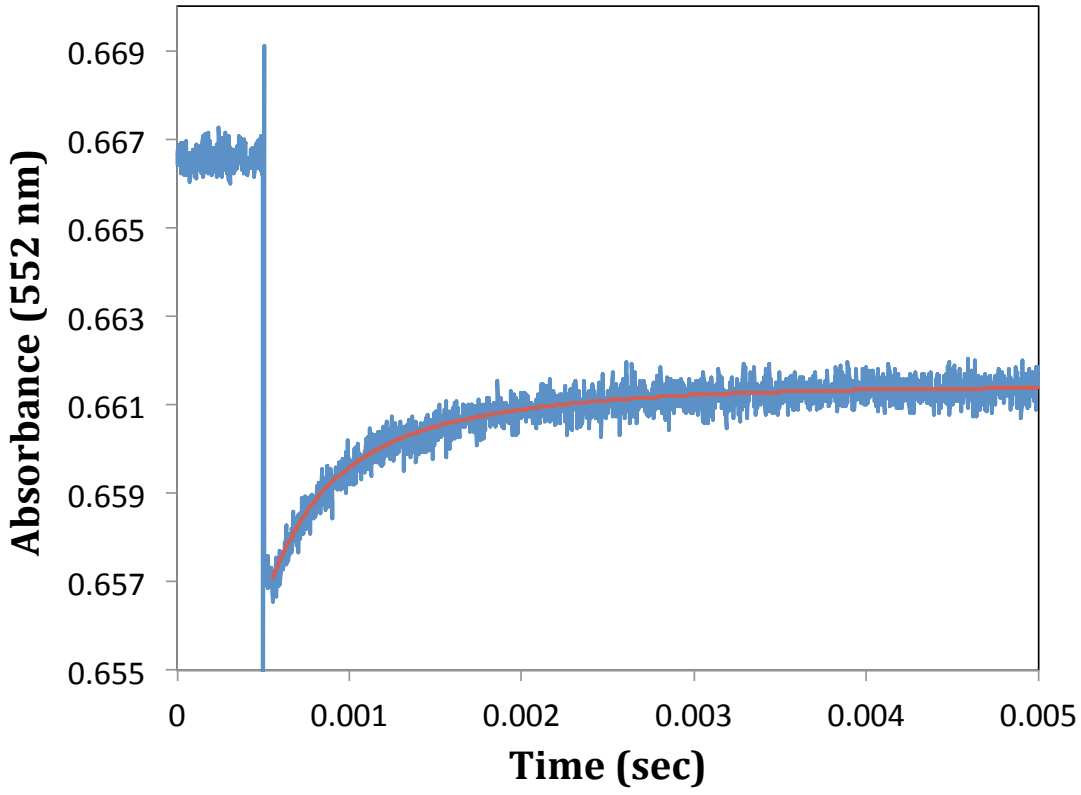

Figure 2.5-4 Same sample as in Figure 2.5-3, with reduction of cyt b_H monitored at 560 nm. The rate constant for reduction of cyt b_H is 1,500 ± 150 s^{-1}.

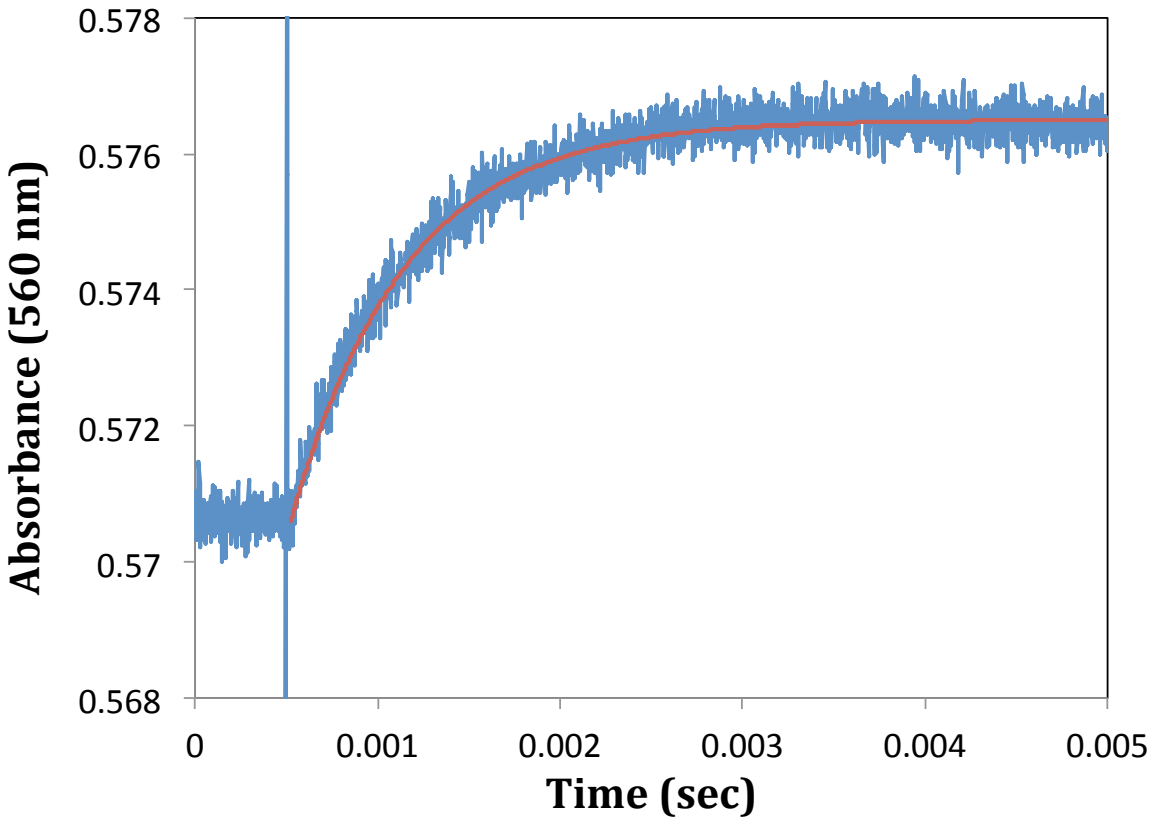

Figure 2.5-5 Effect of stigmatellin on electron transfer within cytochrome bc_1. Reaction conditions consist of 4μM cyt bc_1 in a 300 μL solution of 20 mM TRIS-HCl, pH 8.0, 20 μM Ru_2D, 5 mM $[Co(NH_3)_5Cl]^{2+}$, 100 μM decylubiquinol, 2 mM succinate, 50 nM SCR, 4 μM TMPD, and 1 mM ascorbate. (A) Uninhibited R. cap bc_1 shows electron transfer occurring from [FeS] to heme c_1 with a rate constant of ~5000 ± 1000 s^{-1}; (B) Upon addition of stigmatellin, the 552 nm transient shows negligible electron transfer to heme c_1 from [FeS]

A

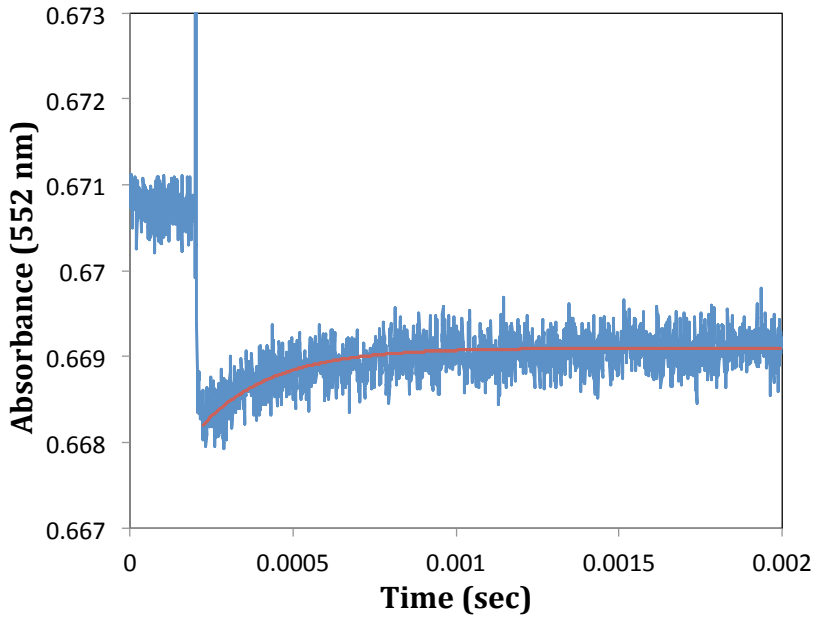

B

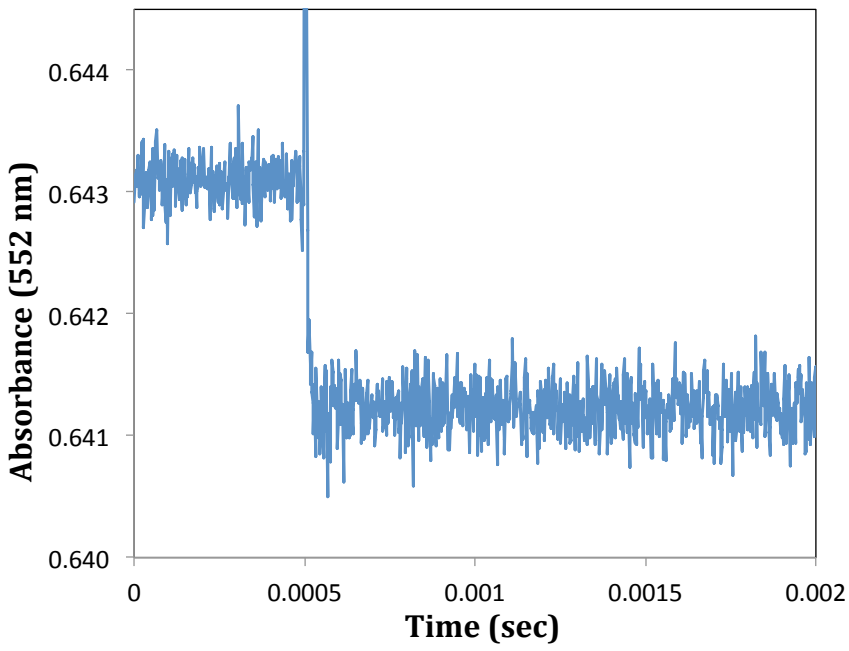

Figure 2.5-6 Electron transfer in mutant Ala+1 *R. cap* cytochrome bc_1 at 552nm. Reaction conditions consist of 4.8 µM cyt bc_1 in a 300 µL solution of 20 mM TRIS-HCl, pH 8.0, 20 µM Ru_2D, 5 mM $[Co(NH_3)_5Cl]^{2+}$, 100 µM decylubiquinol, 2 mM succinate and 50 nM SCR. (A) The 552 nm transient shows the rapid oxidation of heme c_1 by Ru_2D, followed by electron transfer from ISP to cyt c_1 with a rate constant of 690 ± 100 s^{-1}, while (B) shows reduction of b-hemes occurring at 710 ± 100 s^{-1}.

A

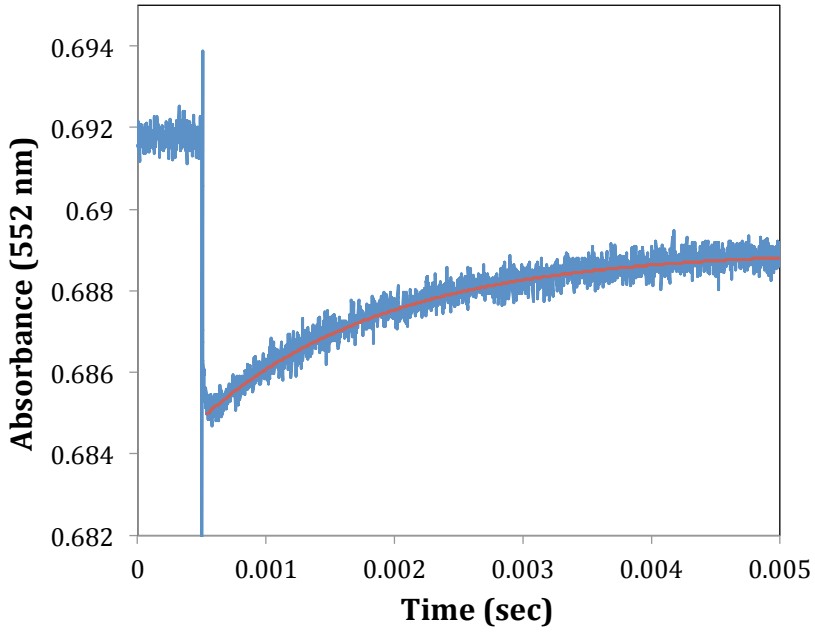

B

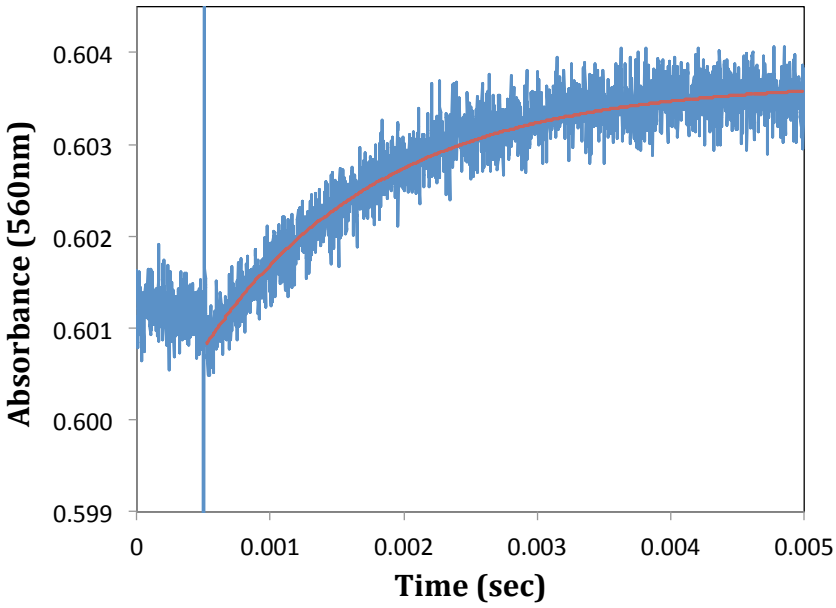

2.6 Discussion

Wild-type cytochrome bc1 derived from *R. capsulatus* was examined for the first time at catalytically relevant timescales (<1 ms). Specifically, we were able to monitor this protein in the complete absence of quinol substrate at relevant wavelengths, as well as examine the biphasic behavior of the protein when substrate is present. As not all samples were deficient in quinol, it seems correct to describe this as a fortunate set of circumstances, presumably resulting from an unspecified step in the preparation. Samples were graciously donated by the Daldal lab and were not all from the same batch. Without quinol in the sample, the rate of electron transfer to flash-oxidized heme c_1 from the pre-reduced FeS is unfettered by occupancy at the Q_o site. The rate constant of this rapid electron transfer is 14,000 s^{-1}, which is considerably less than similar experimental results for R. *sph* (~70,000 s^{-1}). Considering Marcus theory, which would project a much faster rate constant of based purely on redox potentials between the two interacting centers, it is clear that we can attribute this rate to the physical rotation of the [FeS], which is consistent with existing theories describing the ISP rotation as rate-limiting. The addition of P_f-type inhibitor famoxadone to this same sample of native *R. cap* bc_1 reduced the rate to ~5000 s^{-1}. This is consistent with previous studies and has been rationalized by the idea that occupancy of the Q_o site by the inhibitor froms van der Waals contacts with the [FeS] and thus slows the rate of [FeS] rotation in its transit to deliver an electron to heme c_1. No reduction of b-heme was observed, as would be expected for a sample devoid of quinol (47-49).

Interestingly, in samples that had sufficient native ubiquinol substrate for electron transfer to occur, the rate of transfer was 5000 s^{-1}. The occupancy of the Q_o site by the

substrate thus confirms that FeS rotation and the subsequent electron transfer to c_1 is considerably slower for this enzyme when the substrate is present. The rate of reduction of the b-hemes has a rate constant of approximately 1500 s^{-1} under these conditions.

The addition of potent P_f-type inhibitor stigmatellin reduced the rate of electron transfer to c_1 to a negligible level for the *R. cap* bc_1 enzyme. This is consistent with the effect this inhibitor has had on other previously explored species, as this has been characterized as a hydrogen bond between the inhibitor locked into the Q_o site and the [FeS] cluster. This fixes the ISP at the b position, and as it is prevented from rotating to heme c1, electron transfer for the enzyme is effectively stopped (47-49).

Altering the amino acid neck region by inserting alanine(s) had predictable effects on the FeS rotation to c_1. The Ala^{+1} mutant showed marked reduction of the rate of electron transfer, while the Ala^{+2} mutant slowed the rate to only nominal levels. This confirms steady-state kinetics studies by the Daldal laboratory on these neck mutants, which show that altering the neck region by the addition of amino acid residues drastically slows the rate of [FeS] rotation as it changes the physical relationship between the redox centers (50).

Chapter 3: Assessing the effect of redox potential of human cytochrome c on the reaction with bovine cytochrome oxidase

3.1 Introduction to cytochrome oxidase and cytochrome c

As mentioned, efficient energy conservation for eukaryotes occurs via a series of highly organized and conserved electron-transfer reactions. These reactions are catalyzed by several transmembrane multisubunit proteins that ultimately yield considerable amounts of free energy for the cell in the form of ATP. Due to their ubiquitous role in all aerobes, it is of great interest to understand the molecular and atomic details of respiratory proteins. Cytochrome c oxidase (CcO), one of these large integral membrane protein complexes, facilitates the final electron transfer in the respiratory pathway by catalyzing the reduction of O_2 to H_2O. In doing so, the electrochemical gradient that drives ATP synthesis is simultaneously maintained by this protein as it pumps protons across the inner mitochondrial membrane. This study is focused on the final reaction in the mitochondrial electron transfer chain, the reaction between cytochrome c and cytochrome oxidase. Independent discussions of structure and function of CcO and Cc will be followed by a review of their docking and interaction. A method developed by the Millett and Durham research groups to study this relationship will be discussed, where a ruthenium complex attached to cytochrome c (Cc) allows for rapid photoreduction of the protein. Subsequent electron transfer from Cc to CcO can then be studied on a nanosecond time scale. The kinetics of the reaction between Cc and CcO has been previously characterized for the wild-type proteins. We sought to more fully understand this interaction by altering the redox potential of Cc and monitoring concomitant changes in electron transfer. The environment about the heme of cytochrome c has previously been shown to significantly

affect its redox potential. Particularly, axial ligation by the thioether side group of Met80 to the heme prosthetic group is a viable target to greatly alter the redox potential of Cc. By mutating Met80 of Cc, we sought to affect axial ligation and thus redox potential. In doing so, we have explored several specific questions:

1) How does changing the redox potential between Cc and CcO affect the rate of electron transfer?
2) Using Marcus theory, what conclusions can we draw about the important factors involved in the native biological electron transfer event?

In the following sections, the discussion will follow the steps and results used to 1) mutate Met80 and clone these human cytochrome c K39C-M80X) mutated plasmids into E. Coli to express the protein; 2) purify the cytochrome c mutants; 3) covalently label them with photo-active ruthenium complex; 4) perform redox titrations on new mutant proteins to determine redox potential; and 5) perform flash photolysis experiments of the reaction between cytochrome c and cytochrome c oxidase.

3.2 Background and significance of cytochrome oxidase and cytochrome c

CcO sequentially oxidizes 4 molecules of Cc and transfers the electrons to Cu_A and then to heme a and the (Cu_B-heme a_3) binuclear center. The 4 electrons are used to reduce O_2 to 2 H_2O and pump 4 protons across the membrane (Figure 3.2-1). The overall reaction catalyzed by CcO is:

$$4\ C\mathit{c}\ (Fe^{2+}) + O_2 + 8H^+_{in} \rightarrow 4\ C\mathit{c}\ (Fe^{3+}) + 2H_2O + 4H^+_{out}$$

Each Cc molecule carries one electron from cytochrome bc_1 to CcO (52, 53). X-ray crystallographic studies have advanced the understanding of CcO function as it pertains to its structural complexity, although many questions remain unresolved. Tsukihara *et al*. determined a 2.8-Å resolution structure of bovine CcO that has 13 different subunits. As shown in Figure 3.2-2, CcO is a large, integral membrane protein, with approximately 3600 amino acids (54, 55). In a previous study dedicated to the metal centers, the same group identified the two hemes and three copper atoms in each monomer, as well as several membrane-associating phosphatidyl groups. These studies corroborate previous mutagenesis studies in elucidating the likely pathway of electron and proton flow, yet the finer details with respect to proton translocation, consumption, and the timing of these events remain unknown (56). The initial electron transfer from Cc to CcO is to the Cu_A site of CcO, which was long thought to consist of a single copper atom. However, its similarities to a binuclear copper center of nitrous-oxide reductase led to further crystallographic exploration, indicating that Cu_A of CcO is composed of two copper atoms with a (1.5 – 1.5) mixed valence state. Similar to metal centers in other proteins, such as Cc, the sulfurs of cysteine and methionine, as well as the imidazole R-group of histidines, are implicated as

ligands for the copper atoms of Cu_A (57). This understanding helped drive the formation of the mechanism of electron transfer through CcO. The receipt of electrons by heme a is followed by transfer to the binuclear [Cu_B-heme a_3] center, where the catalytic cycle takes place.

The general emphasis of investigation for CcO is the complete characterization, on a molecular and atomic level, of the individual electron transfer events that result in the reduction of O_2 to H_2O, termed the catalytic cycle. As shown in Figure 3.2-3, catalytic cycle includes six different states (given the letters **O**, **E**, **R**, **A**, $\mathbf{P_M}$, and **F**). These states differ by the number of electrons transferred to the [Cu_B-heme a_3] binuclear center and the number of protons taken up in activity. The **O** state represents the cupric/ferric state of the binuclear center. The **E** state is reduced by one electron at the the binuclear center, coupled to uptake of one proton; a second electron and proton are taken up to complete the reductive phase and yield the **R** state. The oxidative phase proceeds by binding diatomic oxygen to form the **A** state (52). The O-O bond is then broken, with O_2 being reduced by three electrons from the binuclear center and a fourth electron from a tyrosine residue (58). The $\mathbf{P_M}$ state is highlighted by the O-O bond scission and the binuclear center is shown to have cupric Cu_B and ferryl heme a_3 at this point in the catalytic cycle. The **F** state follows, where the center uptakes another electron and proton. The fourth and final electron/proton transfer regenerates the **O** state (52). The importance of the catalytic cycle is that it couples the free energy gain of O_2 reduction to continual maintenance of a strong electrochemical gradient via proton pumping, with a net negatively (N) charged inner matrix and a net positively (P) charged intermembrane space. There are two routes of proton translocation from the N to the P side, termed the D- and the K-pathways—these

are named for Asp-91 and Lys-319. The D-pathway conducts all four pumped protons and two chemical protons; the K-pathway is responsible for the first two protons in the catalytic cycle generating the R state. Kaila *et al*. propose a valve mechanism to prevent backwards flow of protons that is regulated by Glu-242. Figure 3.2-4 is shown to visualize the number of amino acid residues involved in proton pumping for CcO through the D and K pathways in a "bucket-brigade" fashion. A subsequent study has corroborated these findings (59-61).

Figure 3.2-1 Schematic of proton pumping from the N-side (high pH) to the P-side (low pH) side as a function of cytochrome c electrons providing electrogenic balance (52).

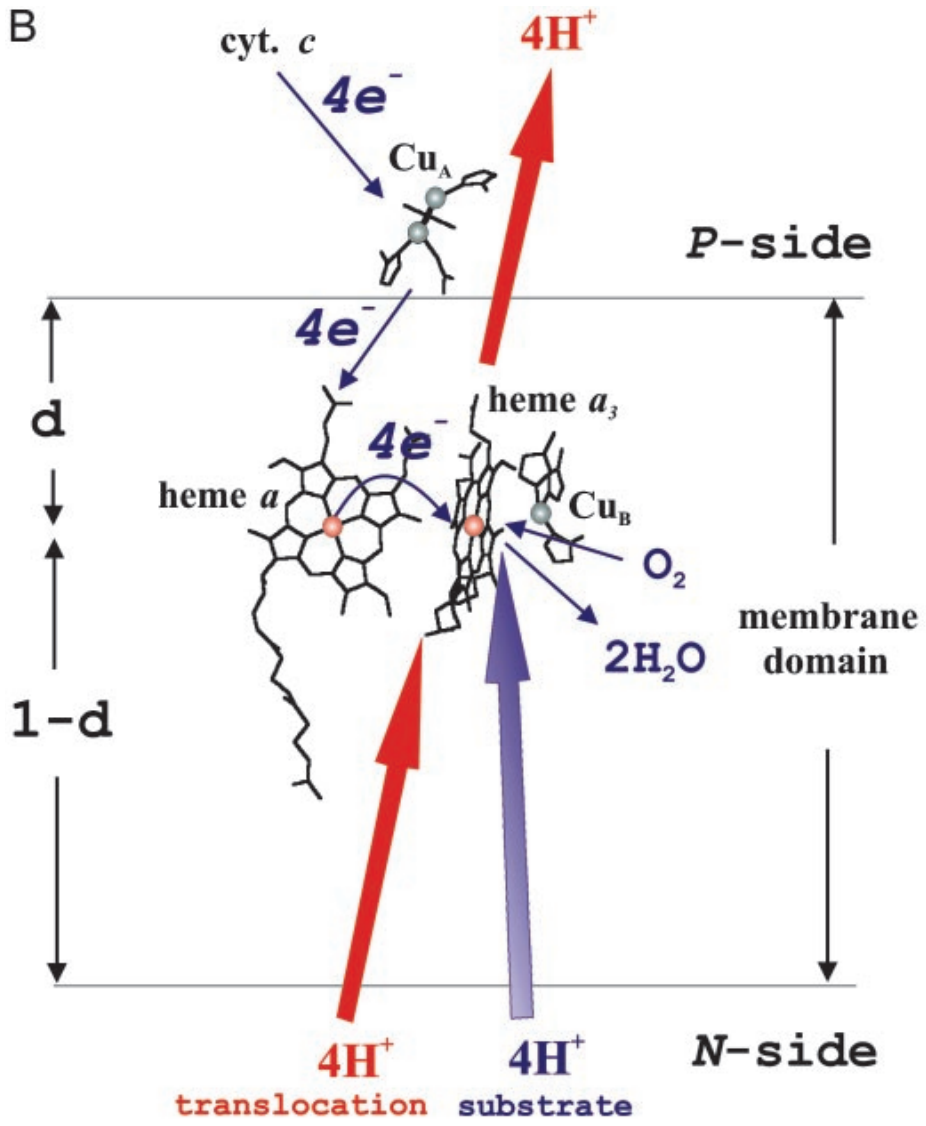

Figure 3.2-2 Ribbon diagram of integral membrane protein cytochrome oxidase (CcO), consisting of 3600 amino acids and anchoring trans-membrane α-helices (54,55).

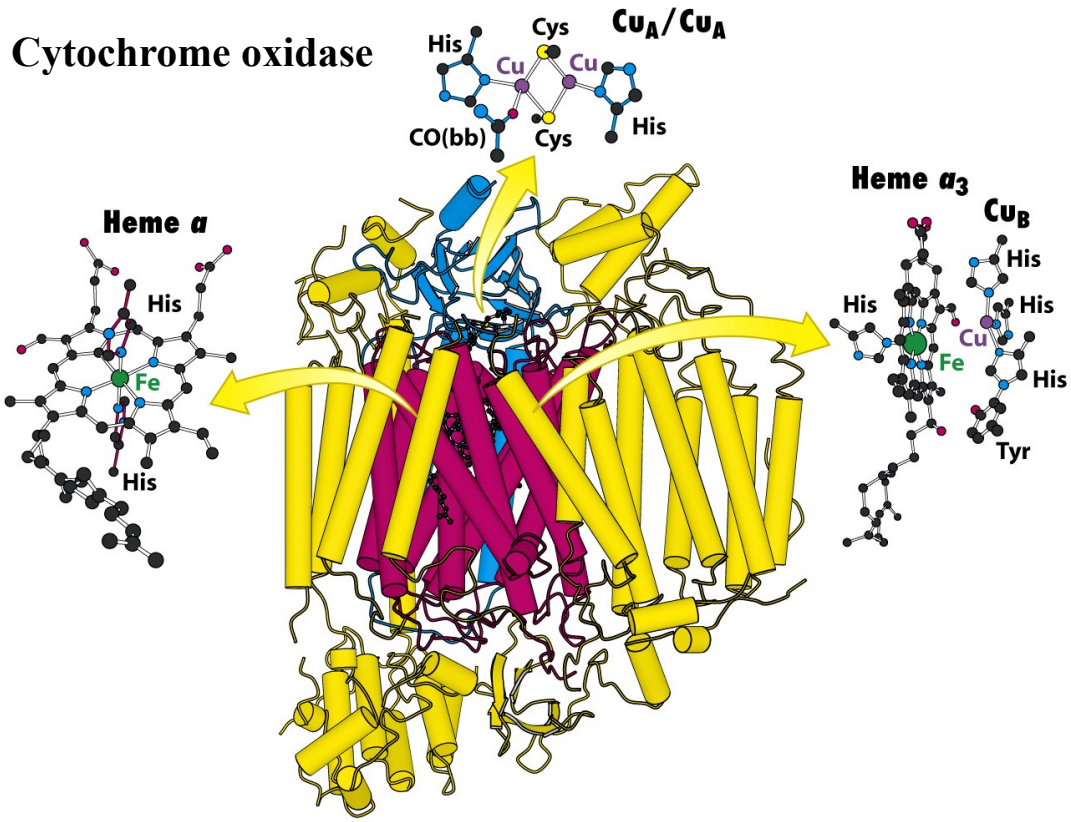

Figure 3.2-3 Figure detailing the cycling of cytochrome oxidase (CcO)

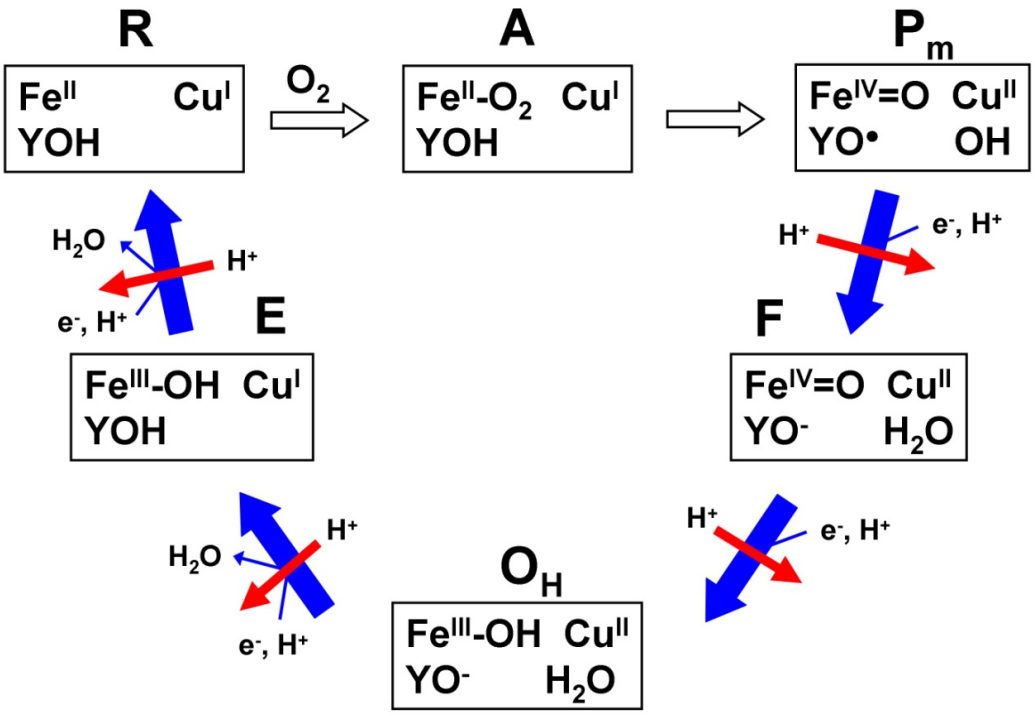

Figure 3.2-4 Schematic of important amino acid residues involving in the pumping of protons for CcO

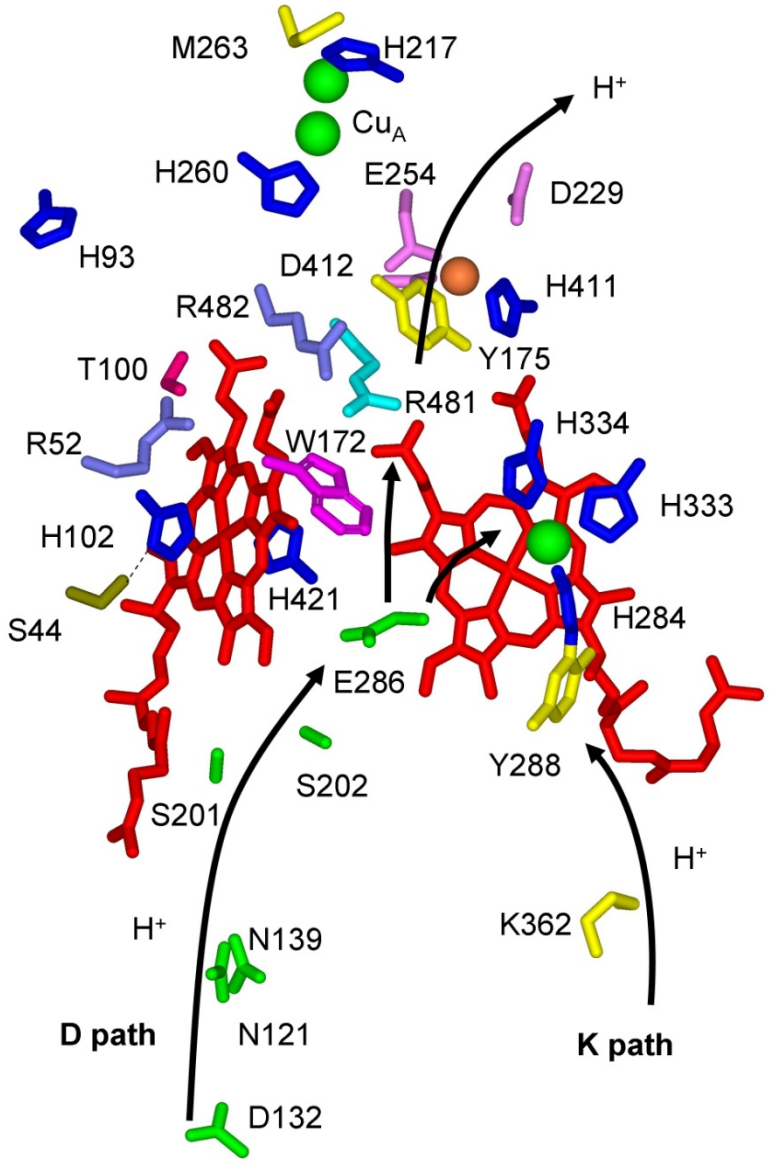

3.3 Structure and function of cytochrome c

Cytochrome c is an efficient and highly specific electron transfer carrier that transfers electrons between Complexes III and IV. One of the most conserved proteins across all species, as well as one of the most studied due to its high solubility and strong folding characteristics, Cc is a useful molecule to explore the effect of redox potential on electron transfer between Cc and CcO. It is composed of a single peptide of 104 amino acid residues. Cysteine residues at positions 14 and 17 form covalent bonds with the porphyrin ring. The four nitrogens in the porphyrin ring serve as equatorial ligands for the iron. His-18 is the 5^{th} ligand, and Met-80 is the sixth ligand.

We mutated Met-80 to alter the redox potential of the cytochrome c (Cc) protein. Figure 3.3-1, shown courtesy of the Protein Data Bank, is provided to show the structure of cytochrome c. The ring of His-18 serves as an axial ligand above the porphyrin ring, while Met80 is shown below. In the wild-type protein with the ligation scheme described above, the $E_{(red)}$ is +260 mV, whereas in the mutant M80A mutant, Sola *et al.* report an $E_{(red)}$ value of -200 mV, representing a change of -460 mV (62). Changing the redox potential of proteins, and specifically Cc, is not without its precedent in the literature. It has been proposed that variation in cytochrome redox potential depends on 3 variables: [1] the type of heme present (i.e. a, b, c); [2] the nature of the axial ligand as explored by replacement of Met80 with imidazole complexes; and [3] protein environment effects (63). Variable [1], the type of heme, is more generic for all cytochromes and does not apply for our mutants, where the heme type does not vary. In terms of Variable [2], Liu *et al*. conclude that M80H mutation represents ~160mV of the redox potential shift, meaning that the bulk of the redox potential shift is related to variable [3] —protein environment effects (64). While

these effects may encompass a number of factors that are difficult to quantify, the large effect axial ligation has on the redox potential of Cc has been attributed to destabilization of the heme microenvironment, resulting in flexibility in the inner core of the protein (62). Whereas a low dielectric interior persists in the native state of Cc, Met80 mutants should expectedly open the heme crevice to solvent exposure. Heme propionate ionization is typically limited for native Cc and plays a crucial role in the establishment of potential for cytochromes in general. With increased exposure to the solvent, the protein-water system is in a high dielectric environment and the propionic acid side chains of the heme group more readily interact with the proximal water molecules (64). As discussed, the Moser-Dutton equation, modified from Marcus theory, mathematically predicts electron transfer rates in biological systems as an exponential function with dependence on the distance between redox centers, redox potential, and reorganization energy:

$$k_{et} = k_o \exp[-\beta(r - r_o)] \exp[(-(\Delta G^{o\prime} + \lambda)^2/4\lambda RT)]$$

with the electronic coupling constant $\beta = 1.4$ Å^{-1}, the nuclear frequency $k_o = 10^{13}$ s^{-1} , and the van der Waals distance $r_o = 3.6$ Å. With these experiments taking place at room temperature (293-298K), the remaining components are r = the distance between redox centers; the free energy $\Delta G^{o\prime} = -nF\Delta E^o$, where ΔE^o = the difference in reduction potential between the two centers; and λ= the reorganization energy (65). We seek to alter the driving force of the redox reaction by changing the redox potential; in mutating Met80 to alter axial ligation to varying degrees (Leu, Lys, Gln, Thr, Ala, Glu, and Cys, specifically), it is expected that the driving force will be increased. This is because the mutants should show increasing readiness to be oxidized after they are flash reduced, based solely on decreased E_{red} values measured for known Met80 mutants. It should be noted that the primary study

of Met80 mutants and their redox potentials was not exhaustive; of the 20 naturally occurring amino acids, only M80C, M80A, and M80H were previously explored due to semi-synthetic technique constraints. Using recombinant methods, this study sought to more fully explore the effect of redox potential on the kinetic activity of Cc (62,66). Given measured redox potential and rate information, the reorganization energy (λ) is an important factor in the Marcus equation of electron transfer that can be calculated. As it is the energy required to make all the necessary nuclear rearrangements in order to match bond angles and geometries between redox partners, it varies as a function of altered redox potential. Measuring rates and redox potentials can be used to gain some information about the reorganizational energy component; however, isolating a specific cause or set of causes of any reorganizational differences in the complex protein interaction presents challenges and goes beyond the scope of the project. One possible hypothesis is that the presumed flexibility introduced at the heme ligation site by Met-80 mutation could change the hydration and/or have one or many changes in atomic orientation. Any such structural difference or alteration in the microenvironment could to some degree alter the reorganization energy as compared to the control. By correlating measured redox potentials of Cc mutants and their respective rates of electron transfer to CcO, and applying these to Marcus theory, we seek to make meaningful commentary about driving force and reorganization energy with regards to this important reaction.

Figure 3.3-1 Cytochrome c and its ligation scheme with respect to the heme porphyrin (red), His 18 imidazole (pink), and methionine (yellow). Surface lysine residues are in blue and are important for proper binding via ionic interactions to negatively charged residues on CcO.

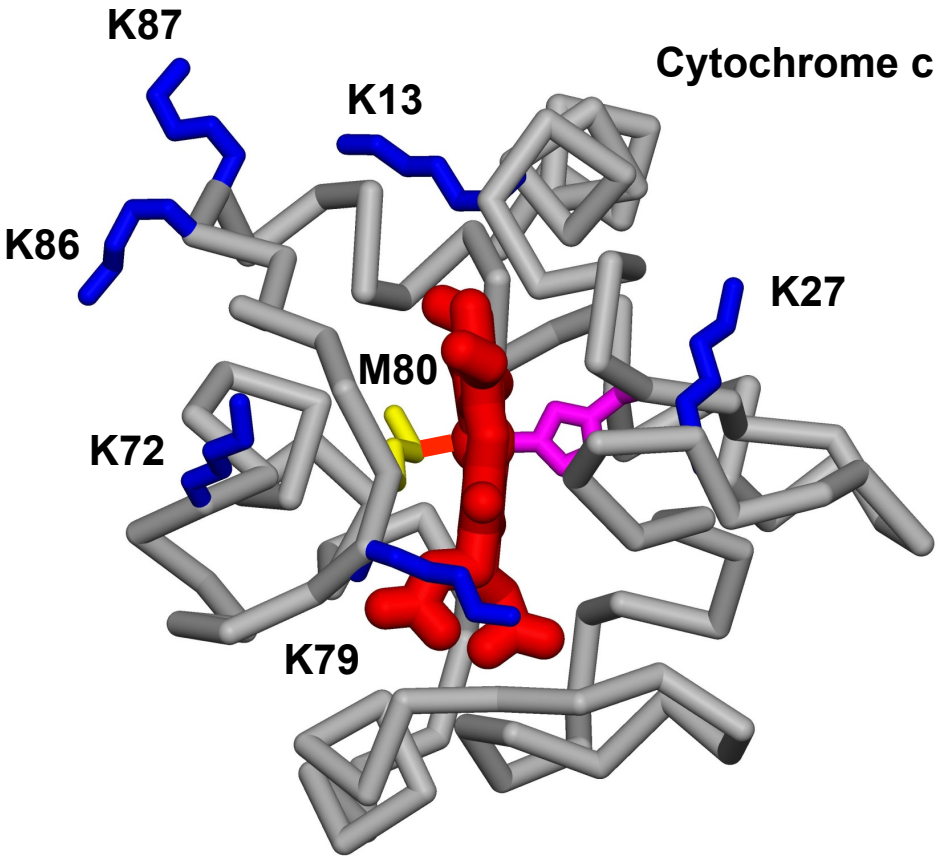

3.4 Interaction of cytochrome c and cytochrome oxidase

Although we do not seek to alter the binding of Cc to CcO, it is important to at least understand how Cc interacts with CcO *in vivo* to accomplish its missive as electron shuttle. The interactions of Cc with its binding partners bc_1 and CcO are transient. It must be able to bind to each protein, either accept or donate an electron, and then leave to maximize turnover at the active site(s). Electrostatic forces largely dictate its association with both bc_1 and CcO (67). Cc is a highly conserved protein; between yeast and human Cc, ~60% of the amino acid sequence remains intact. Interestingly, sequence studies have shown that a rapid mutation of Cc occurred in the anthropoids and primates. Lower mammals differ in amino acid sequence by 11 amino acids, 5 differences of which occur at the proposed binding interface of Cc and CcO (Figure 3.4-1). Lysine residues 8, 13, 72, 86, and 87 create a positively charged surface of Cc, which makes electrostatic interactions possible with the negatively charged residues E148, E157, D151, D195, and D214 at the binding interface (68-70). Due to different distribution of lysine residues on the surface, *R. sphaeroides* and horse Cc interaction with CcO expectedly differ. Furthermore, mutagenesis studies of CcO show that mutations of Trp-143 did not exhibit any effect on K_m values for Cc, meaning that it is not involved in the binding. Trp-143 mutation also does not disturb the Cu_A, yet Trp-143 mutation drastically inhibits the electron transfer between Cc and CcO, suggesting it is a crucial link in the electronic pathway to Cu_A. As shown in Figure 3.4-1, Trp-143 and Asp-214 are close to the site of electron transfer and provide a feasible avenue through which rapid electron transfer can be achieved by these two redox proteins. Figure 3.4-2 shows the various redox centers in Cc and CcO, in addition to ruthenium complex covalently attached at a cysteine residue at position 39. Electron transfer from Cc to Cu_A showed a

rate constant k_a = 4 x 10^4 s^{-1} for wild type, while Trp-143 mutants showed rates of ~450-fold decrease for Phe-143, and ~1200-fold decrease for Ala-143. While the aromatic ring of Phe is able to somewhat modulate the effect, relative to Ala at least, the indole ring of Trp is clearly implicated as a necessary component in the electron transfer event {71-73).

Having established the significance of Cc and CcO, the importance of axial ligand Met80 of Cc on its redox potential, and docking of Cc to CcO and electron transfer to Cu_A, a brief discussion of ruthenium complex attachment to Cc will ensue. The following shows the Cc:CcO interaction we seek to explore, equilibrium states of their binding relationship, and the purpose of photoreduction via laser flash to trigger electron transfer.

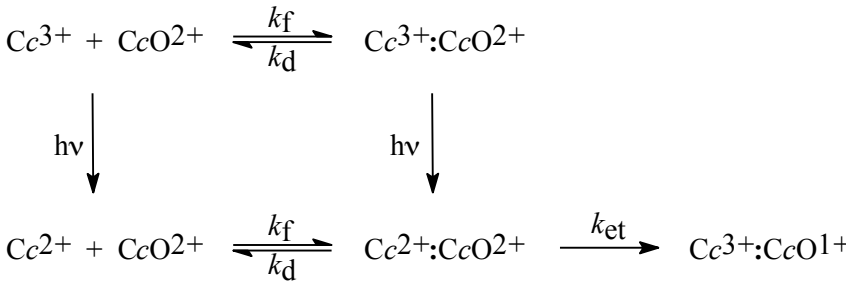

Figure 3.4-1 Important ionic interactions at the surface of Cc and CcO regulate their interaction. Cc has several important, positively charged lysine residues that interact with negatively charged glutamate and aspartate residues. These ionic interactions establish a connection, followed by electron transfer from the heme group of Cc to Cu_A redox center of the CcO complex.

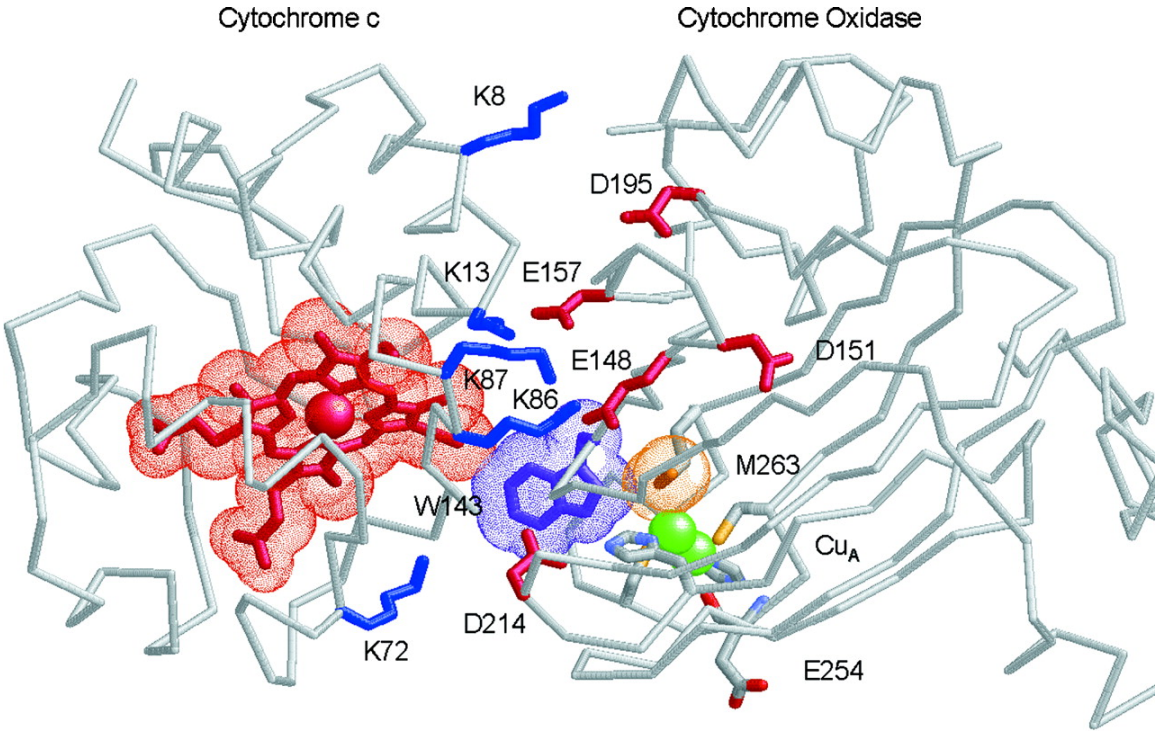

Figure 3.4-2 This figure shows the overall scheme of how cytochrome c (Cc) interacts with cytochrome oxidase (CcO), in addition to the ruthenium complex (green) which is employed to flash reduce heme c. Electron transfer proceeds from heme c to Cu_A; from Cu_A to heme a; and from heme a to heme a_3.

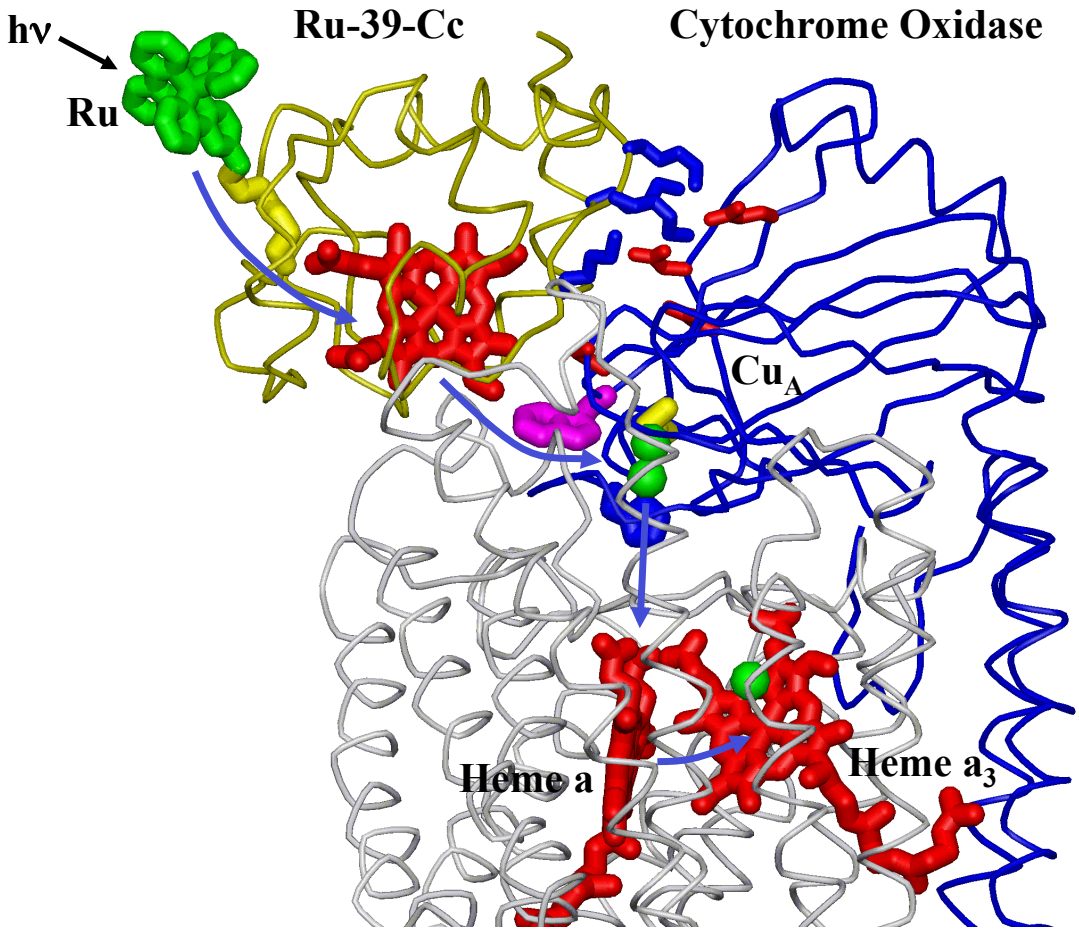

3.5 Materials and methods

Site-Directed Mutagenesis

This work was approved by the Institutional Biosafety Committee under Protocol 12018, with oversight provided by the University of Arkansas Office of Research Compliance. Site-directed mutagenesis was performed in order to produce plasmids encoding Met80 mutants of Cc. Beginning with human Cc plasmid, pBTR(humanCc), as described in Olteanu et al. (74) and provided to the Millett lab as a gift from the Pielak laboratory, primers were designed to change the Met80 codon to affect the axial ligation and thus the redox potential of the protein. The structure of the original plasmid is crucial for Cc expression. As the redox active heme group of Cc is required for Cc folding and electron transfer, early efforts in the 1990's to express the enzyme in *E. coli* vectors failed. Therefore, aside from encoding the amino acid sequence of Cc, the plasmid also encodes for cytochrome c heme lyase, which functions to covalently bond the heme group to the cytochrome c architecture. (75-78). Also, in order to accommodate ruthenium labeling for kinetic experiments (discussed later), a lysine residue at position 39 was modified to a cysteine residue to create the Human Cc-K39C template.

A Stratagene Quik-Change II site-directed mutagenesis kit was used to facilitate the creation of novel Met80(X) mutants. Oligonucleotide sense and antisense primers for various Met80 mutants were designed and ordered from Integrated DNA Technologies, Inc. Plasmid concentration was determined in distilled deionized H2O (ddI) at 260 nm using Beer's Law ($A=\varepsilon cb$) with ε_{260} = 33 mL/(mg*cm) for single-stranded DNA. These stocks were then diluted to be used for reaction mixtures. The K39C-Cc parent plasmids were thawed and their concentration was determined in the same manner, using ε_{260} = 50

mL/(mg*cm) for double stranded DNA. Dpn1 restriction enzyme is added after PCR, which cleaves any methylated or hemi-methylated dsDNA and ensures that any plasmids contain the mutation. The Dpn1-treated DNA was added to XL-1 Blue supercompetent cells, transformed via heat shock, and plated. After incubation, colonies were aseptically picked from each plate, added to broth, and allowed to incubate overnight at 37 °C.

Plasmid preparation, isolation, and sequencing

A Wizard Miniprep DNA Purification System was used to prepare and purify the mutant plasmids for sequencing. Approximately 1.5 mL of the cell suspension was pipetted from the culture tube to sterile Eppendorf tubes. Microcentrifugation at 10,000 rpm created cell pellets. Following kit protocol, cell resuspension buffer, cell lysis buffer, and neutralization buffer were added in sequential fashion. Due to the fragility of the plasmids outside the cell, gentle mixing by inversion is highly recommended. Cell lysate was centrifuged to separate the plasmids (supernatant) from the native bacterial cellular DNA (pellet). Supernatant was added to plasmid-binding resin and pushed through a small column using a syringe plunger. Plasmids were summarily extracted as confirmed by diode array. To ensure that the prepared plasmids contained the desired mutations, they were sent to the University of Arkansas DNA Sequencing Laboratory for sequencing.

Transformation into expression line with mutant plasmid

The mutant Cc plasmids were then individually used to transform *E. coli* BL21-DE3 competent cells in sterile, iron-rich Terrific Broth. This particular cell line is deficient in OmpT and *lon* proteases, which cleave heterologous proteins in the cell; thus, their deletion from the *E.*coli genome in BL21-DE3 cells results in increased protein production. This is especially true for cytochrome c, as determined empirically prior to the studies described

herein. Transformation was performed again using heat shock and plated on 2xYT+AMP agar plates and incubated overnight. Single colonies were aseptically removed and placed into Erlenmeyer flasks containing sterile 2L volumes of Terrific Broth plus AMP and incubated 48 hours at 37 °C.

Cytochrome c Expression and Purification

Protein expression of cytochrome c, using this particular plasmid construct, occurs in a nascent fashion without induction via lactose analog isopropylthiogalactoside (IPTG). Therefore, while traditional *lac* operon plasmids are induced with IPTG at an optical density at 600nm (OD_{600} /Abs) = [.4-.6] in the growth media, where there are a maximal number of healthy cells, this particular system is an exception.

Protein purification was performed with a technique similar to that described in Patel *et al.* (75). The cells in which cytochrome c remains were lysed in 50 mM Tris, pH 8.0/5 mM EDTA/10 mM magnesium sulfate/1 mM calcium chloride, lysozyme, and 50 mM PMSF (phenylmethylsulfonyl fluoride). Pulse sonication on ice was then employed to provide additional lysing via mechanical means. A small amount of DNase was added and allowed to incubate to cleave DNA. The suspension was stored at -80 °C, to be later put through a 2-3 freeze-thaw cycles in order to aid in lysis of the cells.

To purify, the thawed cell lysate to remove any large particles, retaining the supernatant. Ammonium sulfate precipitation at 50% is employed to remove a large fraction of unwanted precipitates -- supernatant is retained post-centrifugation. Ammonium sulfate to 90% precipitates cytochrome c; pellet is resuspended in ddiH_2O and dialyzed into 4.0L of 10mM Tris using 6,000-8,000 molecular weight cutoff (MWCO) dialysis tubing. Rough cation exchange proceeds, using 50 mM Tris, pH 8 as parent buffer,

and [NaCl] from 0mM-500mM. Fractions were collected and assessed via diode array for high (410nm:280nm) ratios, indicating strong presence of heme Soret (410nm) relative to λ_{max} for all proteins at 280nm. These fractions were collected and concentrated in a 10,000 MWCO centrifugal unit, and were then exchanged 5 mM sodium phosphate (P*i*), pH 7.0 for the final step.

The final purification step of Cc was HPLC using a Hitachi LaChrom Elite HPLC system. The Cc is fully oxidized with a small amount of potassium ferricyanide ($K_3Fe(CN)_6$) to maximize interaction with the negatively charged resin of the cation exchange column. Using a continuous gradient of 5mM P*i*, pH = 6.0 up to 500mM P*i*, pH= 6.0, fraction tubes that contained Cc were pooled and concentrated in a 10,000 MWCO concentrator at 6,000 rpm, and frozen at -80 °C (76).

Cytochrome c Oxidase Purification

CcO is purified directly from the muscular tissue of cow hearts ground and blended with 20 mM P*i*, pH = 7.4 buffer to homogenize. The homogenized mixture was centrifuged to remove larger particulate matter and then strained to further remove large debris. The supernatant was then centrifuged using an ultracentrifuge at 15,000 rpm. Pellets containing the Keilin-Hartree particles were collected and resuspended in 50 mM Tris with 250 mM sucrose, pH 7.4. The pellet was resuspended in 0.1 M P*i*, pH 7.4, and ammonium sulfate precipitation was employed to obtain CcO incrementally to precipitate CcO. Steady state assays were utilized to determine catalytically active samples from this purification.

Preparation of Ruthenium Complex

(4-hydroxymethyl-4'methylbipyridine)[bis(bipyridine)] ruthenium^{+2} was prepared by T.J. Anderson using the previously described method of Geren *et al*. (79). The

bromination of this complex was performed under the guidance of Dr. Lois Geren. Using excess HBr and heat, the (4-bromomethyl-4'methylbipyridine) [bis(bipyridine)] ruthenium^{+2}, referred to for simplicity as [$(bpy)_2$(mobpy)Ru^{+2}], was created and dissolved in dimethylformamide. The addition of the bromine to the ruthenium complex provides a good leaving group for the covalent attachment of the compound to a cysteine via a thioether bond. All proteins were labeled with this complex, with the methodology of this discussed below.

Preparation of Ruthenium Labeled Human Cc-K39C (Met80X) derivatives

In order to assess the redox potential and rates of electron transfer from cytochrome c to cytochrome oxidase, the wild-type and mutant Cc constructs were exchanged into 50mM pH= 9.0 borate buffer in the presence of dithiothreitol (DTT) using 5,000 MWCO 2mL centrifugal filter units, which ensures a substantial portion of the protein molecules have a deprotonated cysteine at position 39. It is noteworthy that no other free cysteine residues exists in the cytochrome c sequence, as the other two are involved in covalent attachment to the heme redox center. Thus, labeling occurs at one site that is spatially distal from the binding interface of the Cc/CcO complex, which prevents any secondary effect of ruthenium complex on the binding relationship. The sample was degassed and assessed for molar constitution using Beer's law and an extinction coeffcient of $\varepsilon = .106\ uM^{-1}$. DTT is used to reduce any disulfide bonds between protein molecules that might be in place, which would prevent labeling from taking place. The [$(bpy)_2$(mobpy)Ru^{+2}] is added in some excess, which was explored for optimization. The chemistry here is somewhat conflicting, for though the DTT serves to discourage disulfide bonds between protein molecules to form dimers, it also serves to counter the very

reaction sought in the labeling process: the thioether bond to the Ru^{+2} complex. Therefore, the success of this step depends heavily on finding a proper molar ratio of the components with respect to one another. Various ratios of components in the mixture were explored, and the ideal ratio to generate maximal singly-labeled Cc with minimal dimer formation was determined to be that of a [1 mole Cc : 1mole DTT : 4 mol Ru^{+2}] nature in 2mL total volume. Reaction samples were washed thoroughly with DTT in the borate buffer exchange and then sealed in an airtight vial with septum. Degassing was done using N_2 to minimize oxidation via O_2, which would counter the desired reduction of disulfide bonds. A stock DTT solution was created from the solid in 2.0 mL volumes and added 1:1 (mol:mol) to the degassed protein sample in the 50mM borate pH=9.0 buffer. The Ru^{+2} mobpy compound, previously stored in dimethylformamide at -20 °C, is added in four-fold excess to the Cc construct using Hamilton pipettes that are thoroughly (10-20 fold) rinsed with dry DMF to protect the valuable stock compound from water contamination. Reaction mixtures were incubated at room temperature in the dark overnight. 5000 MWCO centrifugal units were used to remove excess DTT and unreacted Ru^{+2} label, while also exchanging buffer from its current state to 5mM PBS pH = 6.0. Purification was performed via HPLC/cation exchange using the Hitachi LaChrom Elite HPLC system mentioned above. Loading was done under 5mM PBS pH = 6.0 conditions, and elution followed a gradual gradient over 100 minutes from 5mM PBS pH = 6.0 to 500mM PBS pH = 6.0. Fractions were collected every minute and combined as appropriate. Addition spectra of the compound to that of an unlabeled cytochrome c can be used to make the distinction between labeled and unlabeled protein. The primary differences are a moderately decreased (410nm:280nm) ratio for labeled Cc, as a function of the contributive

absorbance of the attached Ru^{+2} label which is on its own greater at 280nm than at 410nm. An even stronger indicator is the evolution of a shoulder in the 450nm range for the labeled protein. The common elution pattern showed unlabeled protein eluting first, followed by singly labeled protein. Dimers and what may be doubly-labeled constructs typically eluted late, sometimes even as the column washing in 1M NaCl. Fractions of individual peaks were combined and washed, using 5mM PBS pH= 7.0 and stored in maximally concentrated aliquots at a temperature of -80 °C.

Redox titration and potential measurements

Redox titrations were performed anaerobically using calomel reference electrode and pH/mV meter to directly measure voltage of Cc derivatives in solution. Mediators of varying redox potentials were used to create a thorough range to interact with the protein components in solution, all at .100mM concentrations: (potassium ferricyanide = +430mV; phenazine methosulfate = +80mV; $Ru(NH_3)_6$ = ~0mV; 2-hydroxy-1,4-naphthoquinone = -145mV; anthraquinone-2-sulfonate = -230mV) in cuvette with 10-15μM Cc. Dithionite and ferricyanide were used (~.05M in 1mL amounts) as titrants to decrease or increase solution voltage, respectively. Reduction of Cc was monitored by A_{550} (HP diode array). Correlation of E_{meas} and respective (Cc_{red}:Cc_{ox}) plotted in y vs. ln x fashion per Nernst; least squares trendline applied (y-int = redox potential; slope = (-nF/RT), which at 298K should represent a slope of -25.17 for a single electron transfer).

Flash photolysis

The intermolecular electron transfer between ruthenium-labeled Cc constructs (wild type and Met80 mutants) and bovine oxidase was studied using a Phase R Model DL 1400 flash-pumped dye laser with Exciton coumarin LD 490 dye. This produces a pulse

with duration of less than 500ns at 490nm. The instrumentation setup can be found in Figure 1.3-1, where a monochromator is used. At 550nm the flash-induced reduction and subsequent re-oxidation of the heme redox center of Cc is observed as it delivers its electrons to Cu_A of cytochrome oxidase. The 605nm wavelength is also monitored, as it indicates the rate of electron transfer internal to the cytochrome oxidase protein from Cu_A to heme a. The samples are maintained in an oxidized, fully aerobic state prior to the laser flash. Buffer conditions of these experiments consist of 5mM sodium phosphate, pH= 7.0 at room temperature with 10-15 μM Cc and .1% lauryl maltoside to provide a proper micellular, lipid-like environment for CcO. In order to conserve Cc sample, a minimal volume of 270-300 μL is achieved. Although additional components are not necessary to maintain oxidized Cc and CcO prior to flash, as atmospheric O_2 is sufficient for this, aniline and 3-carboxy-2,2,5,5-tetramethyl-1-pyrrolidinyloxy free radical (3CP) are added. Their importance is described below.

Upon laser flash, the Ru^{II} mobpy compound goes to an Ru^{II}* excited state. It rapidly donates the electron to the Fe^{III} oxidized redox center of Cc, yielding a ruthenium in the powerful oxidized form Ru^{III} and a reduced Fe^{II} heme on Cc. At this point, with a redox potential of 1.27V, the Ru^{III} could simply take the electron back from the heme of Cc to regenerate the original pre-flash (Ru^{II}/ Fe^{III}) situation. Allowing this to occur unchecked would not allow electron transfer to cytochrome oxidase Cu_A. Therefore, aniline acts as an electron donor to immediately donate an electron to Ru^{III} upon its flash-induced formation, so the electron that was just donated to the c-heme will have no other avenue other than to proceed to cytochrome oxidase -- thus, this prevents the back reaction. Aniline's presence in 500-1000 fold excess to the Ru-Cc(K39C) construct ensures that it will not be exhausted

for the duration of the experiment. 3CP is maintained at 1mM, and it is a free radical and therefore, in itself, also a willing donor of electrons. 3CP donates electrons to aniline, which prevents aniline dimers from being formed as the aniline undergoes oxidation. The aniline dimer produces a blue color, which can introduce spectral complications, while the 3CP is colorless in both its free radical and oxidized states. A scheme is provided as Figure 3.5-1 to illustrate these photoexcitation events as they are initiated by laser flash. The first-order phase will occur upon laser excitation, which represents Cc that is already bound to the surface of CcO. This rate is therefore independent of concentration and is only limited by the electron transfer itself. A slower, second-order phase represents free Cc interacting with CcO, which is concentration-dependent, is limited by rate of binding and dissociation (k_f and k_d, respectively), and can be influenced by the presence of salt, which interferes with the ionic interaction of surface residues between the proteins.

Figure 3.5-1 Schematic of light excitation to generate the excited state of the ruthenium complex (Ru) is followed by rapid oxidation of Ru as it donates an electron to heme iron (Fe) of cytochrome c.

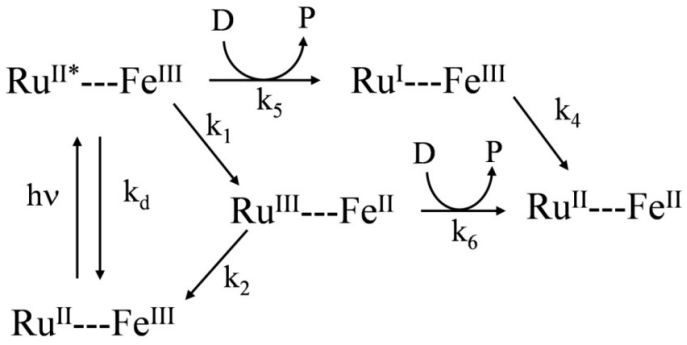

3.6 Results

Site directed mutagenesis

While working within the parameters of primer design software available from IDT, optimization was necessary as the length of certain primers were simply too long. Also, the expected melting temperature of any given primer varies from source to source, presumably as a function of the particular algorithms provided. Primers in excess of 35 base pairs did not successfully yield mutant proteins, presumably due to secondary structure formation of ssDNA that can occur within the temperature range of the PCR thermocycling. Despite meeting desired 60% cytosine-guanosine (CG), maximizing CG content at the 3' and 5' termini, and overall melting temperature constraints, longer primers (which were predicted for codon swapping of 3 base pairs at position 80, rather than 1 or 2) failed. As the mutagenesis kits are expensive and contain reagents (particularly Dpn1) that are particularly sensitive to freeze/thaw, it is important to adjust strategy of primer design to < 35 base pairs, and consult with several primer design websites for possible hairpin issues rather than just relying on a single source. Seven Human Cc -K39C (M80X) mutant plasmids were created, successfully sequenced, analyzed using 4Peaks software, and compared to human cytochrome c as found on UniProt (www.uniprot.org). All sequences confirmed the existence of a cysteine at position 39 (rather than the native lysine), and the proper M80 variants. These include: M80T, M80K, M80L, M80Q, M80A, M80C, and M80E.

Transformation and Purification

All Human Cc-K39C M80X mutants, and K39C-Met80 (wild type at the axial heme ligation site, WT) were successfully transformed into BL21-DE3 as confirmed by plating in 2xYT agar plates with ampicillin.

The WT, M80T, M80K, M80L, and M80Q mutants expressed quite well, as indicated with a robust pink/orange color. Despite identical growing conditions (time, broth type and volume, etc.), the M80A, M80C, and M80E mutants did not grow or express very well in the several attempts made to do so. Specifically, in terms of cellular mass/liter of Terrific broth, cell yield was low and colony color was characteristic of normal *E. coli*, qualitative observations which predicated the low yields obtained in purification. Purification for the WT, M80T, M80K, M80L, and M80Q proceeded without issue per established protocol as described above in Section 3.5.

Preliminary Redox Activity Assay

In order to assess viability of redox variants, preliminary qualitative experiments were conducted on purified Human Cc-K39C using the reductants ascorbate and dithionite. Ascorbate, while capable of reducing the WT form of the protein, was not able to reduce the other mutants. A standard spectrum of human CC-K39C is provided as Figure 3.6-1A, which, when compared to Figure 3.6-1B where ascorbate has been added, clearly indicates reduction of the heme. Distinctive features include Soret peak blue shift upon reduction, increased A_{max}, and characteristic peaks at 550nm. Figures 3.6-2 and Figures 3.6-3 show markedly different behavior, indicating altered redox behavior for Met80 mutants.

Figure 3.6-1 Spectrum of purified WT Cc (K39C-Met80) in (A) oxidized and (B) reduced with ascorbate. Distinctive features include Soret peak blue shift upon reduction, increased A_{max}, and characteristic peaks at 550nm.

A

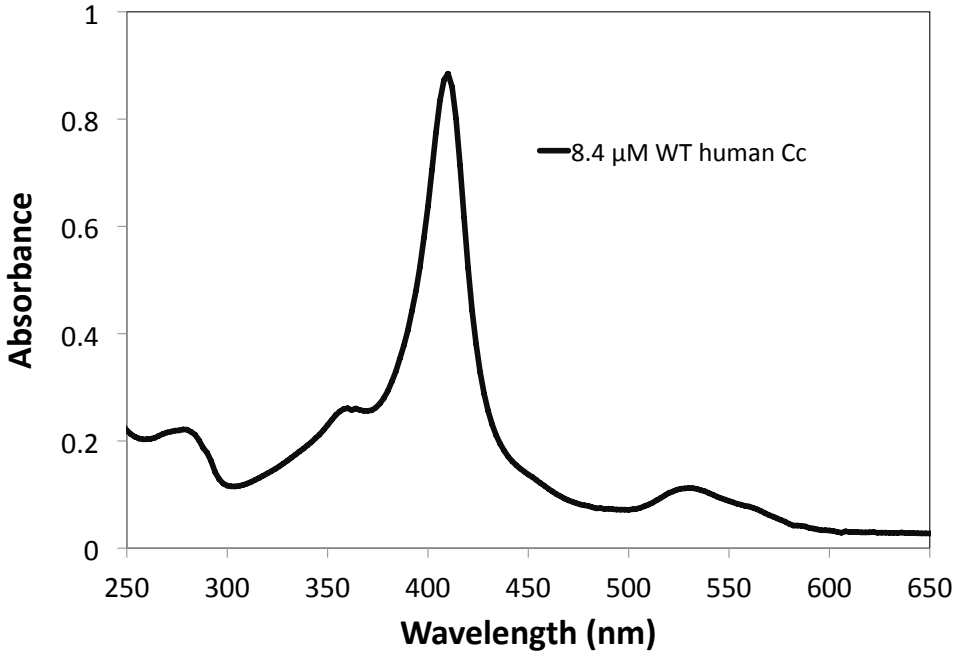

B

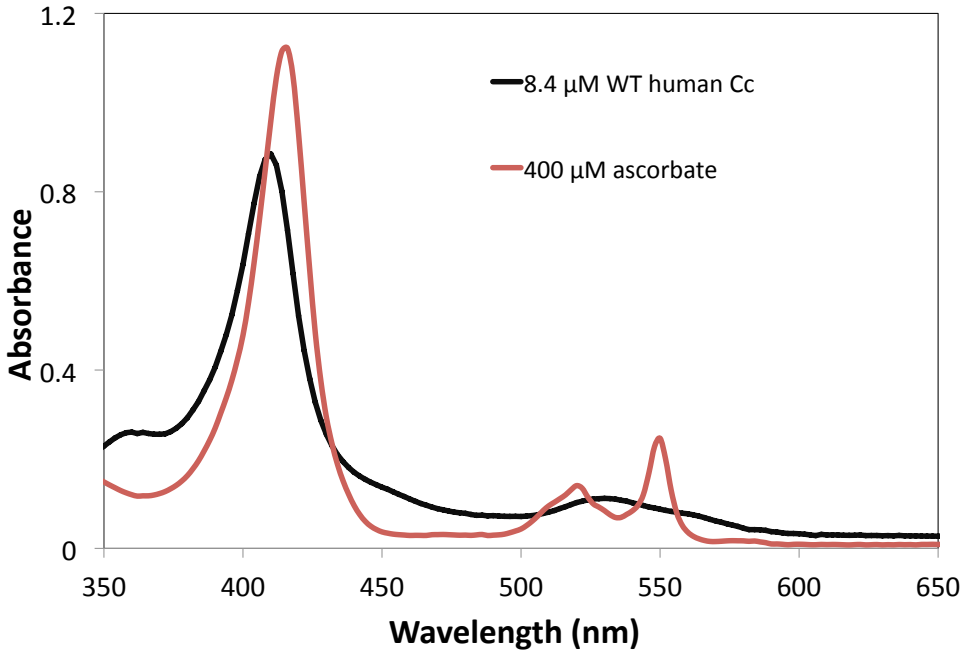

Figure 3.6-2 (A) Spectrum of oxidized human Cc-K39C-M80L; (B) ascorbate does not reduce mutant M80L, but dithionite does

A

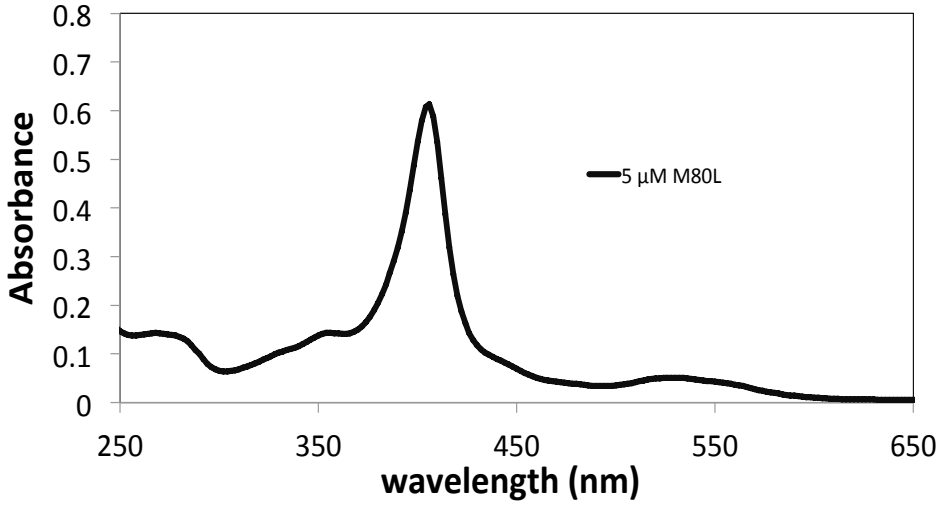

B

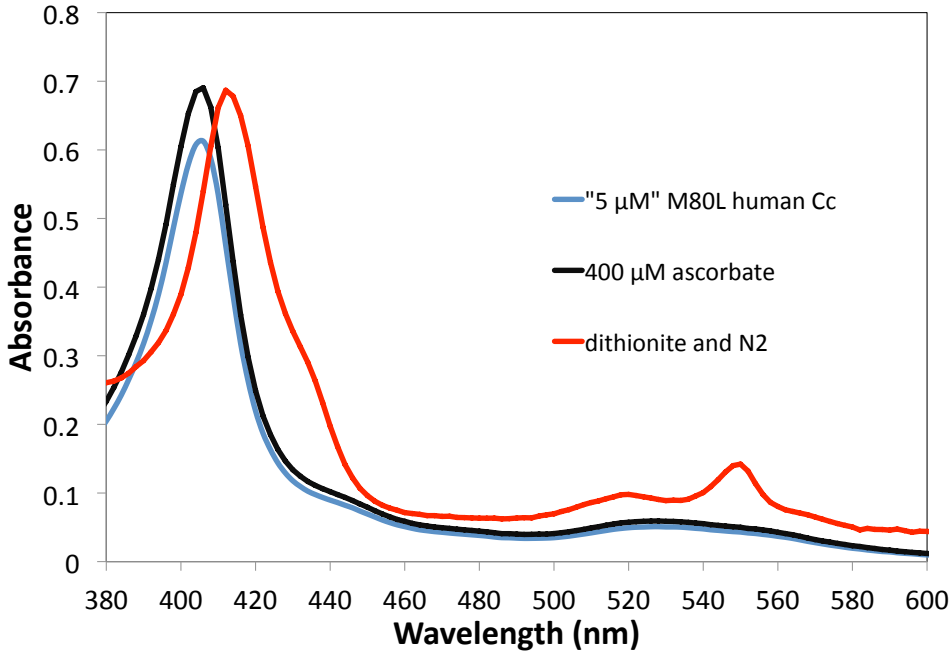

Figure 3.6-3 Similar preliminary redox results were obtained for the M80Q mutant (A) oxidized; (B) reduction via dithionite, but not ascorbate

A

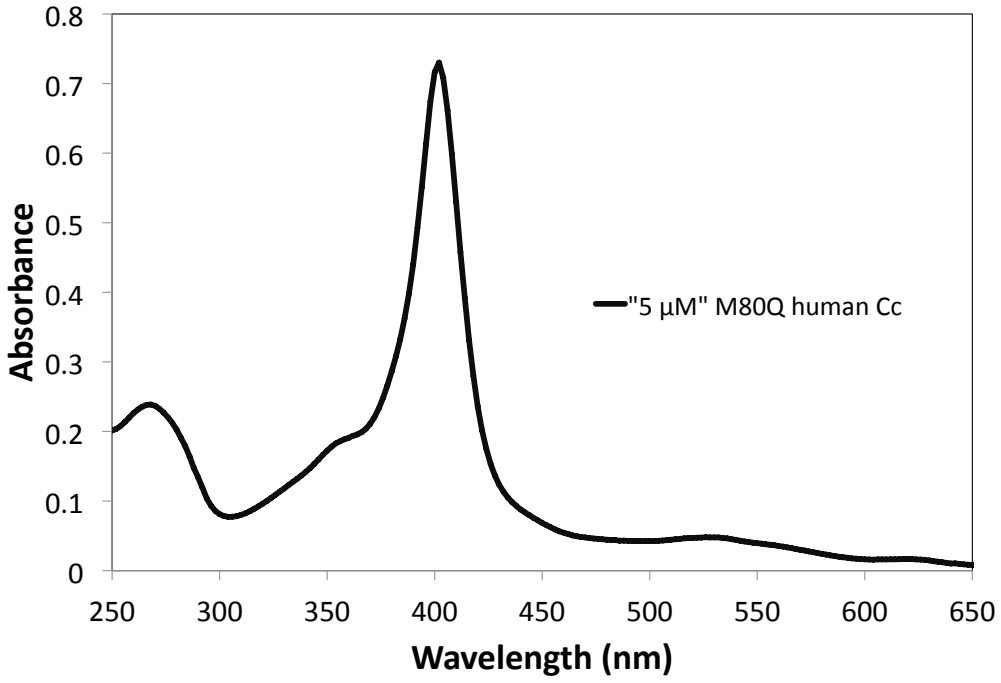

B

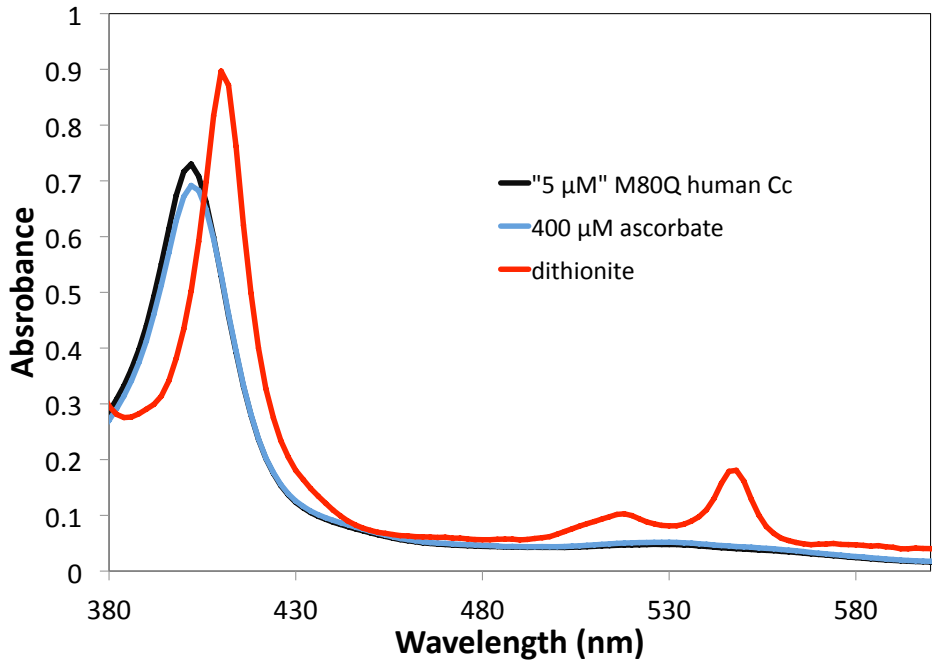

Cytochrome oxidase purification

The activity of bovine heart oxidase was assessed by Marti Scharlau via usage of steady-state kinetic assays to confirm consistent behavior for the protein (results not shown).

Preparation of Labeled Derivatives

This task required significant optimization, as described in Section 3.5 (Materials and Methods). The M80Q mutant protein stock was exhausted without successful labeling, while the M80L, M80T, M80K, and WT proteins showed labeling, as indicated by the evolution of 450nm shoulder even after significant washing and buffer exchange. Figure 3.4-4 shows the labeled mutants with a characteristic shoulder at 450-460nm not observed in unlabeled protein. Samples are purified via HPLC in a gradient from 5-500mM phosphate buffer at pH =6.0 over 100 minutes to achieve well separated peaks. Singly-labeled constructs can be discerned from unwanted populations via UV/Vis and comparison to addition spectra for the components. These undesired populations include unlabeled fractions, the possibility of multi-labeled fractions, and any protein dimers that might occur (presumably as a function of aggregation or C39 disulfide bonding between protein molecules). The (410:280) peak ratio and 450-460nm shoulder are of importance in this assessment. Theoretical addition spectra of 1:1 (mol Ru: mol Cc) have been provided as Figure 3.4-4, while Figure 3.5-5 shows the experimental spectra of successfully purified, singly-labeled constructs.

Figure 3.6-4: Theoretical addition spectra of Ru-mobpy and cytochrome c acquired independently, then added together to show expected spectra for 1:1 (mol Ru:mol Cc) labeling

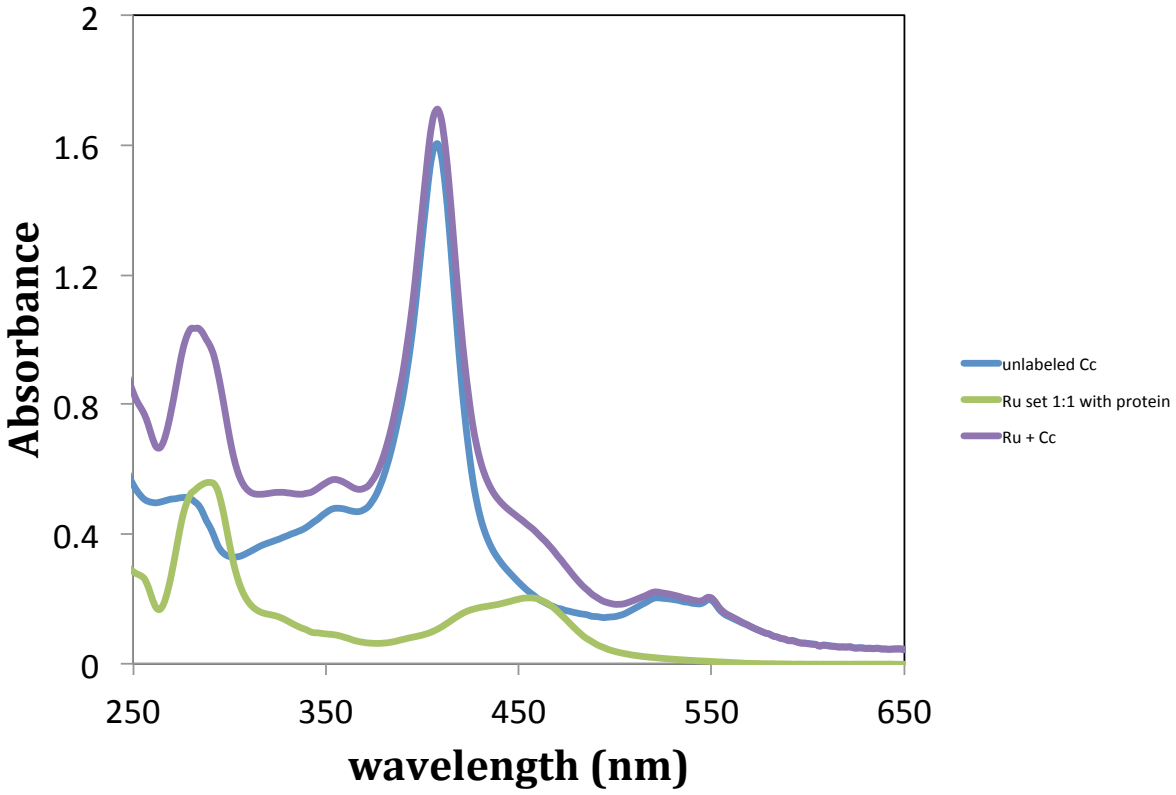

Figure 3.6-5 Labeled Ru39-Cc (WT and M80X) proteins as purified and observed via diode array, which tracks the theoretical spectra of Figure 3.6-4 in terms of the "shoulder" around 450nm and the (410:280) peak ratio increase for the labeled Cc construct as compared to unlabeled

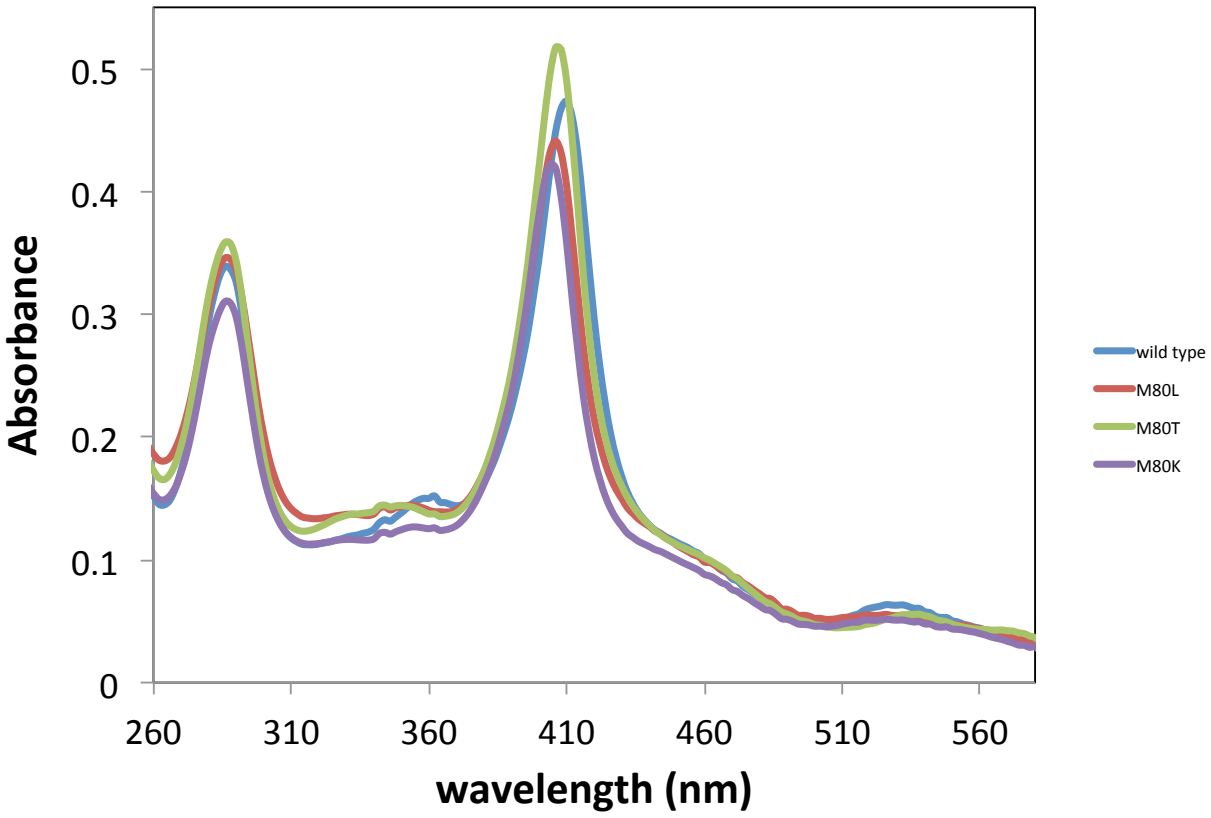

Redox titrations

Given preliminary evidence of unique redox mutant behavior, redox titrations performed as described in Methods and Materials section. Least-squares fit to data yields line of slope = (-nF/RT) and y-intercept = the redox potential of the mutant. The theoretical line of single-electron transfer would have slope = 25.7mV at 298K. M80T had an intermediate redox potential of +11.7 mV, while that of M80L was -69.4mV using this method, compared to a literature value of -45 reported for M80L and significantly lower than +260mV reported for Cc-WT (79). The M80K mutant yielded a redox potential of approximately +50mV, higher than the M80T mutant by a margin of 40mV and the M80L mutant by about 120mV. Redox titration data presented as Figures 3.6-6, 3.6-7, and 3.6-8. Error for these experiments was determined to be (± 20mV).

Figure 3.6-6 Redox titration of Human Cc-K39C/M80T (Emeas vs. ln Ccred/Ccox).

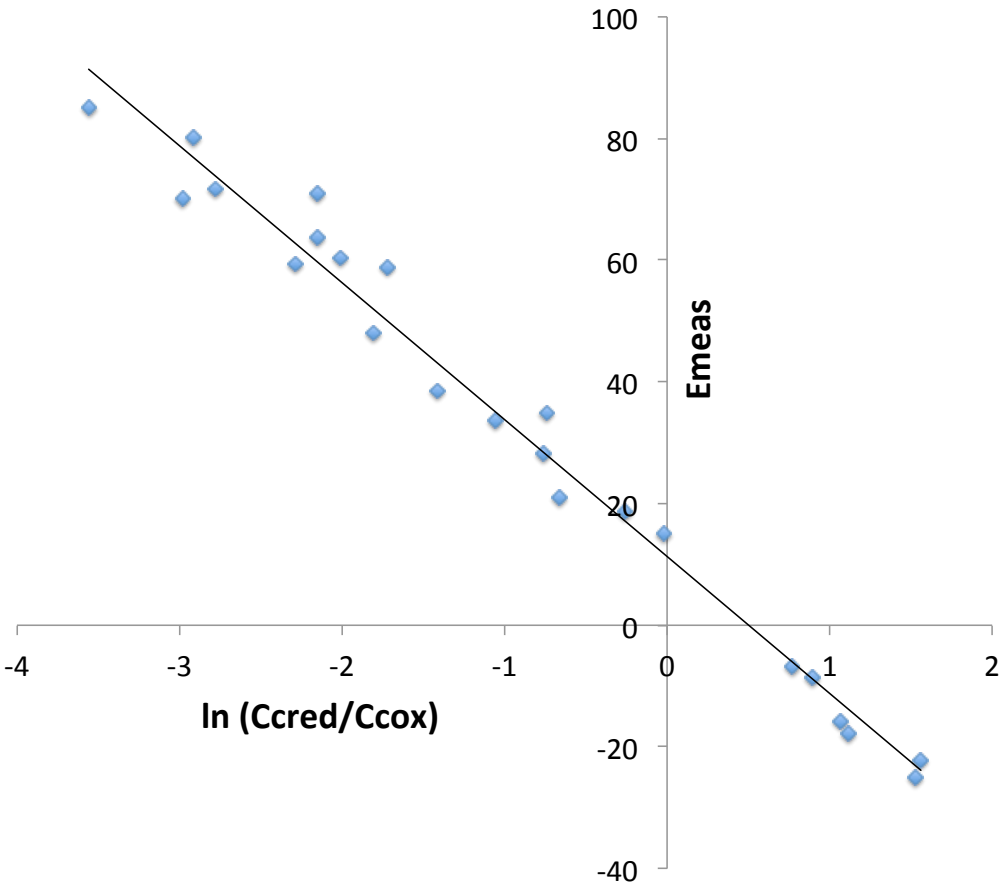

Figure 3.6-7 Redox titration of Human Cc-K39C/M80L (Emeas vs. ln Ccred/Ccox)

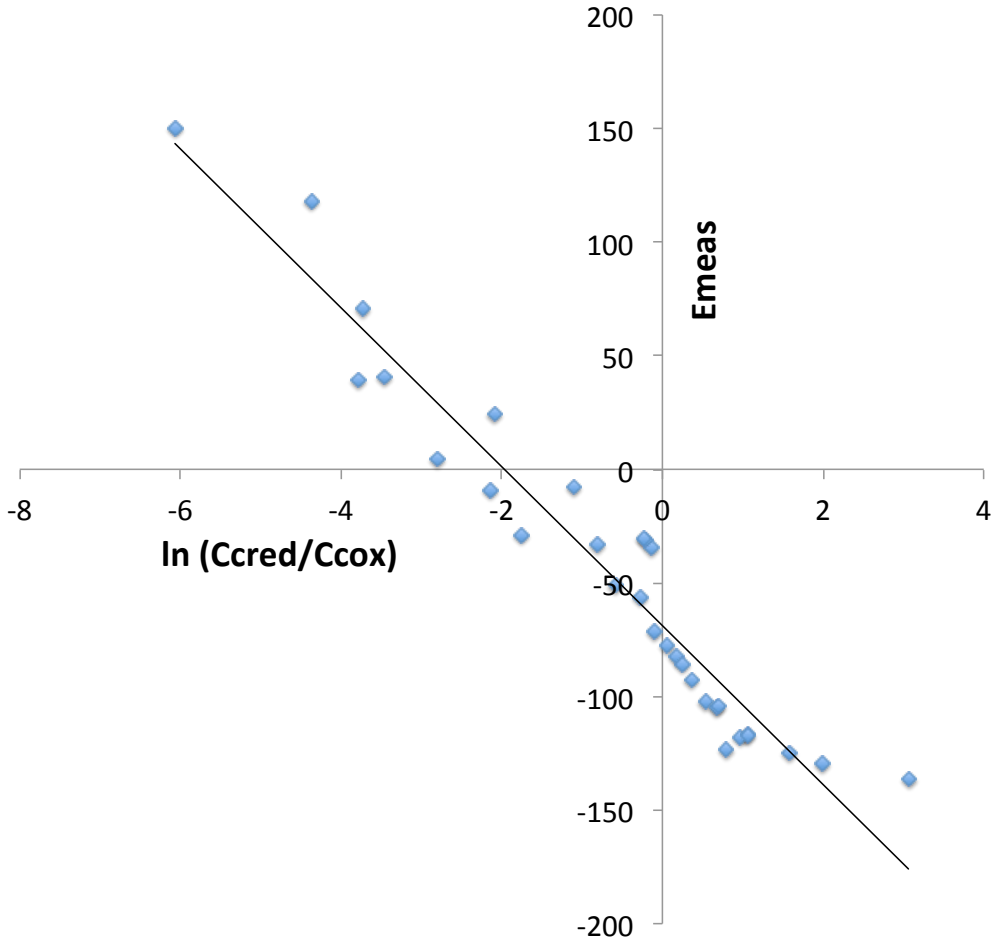

Figure 3.6-8 Redox titration of Human Cc-K39C/M80K (Emeas vs. ln Ccred/Ccox)

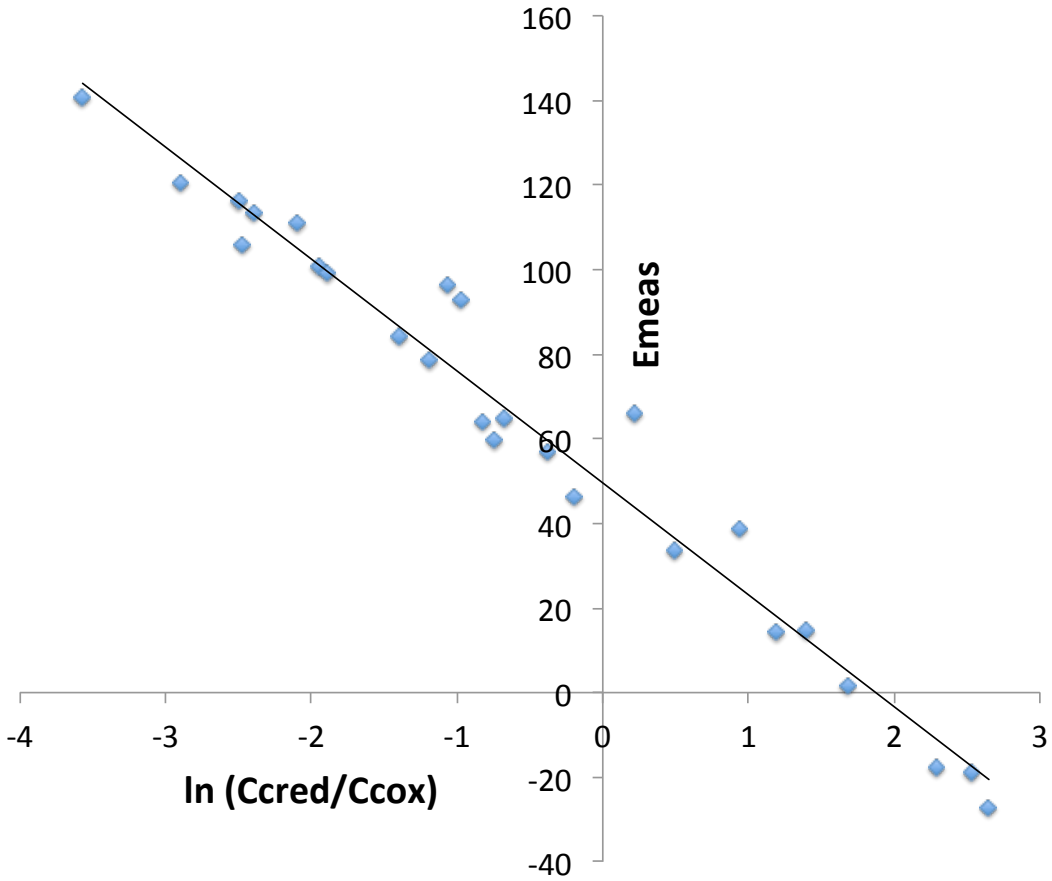

Flash photolysis kinetics

In order to assess that the reaction components were behaving consistently with respect to previous experimental data, ruthenium labeled cytochrome C WT-K39C, Ru-39-Cc, was combined first with a catalytic amount of oxidase to oxidize flash-reduced Cc. Aniline and 3CP were added at 10mM and 1mM, respectively. The 550nm transient indicates a rapid electron transfer from the laser-excited ruthenium Ru^{II*} to the heme of Cc (Figure 3.6-9). The previously published value of the rate constant of this electron transfer is $6 \times 10^5\ s^{-1}$, a value which was directly measured using a YAG laser in previous studies. Since the YAG laser was not operational and instead we used a dye laser and detection system that has a slower response time of ~ 4μs, the light scattering artifact resulted in complications directly measuring this rapid rate (70).

Upon addition of 17μM bovine CcO to this sample, the 550nm transient changes shape, due to the formation of a 1:1 complex between Ru-39-Cc and CcO at low ionic strength (Figures 3.6-10). Heme c in Ru-39-Cc is photoreduced by Ru^{II*} with a rate constant of $\sim 6 \times 10^5\ s^{-1}$, followed by electron transfer to Cu_A in CcO with a rate constant of $6 \times 10^4\ s^{-1}$. Under the same conditions, the concomitant rate of electron transfer from Cu_A to heme a within CcO was assessed at the 605nm wavelength and measured to be $\sim 28{,}000\ s^{-1}$ **(**Figure 3.6-11) which is within the error margin for the previously published value for this transfer of $\sim 20{,}000\ s^{-1}$ (70). This control experiment indicates that the composite system (laser, proteins, reagents, etc.) were functioning in accordance with previous experiments (70). These rate constants are independent of the concentration of CcO at low ionic strength, indicating that they are due to electron transfer within the 1:1 Ru-39-Cc:CcO complex.

Figure 3.6-9 550nm transient indicating a rapid electron transfer from the laser-excited ruthenium Ru^{II*} to the heme of Cc for Ru39C-Cc-WT. This particular fit represents the recovery time of the system, while a YAG laser (data not shown) determined the rate of electron transfer from Ru^{II*} to heme c to be approximately 6.5e5 s^{-1}. Error is ± 20%. Reaction conditions are 11µM Cc, 5mM phosphate pH =7.0, .1% lauryl maltoside, 10mM aniline, 1mM 3CP, and a catalytic amount of oxidase.

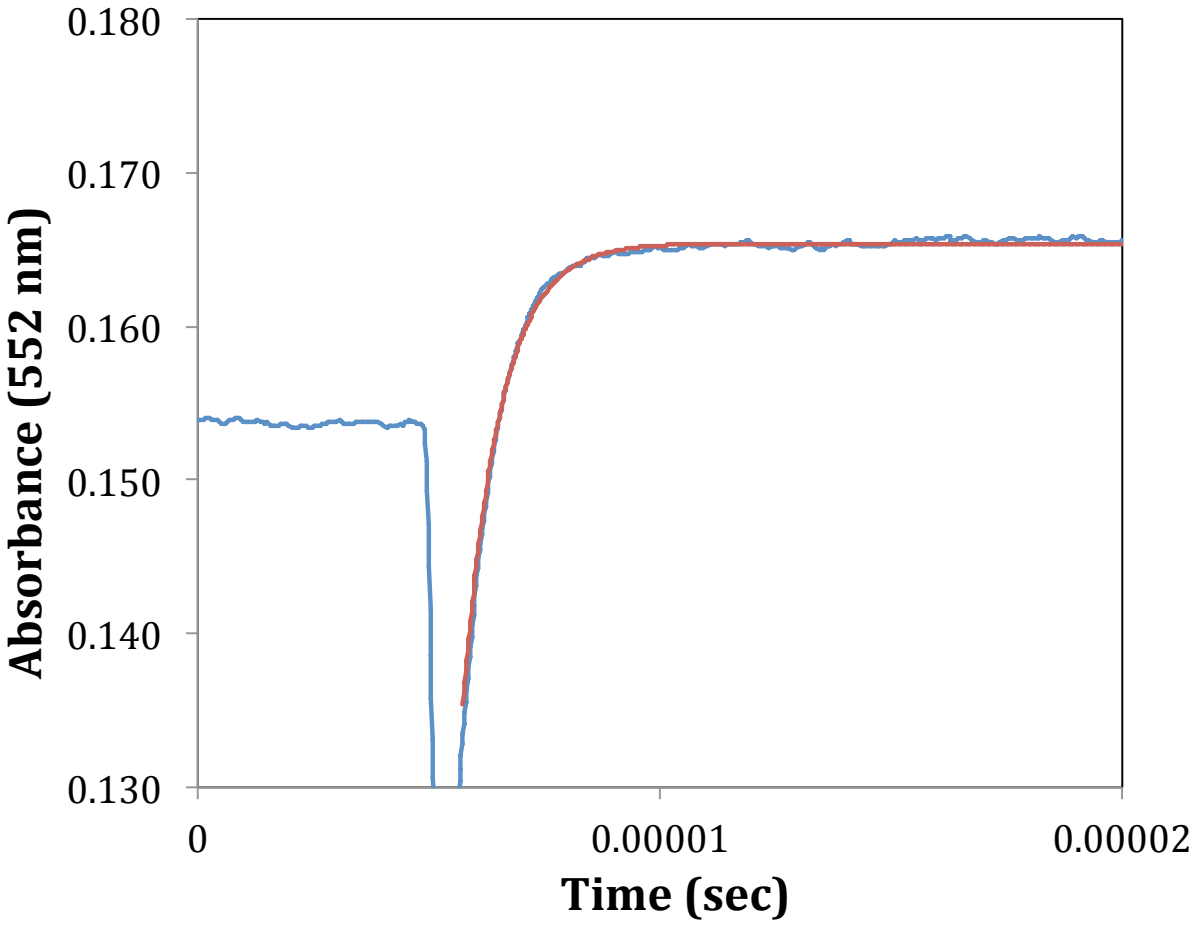

Figure 3.6-10 552nm transient indicating heme c of Ru-39-Cc is photoreduced by Ru^{II*} with a rate constant of 6 x 10^5 s^{-1}, followed by electron transfer to Cu_A in CcO with a rate constant of 6 x 10^4 s^{-1}. Error is ± 20%. Reaction conditions are 11μM Cc, 5mM phosphate pH =7.0, .1% lauryl maltoside, 10mM aniline, 1mM 3CP, and 18μM oxidase.

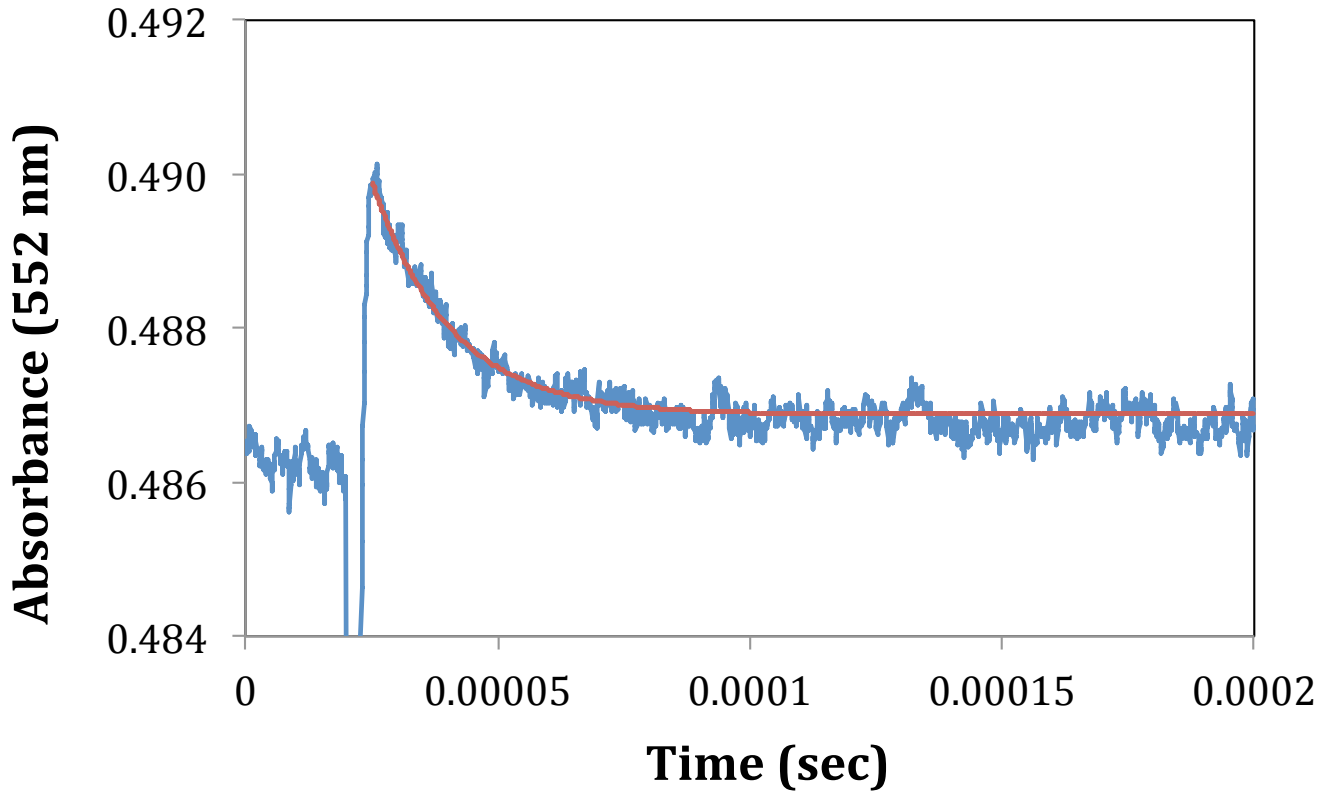

Figure 3.6-11 The rate of electron transfer from Cu_A to heme a within CcO assessed at the 605nm wavelength and measured to be ~28,000 s^{-1}, within the error margin for the previously published value for this transfer of ~20,000 s^{-1}. Error is estimated to be ± 20%. Reaction conditions are 11μM Cc, 5mM phosphate pH =7.0, .1% lauryl maltoside, 10mM aniline, 1mM 3CP, and 18μM oxidase.

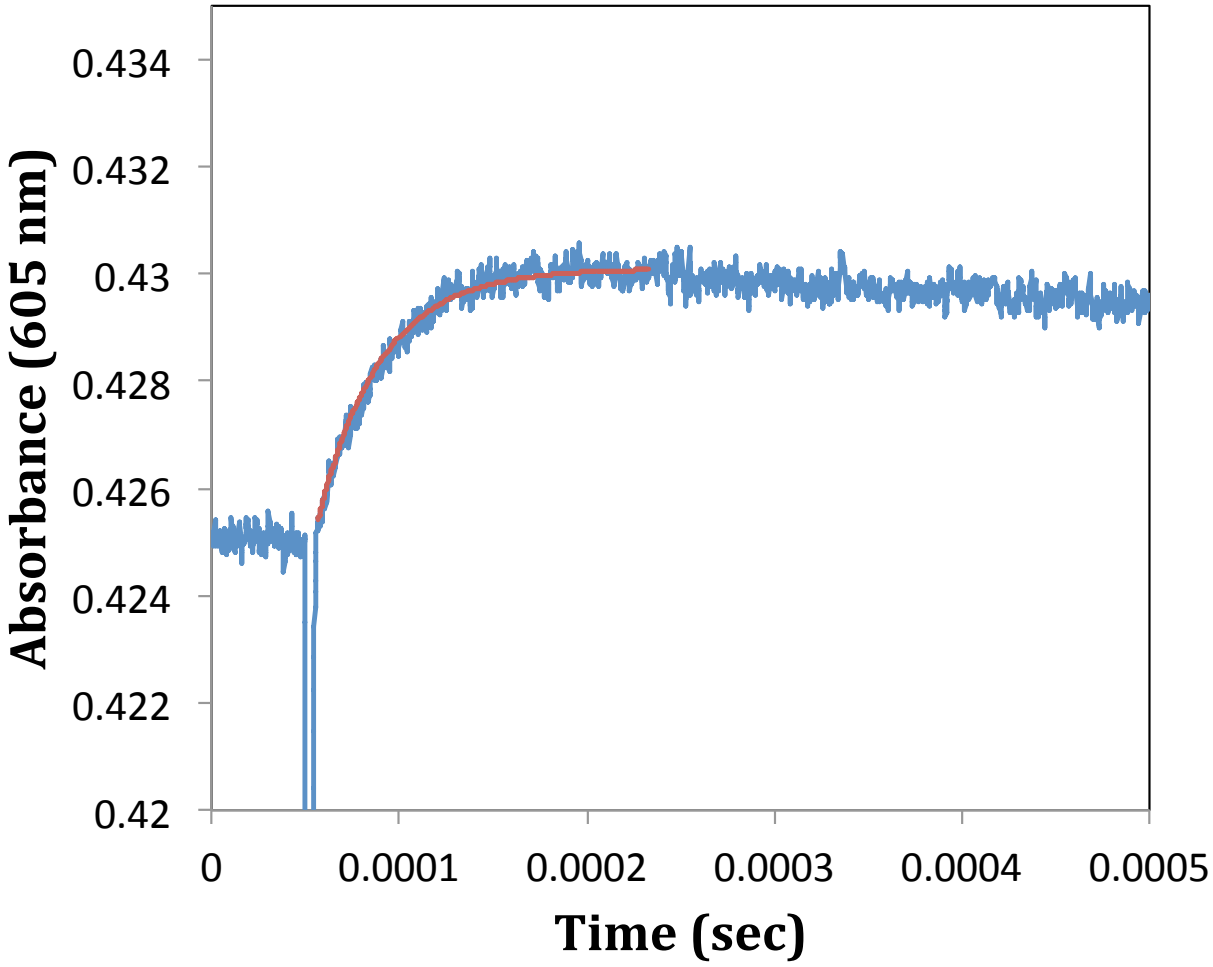

The M80K Ru-39-Cc mutant, with a measured redox potential of ~+50 mV, yielded some very interesting kinetic results. Based on Marcus Theory, the decreased redox potential of the Cc mutants should provide less impetus for an electron transfer from laser excited Ru^{II*} to heme c. Consistent with this result, the 550 nm transient of 15 μM M80K Ru-39-Cc with catalyic CcO present indicated a rate constant k_1 of electron transfer from Ru^{II*} to heme c less than wild-type, which is 6×10^5 s^{-1} for Ru-39-Cc. Again, because of the use of the laser dye and detection system, rather than YAG laser system, we were unable to directly obtain this rate constant due to missing a large portion of the signal in the 4μs dead time. However, the application of Marcus Theory allows us to put an upper limit on the number of 4.3×10^5 s^{-1}. The decreased rate constant k_1 for the M80K Ru-39-Cc mutant compared to wild-type Ru-39-Cc is consistent with the decreased heme c redox potential to ~+50 mV, which would decrease the driving force ΔE of electron transfer from Ru^{II*} to heme Fe^{III} by ~200 mV (Figure 3.6-12).

When 20 μM CcO was added to 15 μM M80K Ru-39-Cc to form a 1:1 complex at low ionic strength, the 550 nm transient seemed to indicate no apparent change in absorbance from pre- to post-flash. This was initially interpreted to mean that electron transfer was not occurring at all. However, the 605nm transient indicated that M80K Ru-39-Cc was in fact transferring electrons to heme a, and the rate constant k_b for electron transfer from Cu_A to heme a was the same as seen with Ru39-Cc-WT. Simply put, electrons were being internally transferred within CcO **(figure not shown).** Given that [1] the conditions of the experiment were aerobic, maintaining an oxidized population of CcO; [2] electrons were successfully conferred to Cc from the flash-reduced ruthenium complex; and [3] electrons were being conferred from Cu_A to heme a of CcO, the only possible conclusion was that

electron transfer from heme c of Cc to Cu_A of CcO must be occurring for this mutant. The fact that a signal is not seen in the transient indicates that within the 3-4 μs timescale of the light scattering associated with the laser flash and the unavoidable delay with signal detection, the electron transfer has taken place. In short, the electron transfer is too fast to observe. This indicates that the rate constant for electron transfer from heme c of M80K Ru-39-Cc to Cu_A in CcO must be larger than 7.0×10^5 s^{-1}, so that the formation and decay of reduced heme c is very rapid and is completed during the light scattering pulse 4μs down time for system response in the post-laser window. Applying theoretical fits to the raw transient of the 550nm was deemed necessary. Using the accepted rate constant $k_1 = 4.3 \times 10^5$ s-1 for the Ru^{II*} to Cu_A electron transfer, and the measured value of $k_2 = 6 \times 10^4$ s^{-1} for wild-type Ru-39-Cc, the theoretical transient did not match the data (Figure 3.6-13). The rate constant for electron transfer from M80K Ru-39-Cc heme to Cu_A must be much faster in order to have returned to the baseline. The estimated rate constant for electron transfer from heme c to Cu_A must be no less than 7.0×10^5 s^{-1} to match these experimental results (Figure 3.6-14). This represents a >10-fold increase in the rate constant k_a for the ~200mV reduction in the redox potential for the mutant.

While the M80T and M80L mutants were successfully labeled, we observed a very small signal from Ru^{II*} to heme c at the outset of these experiments. This is hypothesized to be the result of the larger decrease in driving force for these mutants with respect to Ru^{II*}. While our results indicated electron transfer was taking place from ruthenium to Cc, signal strength was insufficient to apply reasonable fits and obtain rate data (results not shown). As these two mutants have lower redox potential than the M80K variant, it was

hypothesized that the effect on the rate of electron transfer from heme c to Cu_A of CcO would be even more drastic than witnessed for the M80K mutant.

In an effort to correlate the results of this work to Marcus Theory, we applied Marcus Theory as shown in the following tables. Table 3.1 shows the Marcus Theory prediction for the rates of electron transfer from Ru^{II*} to heme c of Cc for the various mutants. To calculate k_{et}, we used a simplified equation from Moser/Dutton, below:

$$\log k_{et} = 15 - (0.6*R-3.1)*((\Delta G + \lambda)^2)/\lambda)$$

Table 3.1

protein	R (Å) DA distance	E_{red} (V) Ru^{II*}	E_{red} (V) heme c	ΔG (V) Ered(Ru)-Ered(c)	λ (V) reorganization energy	k_{et} (s^{-1}) rate of electron transfer
WT	15.4	-.84	.2600	-1.100	1.1	5.8×10^5
M80K	15.4	-.84	.0496	-.8896	1.1	4.3×10^5
M80T	15.4	-.84	.0117	-.8517	1.1	3.9×10^5
M80L	15.4	-.84	-.0694	-.7706	1.1	2.8×10^5

As might be expected, the decreased redox potentials for the mutant relative to WT result in slower rates of electron transfer, although the magnitude of (-ΔG) values remains quite

large as a function of the favorable drive for electrons to be transferred from the laser excited Ru^{II*} state.

From a theoretical standpoint, and given the calculated redox potentials, it was also important to assess the rate of electron transfer between heme c and Cu_A. Table 3.2 shows the expected rates of electron transfer from heme c of Cc to Cu_A of CcO, provided that the relationship obeys Marcus Theory. To calculate k_{et}, we used the same simplified equation we used for Table 3.1:

Table 3.2

protein	R (Å) DA distance	E_{red} (V) heme c	E_{red} (V) Cu_A	ΔG (V) Ered(c)-Ered (Cu_A)	λ (V) reorganization energy	k_{et} (s^{-1}) rate of electron transfer
WT	13	.26	.29	-.03	.84	6.0×10^4
M80K	13	.05	.29	-.24	.84	7.4×10^5
M80T	13	.0117	.29	-.2783	.84	1.1×10^6
M80L	13	-.0694	.29	-.3594	.84	2.2×10^6

As shown, Marcus Theory predicts that, for Ru39-Cc-WT, we would expect a rate constant of $k = 6.0 \times 10^4$ for heme c (of Cc) to Cu_A (of CcO). This has been confirmed experimentally

and corroborated in this study. Furthermore, our experimental fit and the rationale applied for Ru39C-Cc-M80K are both supported by theoretical application of Marcus Theory. We provide an experimental fit that almost identically matches the Marcus Theory prediction of the rate constant of $k = 7.4 \times 10^5\ s^{-1}$. This is direct evidence that altering redox potential of heme c in Cc can result in altering the rate of electron transfer to Cu_A. Moreover, this relationship could be described as behaving in accordance to Marcus' nobel winning work in summarizing electron transfer in biololgical systems. Finally, it can be concluded that the interaction between Cc and CcO does not include any type of conformational gating that results in rate limitations on the timescale of the above experiments.

Figure 3.6-12 552nm transient of Ru39-Cc-M80K indicating electron transfer from Ru^{II*} to heme c. Fit applied using Marcus Theory value from Table 3.1 for Ru39-Cc-M80K of 4.3 x 10^5 s^{-1}. Error is ± 20%. Reaction conditions are 11.5 μM M80K-Cc, 5mM phosphate pH = 7.0, .1% lauryl maltoside, 10 mM DMAB, and catalytic oxidase.

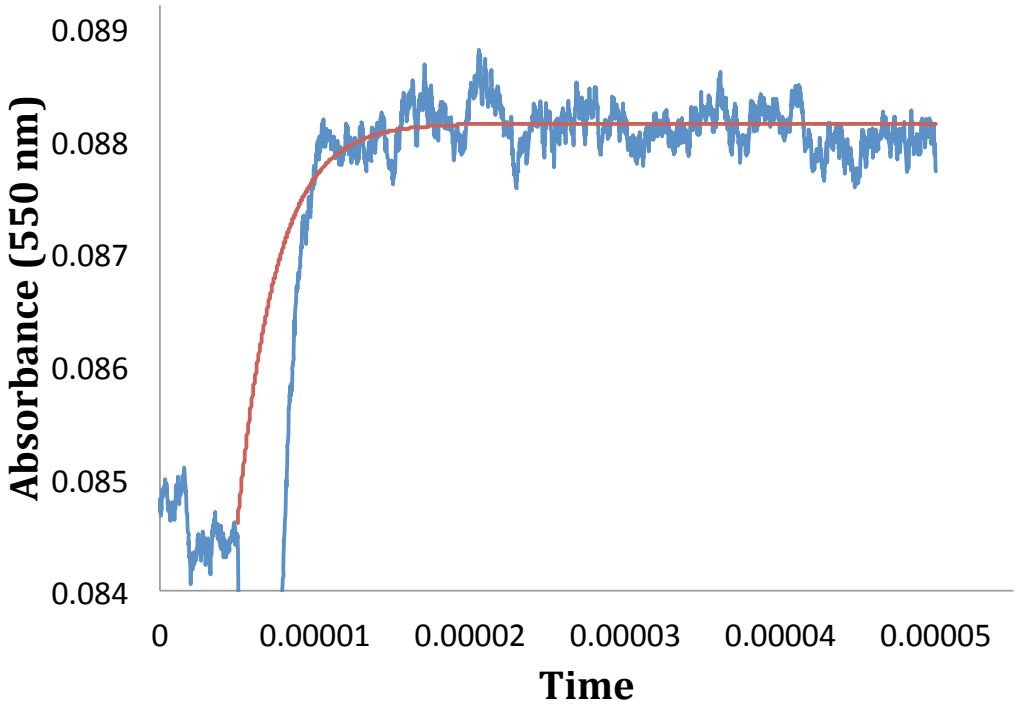

Figure 3.6-13 Theoretical fit of Ru39-Cc-M80K data using established rate data of Ru39-Cc-WT. As clearly indicated, the rate of electron transfer from heme c of Cc to Cu_A of CcO for the M80K mutant is much faster than that of WT. Fit applied using value of $k_1 = 4.3 \times 10^5\ s^{-1}$ and a value of $k_2 = 6.0 \times 10^4\ s^{-1}$. The applied fit with these parameters clearly does not accurately describe the experimental data. Reaction conditions are 11.5 μM M80K-Cc, 5mM phosphate pH = 7.0, .1% lauryl maltoside, 10 mM DMAB, and 18 μM oxidase.

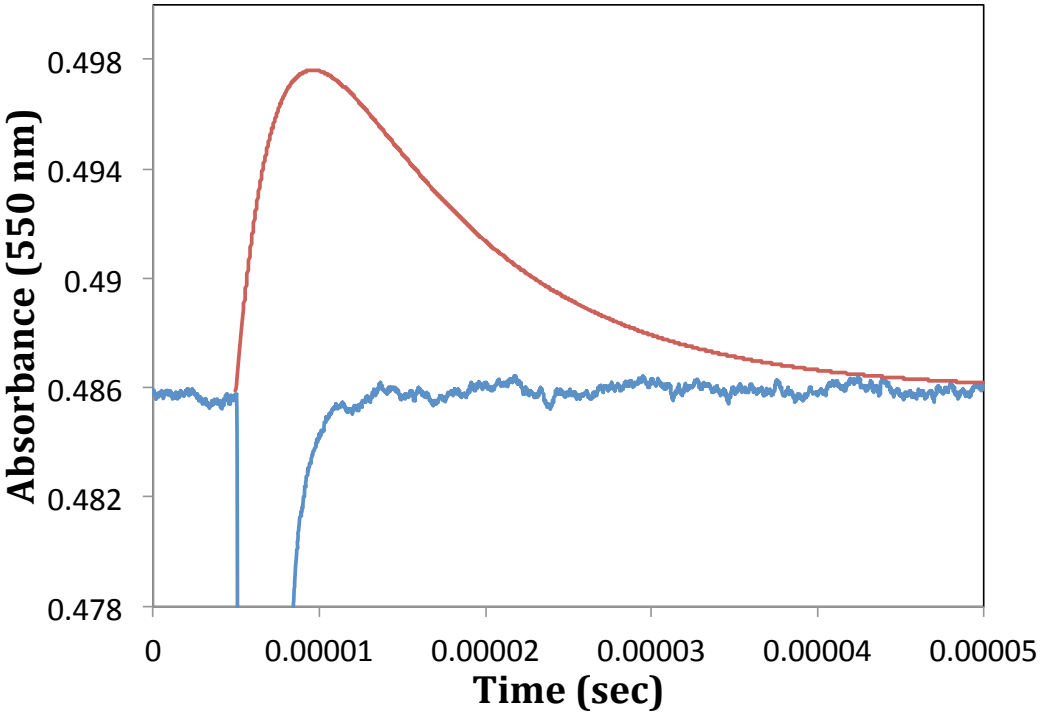

Figure 3.6-14 Theoretical fit of Ru39C-Cc-M80K depicting a more accurate set of parameters, showing the rate constant k_2 drastically increased from heme c of Cc to Cu_A of CcO, closer to $k_2 = 7.0x10^5\ s^{-1}$ as a function of altered redox potential. Rate constant k_1 remains unchanged at $4.3 \times 10^5\ s^{-1}$. Experimental conditions noted in Figure 3.6-13.

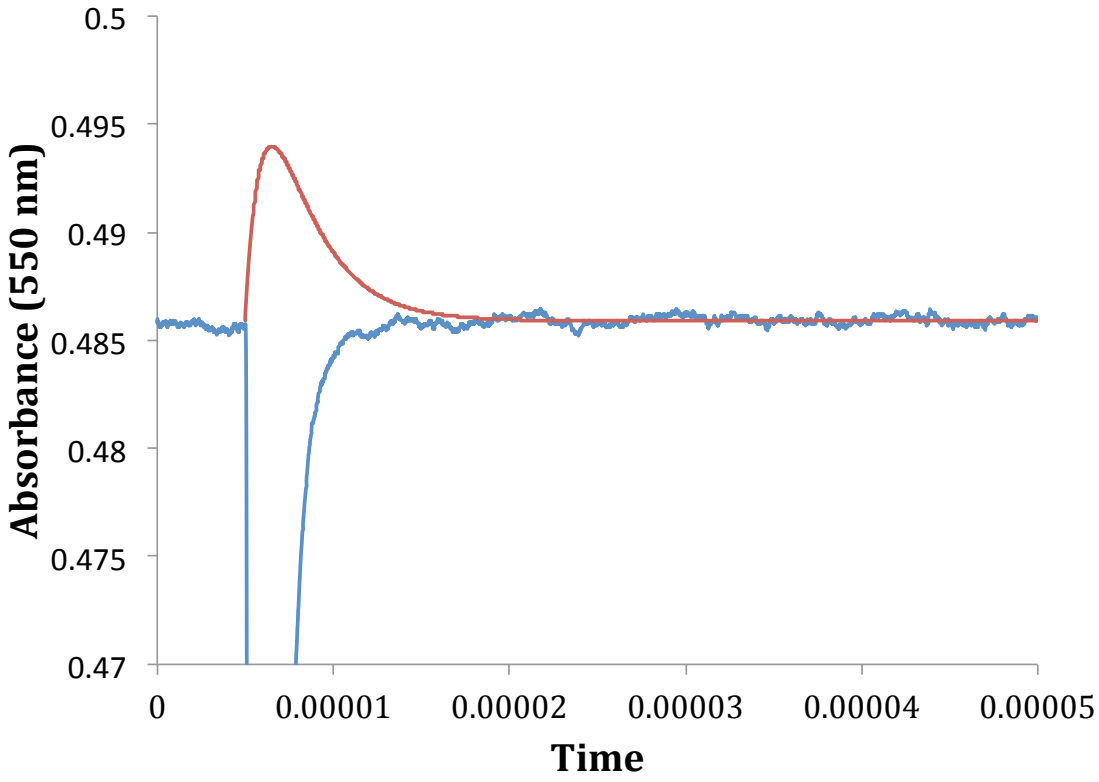

3.7 Discussion

In conclusion, we were able to successfully create several novel human Cc-M80X plasmids to explore the effect of redox potential on the rate of electron transfer between Cc and CcO. Several of these proteins did not express very well in multiple attempts, perhaps indicating a folding problem at the thermodynamic level as a function of altering the architecture about the heme. This possibility is not without some precedent, as the histidine residue that serves as the opposite point of ligation has been shown to be absolutely mandatory for proper protein expression and activity. While the Met80 is amenable to some replacement, as indicated in this recombinant study as well as in semi-synthetic attempts in the early 1990's, some amino acid substitutions may cause complications for the protein molecules to achieve a proper fold under these conditions. Successful labeling the proteins with the brominated ruthenium compound was followed by redox titration, indicating a decreased redox potential for the proteins as compared to that of +260mV of WT.

For the kinetics experiments, as we could only apply upper and lower limits to these rate constants given instrumental constraints, determining information about any changes in reorganization energy proved challenging. We were able to conclude, unsurprisingly, that the rate constant for electron transfer from Cu_A to heme a of CcO remains unaffected by altered redox potential of Cc (81,82). We were also able to corroborate previous rate data regarding the Ru39-Cc-WT.

By far the most relevant contribution of this work to the subject of mitochondrial electron transfer is as follows. The kinetics experiments of the Ru39-Cc-M80K mutant, as compared to Ru39-Cc-WT control, lead to the first known proof that the rate of electron

transfer between Cc and CcO is consistent with the Marcus Theory of biological electron transfer. Although hypotheses have been put forth based on structural information about the interaction of the two proteins, no one has kinetically assessed the effect of altering redox potential on the rate and correlated these findings with Marcus Theory. There is little reason to conclude that there are significant structural shifts (conformational gating, etc.) necessary for Cc to donate an electron to CcO, given the rapid rates witnessed for redox mutants of Cc. We have thus shown that conformational gating is not a factor in the Cc/CcO electron transfer relationship. In sharp contrast, it is noteworthy that the subject of the study in Chapter 2, cytochrome bc_1, does not obey Marcus Theory and is regulated by conformational gating -- specifically, the rotation of the ISP is the rate-limiting step for the enzyme and prior studies of redox mutants of bc_1 showed that the rate of electron transfer was not sensitive to changes in the driving force between donor and acceptor. From an evolutionary standpoint, it is interesting to observe the juxtaposition of, and imagine the interplay between, redox tuning and conformational gating in the drive towards a more efficient electron transfer system. It is reasonable to conclude that the forces acting on these specific proteins in the system differ as a function of the number of electrons involved. Specifically, the ISP gating mechanism has been thought to function as a means to ensure that radicals and ROS are not produced. Since two electrons must leave quinol, and only one can take the high potential chain, the ISP rotation might be thought to act as a metronome to control enzyme turnover. The second electron going through the b-heme, low potential chain towards the Q_i site must be clear before the enzyme can process more substrate. With two paths for two electrons, and the complications therein, it stands to reason that the forces that acted on this enzyme differed with respect to those that would

have acted on Cc. Cc is a single-electron carrier; therefore, analogous conformational gating, as present in the bc_1 scenario, would only present an obstacle to the rate of electron transfer without any gain. There is little chance for short circuit or ROS creation in a single-electron transfer. Optimum binding facilitated by charged amino acid residues, redox driving force, and reorganization energy might be expected to be on the forefront of selective evolutionary pressures, with conformational gating less of a priority for the advantage of improving efficiency and survivability for an organism.

References

1. Cordes M, Giese B. Electron transfer in peptides and proteins (2009) *Chem Soc Rev (38(4))*: 892-901.

2. Garrett R, Grisham M. Biochemistry (2005), 2nd edition.

3. Baradaran R, Berrisford JM, Minhas GS, Sazanov LA. Crystal structure of the entire respiratory complex I (2013) *Nature (494(7438))*: 443-448.

4. Mitchell, P. The protonmotive Q cycle: a general formulation (1975) *FEBS Letters (59(2))*: 137-139.

5. Davidson, VL. What controls the rates of interprotein electron-transfer reactions (2000), *Acc Chem Res (33(2))*: 87-93.

6. Gray HB, Winkler JR. Electron tunneling through proteins (2003) *Q Rev Biophys (36(3))*: 341-372.

7. Gray HB, Winkler JR. Electron transfer in proteins (1996) *Ann Rev Biochem (65)*: 537-561.

8. Marcus RA. Electron transfer reactions in chemistry. Theory and experiment (1997) *Pure and Appl Chem (69(1))*: 13-29.

9. Marcus RA. Electron-Transfer Reactions in Chemistry -- Theory and Experiment (1993) *Rev Mod Phys (65(3))*: 599-610.

10. Marcus RA. Theory, Experiment, and Reaction-Rates -- A Personal View (1986) *J Phys Chem-Us (90(16))*: 3460-3465.

11. Sharp RE, Chapman SK. Mechanisms for regulating electron transfer in multi-center redox proteins (1999) *Biochem Biophys Acta* (*1432(2))*: 143-158.

12. Page CC, Moser CC, Chen X, Dutton PL. Natural engineering principles of electron tunneling in biological oxidation-reduction (1999) *Nature* (*402(6757))*: 47-52.

13. Miller JR, Calcaterra LT, Closs GL. Intramolecular long-distance electron transfer in radical anions. The effects of free energy and solvent on the reaction rates (1984) *J Am Chem Soc (106(10))*: 3047–3049.

14. Hopfield JJ. Photo-induced electron transfer -- A critical test of the mechanism and range of biological electron transfer processes (1977) *Biophys J* (*18(3))*: 311-321.

15. Onuchic JN, Beratan, Winkler, Gray. Pathway analysis of protein electron-transfer reactions (1992) *Ann Review in Biophys and Bimol Structure (21)*: 349-377.

16. Moser CC, Keske, Warncke, Dutton PL. Nature of Biological electron transfer (1992) *Nature (355 (6363))*: 796-802.

17. Moser CC, Page, Chen, Dutton PL. Biological electron tunneling through native protein media (1997) *Journal of Biological Chemistry (2(3)):* 393-398.

18. Crofts AR, Rose. Marcus treatment of endergonic reactions: a commentary (2007) *Biochem Biophys Acta* (*1767 (10))*: 1228-1232.

19. Moser CC, Chobot, Page, Dutton PL. Distance metrics for heme protein electron tunneling (2008) *Biochem Biophys Acta* (*1777 (7-8))*: 1032-1037.

20. Noy, Moser, Dutton PL. Darwin at the molecular scale: selection and variance in electron tunneling proteins including cytochrome c oxidase (2006) *Philos Trans R Soc London, B Biol. Sci* (*361(1472))*: 1295-1305.

21. Moser CC, Page, Cogdell, Barber, Wraight, Dutton PL. Length, time, and energy scales of photosystems (2003) *Adv Protein Chem (63)*: 71-109.

22. Marcus RA, Sutin N. Application of electron transfer theory to several systems of biological interest (1985) osti.gov

23. Crofts AR, Holland JT, Victoria D, Kolling DR, Dikanov SA, Gilbreth R, Lhee S, Kuras R, Kuras MG. The Q-cycle reviewed: How well does a monomeric mechanism of the bc(1) complex account for the function of a dimeric complex? (2008) *Biochem Biophys Acta (1777(7-8))*: 1001-1019.

24. Crofts, AR. Life, Information, Entropy, and Time: Vehicles for Semantic Inheritance (2007) *Complexity (13(1))*: 14-50.

25. Sun J, Trumpower BL. Superoxide anion generation by the cytochrome bc1 complex (2003) *Arch Biochem Biophys (419(2))*: 198-206.

26. Brand, MD. The sites and topology of mitochondrial superoxide production (2010) *Exp Gerontol (45)*: 466-472.

27. Kim HY, Chung JM, Chung K. Increased production of mitochondrial superoxide in the spinal cord induces pain behaviors in mice: The effect of mitochondrial electron transport complex inhibitors (2008) *Neurosci Lett (447(1))*: 87-91.

28. Dröse, S., and Brandt, U. (2008) The mechanism of mitochondrial superoxide production by the cytochrome bc1 complex, *J Biol Chem (283(31))*: 21649-21654.

29. Sasaki T, Unno K, Tahara S, Shimada A, Chiba Y, Hoshino M, Kaneko T. Age-related increase of superoxide generation in the brains of mammals and birds (2008) *Aging Cell (7(4))*, 459-469.

30. Boveris A, Navarro A. Brain mitochondrial dysfunction in aging (2008) *IUBMB Life (60(5))*: 308-314.

31. Figueiredo PA, Mota MP, Appell HJ, and Duarte JA. The role of mitochondria in aging of skeletal muscle (2008) *Biogerontology (9(2))*: 67-84.

32. Pathak RU, Davey GP. Complex I and energy thresholds in the brain (2008) *Biochem Biophys Acta (1777(7-8))*: 777-782.

33. Chen YR, Chen CL, Yeh A, Liu X, Zweier JL. Direct and indirect roles of cytochrome b in the mediation of superoxide generation and NO catabolism by mitochondrial succinate-cytochrome c reductase (2006) *J Biol Chem (281(19))*: 13159-68.

34. Rottenberg H, Covian R, Trumpower BL. Membrane potential greatly enhances superoxide generation by the cytochrome bc1 complex reconstituted into phospholipid vesicles (2009) *J Biol Chem* (*284)*: 19203-19210.

35. Berry EA, Guergova-Kuras M, Huang LS, Crofts AR. Structure and function of cytochrome bc complexes (2000) *Annu Rev Biochem (69)*: 1005-1075.

36. Yu L, Tso SC, Shenoy SK, Quinn BN, Xia D. The role of the supernumerary subunit of Rhodobacter sphaeroides cytochrome bc1 complex 9 (1999) *J Bioenerg Biomembr (31(3))*: 251-257.

37. Crofts AR, Berry EA. Structure and function of the cytochrome bc1 complex of mitochondria and photosynthetic bacteria (1998) *Curr Opin Struct Biol (8(4))*: 501-509.

38. Esser L, Elberry M, Zhou F, Yu CA, Yu L, Xia D. Inhibitor-complexed structures of the cytochrome bc1 from the photosynthetic bacterium Rhodobacter sphaeroides (2008) *J Biol Chem (283(5))*: 2846-2857.

39. Obungu V, Yu LP, Japa S, Beattie DS. The role of the membrane- spanning and extra-membranous regions of the iron-sulfur protein in its assembly into the cytochrome bc1 complex of yeast mitochondria (1997) *Biochem Biophys Acta (1321(3))*: 229-237.

40. Crofts AR, Hong S, Zhang Z, Berry EA. Physicochemical aspects of the movement of the rieske iron sulfur protein during quinol oxidation by the bc(1) complex from mitochondria and photosynthetic bacteria (1999) *Biochemistry (38(48))*: 15827-15839.

41. Darrouzet E, Moser CC, Dutton PL, Daldal F. Large scale domain movement in cytochrome bc1: a new device for electron transfer in proteins (2001) *Trends Biochem Sci (26(7))*: 445-451.

42. Millett F, Durham B. Kinetics of Electron Transfer within Cytochrome bc (1) and Between Cytochrome bc (1) and Cytochrome c (2004) *Photosyn Res (82(1))*: 1-16.

43. Xiao K, Yu L, Yu CA. Confirmation of the involvement of protein domain movement during the catalytic cycle of the cytochrome bc1 complex by the formation of an intersubunit disulfide bond between cytochrome b and the iron- sulfur protein (2000) *J Biol Chem (275(49))*: 38597-38604.

44. Xia D, Kim H, Yu CA, Yu L, Kachurin A, Zhang L, Deisenhofer J. A novel electron transfer mechanism suggested by crystallographic studies of mitochondrial cytochrome bc1 complex (1998) *Biochem Cell Biol (76(5))*: 673-679.

45. Yu CA, Wen X, Xiao K, Xia D, Yu L. Inter- and intra-molecular electron transfer in the cytochrome bc_1 complex (2002) *Biochem Biophys Acta (1555(1-3))*: 65-70.

46. Kim H, Xia D, Yu CA, Xia JZ, Kachurin AM, Zhang L, Yu L, Deisenhofer J. Inhibitor binding changes domain mobility in the iron-sulfur protein of the mitochondrial bc1 complex from bovine heart (1998) *Proc Natl Acad Sci (95(14))*: 8026-8033.

47. Millett F, Havens J, Rajagukguk S, Durham B. Design and use of photoactive ruthenium complexes to study electron transfer within cytochrome bc_1 and from cytochrome bc_1 to cytochrome c (2013) *Biochem Biophys Acta* (*1827(11-12))*: 1309-19.

48. Havens J, Castellani M, Kleinschroth T, Ludwig B, Durham B, Millett F. Photoinitiated Electron Transfer within the *Paracoccus denitrificans* Cytochrome bc_1 Complex: Mobility of the Iron–Sulfur Protein Is Modulated by the Occupant of the Q_o Site (2011) *Biochemistry* (*50(48))*: 10462-72.

49. Engstrom G, Xiao K, Rajagukguk S, Yu CA, Yu L, Durham B, Millett F. Photoinduced Electron Transfer between the Rieske Iron-Sulfur Protein and Cytochrome c_1 in the*Rhodobacter sphaeroides* Cytochrome bc_1 Complex (2003) *J Biol Chem (278(13))*: 11419-26.

50. Cooley JW, Lee DW, Daldal F. Across Membrane Communication between the Q_o and Qi Active Sites of Cytochrome *bc*1 (2009) *Biochemistry (48(9))*: 1888–1899.

51. Bloch D, Belevich I, Jasaitis A, Ribacka C, Puustinen A, Verkhovsky MI, Wikström M. The catalytic cycle of cytochrome *c* oxidase is not the sum of its two halves (2004) *Proc Natl Acad Sci (101(2))*: 529-33.

52. Esser L, Gong X, Yang S, Yu L, Yu CA, Xia D. Surface-modulated motion switch: capture and release of iron-sulfur protein in the cytochrome bc1 complex (2006) Proc Natl Acad Sci, 13045-50.

53. Lee HJ, Svahn E, Swanson JM, Lepp H, Voth GA, Brzezinski P, Gennis RB. Intricate Role of Water in Proton Transport through Cytochrome *c* Oxidase (2010) *J Am Chem Soc (132(45))*: 16225-39.

54. Tsukihara T, Aoyama H, Yamashita E, Tomizaki T, Yamaguchi H, Shinzawa-Itoh K, Nakashima R, Yaono R, Yoshikawa S. The whole structure of the 13-subunit oxidized cytochrome c oxidase at 2.8 angstrom (1996) *Science (272(5265))*: 1136-44.

55. Tsukihara T, Yoshikawa S. Crystal structural studies of a membrane protein complex, cytochrome c oxidase from bovine heart (1998) *Acta Crystallogr A* (*54(Pt 6 Pt 1))*: 895-904.

56. Tsukihara T, Aoyama H, Yamashita E, Tomizaki T, Yamaguchi H, Shinzawa-Itoh K, Nakashima R, Yaono R, Yoshikawa S. Structures of metal sites of oxidized bovine heart cytochrome c oxidase at 2.8 Angstroms (1995) *Science* (*269(5227))*: 1069-74.

57. Wilmanns M, Lappalainen P, Kelly M, Sauer-Eriksson E, Saraste M. Crystal structure of the membrane-exposed domain from a respiratory quinol oxidase complex with an engineered dinuclear copper center (1995) *Proc Natl Acad Sci (26)*: 11955-9.

58. Gorbikova EA, Wikström M, Verkhovsky MI. The protonation state of the cross-linked tyrosine during the catalytic cycle of cytochrome *c* oxidase (2008) *J Biol Chem* (*283(50))*: 34907-34912.

59. Proshlyakov DA, Pressler MA, DeMaso C, Leykam JF, DeWitt DL, Babcock GT. Oxygen activation and reduction in respiration: involvement of redox-active tyrosine 244 (2000) *Science (290(5496))*: 1588-91.

60. Kaila VR, Verkhovsky MI, Hummer G, Wikström M. Glutamic acid 242 is a valve in the proton pump of cytochrome c oxidase (2008) *Proc Natl Acad Sci (105(17))*: 6255-9.

61. Kim YC, Wikström M, Hummer G. Kinetic gating of the proton pump in cytochrome *c* oxidase (2009) *Proc Natl Acad Sci (106(33))*: 13707-12.

62. Casalini S, Battistuzzi G, Borsari M, Bortolotti CA, Ranieri A, Sola M. Electron Transfer and Electrocatalytic Properties of the Immobilized Methionine80Alanine Cytochrome *c* Variant (2008) J Phys Chem (*112(5))*: 1555-63.

63. Churg AK, Warshel A. Control of the redox potential of cytochrome and microscopic dielectric effects in proteins (1986) *Biochemistry (25(7))*: 1675-1681.

64. Liu G, Shao W, Zhu S, Tang W. Effects of axial ligand replacement on the redox potential of cytochrome *c* (1995) *J Inorg Biochem (60(2))*: 123-131.

65. Moser CC, Keske JM, Warncke K, Farid RS, Dutton PL. Nature of biological electron transfer (1992) *Nature (355(6363))*: 796-802.

66. Wallace CJ, Clark-Lewis I. Functional role of heme ligation in cytochrome c. Effects of replacement of methionine 80 with natural and non-natural residues by semisynthesis (1992) *J Biol Chem (267(6))*: 3852-61.

67. Maneg O, Malatesta F, Ludwig B, Drosou V. Interaction of cytochrome *c* with cytochrome oxidase: two different docking scenarios (2004) *Biochem Biophys Acta (1-3)*: 274-81.

68. Baba ML, Darga LL, Goodman M, Czelusniak J. Evolution of cytochrome *c* investigated by the maximum parsimony method (1981) *J Mol Evol (17(4))*: 197-213.

69. Roberts VA, Pique ME. Definition of the Interaction Domain for Cytochrome *c*on Cytochrome *c* Oxidase (1999) *J Biol Chem (274(53))*: 38051-60.

70. Schmidt TR, Wildman DE, Uddin M, Opazo JC, Goodman M, Grossman LI. Rapid electrostatic evolution at the binding site for cytochrome c on cytochrome c oxidase in anthropoid primates (2005) *Proc Natl Acad Sci (102(18))*: 6379-84.

71. Wang K, Zhen Y, Sadoski R, Grinnell S, Geren L, Ferguson-Miller S, Durham B, Millett F. Definition of the Interaction Domain for Cytochrome *c*on Cytochrome *c* Oxidase (1999) *J Biol Chem (274(53))*: 38042-50.

72. Zhen Y, Hoganson CW, Babcock GT, Ferguson-Miller S. Definition of the Interaction Domain for Cytochrome *c*on Cytochrome *c* Oxidase (1999) *J Biol Chem (274(53))*: 38032-41.

73. Dutton PL. Oxidation-reduction potential dependence of the interaction of cytochromes, bacteriochlorophyll and carotenoids at 77°K in chromatophores of *Chromatium* D and *Rhodopseudomonas gelatinosa* (1971) *Biochem Biophys Acta (226(1))*: 63-80.

74. Olteanu A, Patel CN, Dedmon MM, Kennedy S, Linhoff MW, Minder CM, Potts PR, Deshmukh M, Pielak GJ. Stability and apoptotic activity of recombinant human cytochrome c (2003) *Biochem Biophys Res Comm (312)*: 733–740.

75. Pollock WBR, Rosell FI, Twitchett MB, Dumont ME, Mauk AG. Bacterial expression of a mitochondrial cytochrome c. Trimethylation of Lys72 in yeast iso-1-cytochrome c and the alkaline conformational transition (1998) *Biochemistry (37)*: 6124–6131.

76. Patel CN, Lind MC, Pielak GJ. Characterization of Horse Cytochrome c Expressed in Escherichia coli (2001) *Protein Expression and Purification* (*22)*: 220–224.

77. Morar AS, Kakouras D, Young GB, Boyd J, Pielak GJ. Expression of 15N-labeled eukaryotic cytochrome c in Escherichia coli (1999) *J Biol Inorg Chem (4)*: 220–222.

78. Kranz R, Lill R, Goldman B, Bonnard G, Merchant S. Molecular mechanisms of cytochrome c biogenesis: three distinct systems (1998) *Mol Microbiol* (*29)*: 383–396.

79. Geren L, Sahm S, Millett F, Durham B. Photoinduced electron transfer between cytochrome c peroxidase and yeast cytochrome c labeled at Cys 102 with (4-bromomethyl-4'-methylbipyridine)[bis(bipyridine)]ruthenium2+ (1991) *Biochemistry (30(39))*: 9450-9457.

80. Raphael AL, Gray HB. Semisynthesis of axial-ligand (position 80) mutants of cytochrome c (1991) *J Am Chem Soc (113(3))*: 1038-1040.

81. Wang K, Geren L, Zhen Y, Ma L, Ferguson-Miller S, Durham B, Millett F. Mutants of the CuA site in cytochrome oxidase of Rhodobacter sphaeroides: II. Rapid kinetic analysis of electron transfer (2002) *Biochemistry (41(7))*: 2298-2304.

82. Durham B, Millett F. Design of photoactive ruthenium complexes to study electron transfer and proton pumping in cytochrome oxidase (2012) *Biochem Biophys Acta (1817(4))*: 567-74.

UNIVERSITY OF ARKANSAS

Office of Research Compliance

February 10, 2012

MEMORANDUM

TO: Dr. Frank Millett

FROM: W. Roy Penney
Institutional BioSafety Committee

RE: IBC Protocol Approval

IBC Protocol #: 12018

Protocol Title: "Characterization of Specific Electron Transfer Interactions Between Cytochrome b5 and Cytochrome C"

Approved Project Period: Start Date: February 9, 2012
Expiration Date: February 8, 2015

The Institutional Biosafety Committee (IBC) has approved Protocol 12018, "Characterization of Specific Electron Transfer Interactions Between Cytochrome b5 and Cytochrome C" You may begin your study.

If further modifications are made to the protocol during the study, please submit a written request to the IBC for review and approval before initiating any changes.

The IBC appreciates your assistance and cooperation in complying with University and Federal guidelines for research involving hazardous biological materials.